NASA/TP—2010–216435

Design of Refractory Metal Life Test Heat Pipe and Calorimeter

J.J. Martin, R.S. Reid, and S.M. Bragg-Sitton
Marshall Space Flight Center, Marshall Space Flight Center, Alabama

August 2010

The NASA STI Program…in Profile

Since its founding, NASA has been dedicated to the advancement of aeronautics and space science. The NASA Scientific and Technical Information (STI) Program Office plays a key part in helping NASA maintain this important role.

The NASA STI program operates under the auspices of the Agency Chief Information Officer. It collects, organizes, provides for archiving, and disseminates NASA's STI. The NASA STI program provides access to the NASA Aeronautics and Space Database and its public interface, the NASA Technical Report Server, thus providing one of the largest collections of aeronautical and space science STI in the world. Results are published in both non-NASA channels and by NASA in the NASA STI Report Series, which includes the following report types:

- TECHNICAL PUBLICATION. Reports of completed research or a major significant phase of research that present the results of NASA programs and include extensive data or theoretical analysis. Includes compilations of significant scientific and technical data and information deemed to be of continuing reference value. NASA's counterpart of peer-reviewed formal professional papers but has less stringent limitations on manuscript length and extent of graphic presentations.

- TECHNICAL MEMORANDUM. Scientific and technical findings that are preliminary or of specialized interest, e.g., quick release reports, working papers, and bibliographies that contain minimal annotation. Does not contain extensive analysis.

- CONTRACTOR REPORT. Scientific and technical findings by NASA-sponsored contractors and grantees.

- CONFERENCE PUBLICATION. Collected papers from scientific and technical conferences, symposia, seminars, or other meetings sponsored or cosponsored by NASA.

- SPECIAL PUBLICATION. Scientific, technical, or historical information from NASA programs, projects, and missions, often concerned with subjects having substantial public interest.

- TECHNICAL TRANSLATION. English-language translations of foreign scientific and technical material pertinent to NASA's mission.

Specialized services also include creating custom thesauri, building customized databases, and organizing and publishing research results.

For more information about the NASA STI program, see the following:

- Access the NASA STI program home page at <http://www.sti.nasa.gov>

- E-mail your question via the Internet to <help@sti.nasa.gov>

- Fax your question to the NASA STI Help Desk at 443–757–5803

- Phone the NASA STI Help Desk at 443–757–5802

- Write to:
  NASA STI Help Desk
  NASA Center for AeroSpace Information
  7115 Standard Drive
  Hanover, MD 21076–1320

NASA/TP—2010–216435

Design of Refractory Metal Life Test Heat Pipe and Calorimeter

J.J. Martin, R.S. Reid, and S.M. Bragg-Sitton
Marshall Space Flight Center, Marshall Space Flight Center, Alabama

National Aeronautics and
Space Administration

Marshall Space Flight Center • MSFC, Alabama 35812

August 2010

TRADEMARKS

Available from:

NASA Center for AeroSpace Information
7115 Standard Drive
Hanover, MD 21076–1320
443–757–5802

This report is also available in electronic form at
<https://www2.sti.nasa.gov>

TABLE OF CONTENTS

TABLE OF CONTENTS (Continued)

LIST OF FIGURES

LIST OF FIGURES (Continued)

LIST OF FIGURES (Continued)

LIST OF TABLES

LIST OF TABLES (Continued)

LIST OF ACRONYMS AND SYMBOLS

Ar	argon
ARO	after receipt of order
ASTM	American Society for Testing and Materials
B	boron
C	carbon
Ca	calcium
CAD	computer-aided design
CH_4	methane
Co	cobalt
CO_2	carbon dioxide
EB	electron beam
EBR–II	Experimental Breeder Reactor–II
ESCA	electron spectroscopy for chemical analysis
F	Fisher series designee
Fe	iron
G	mass flux G68–80 series designee
GASP	gas properties
GDMS	glow discharge mass spectroscopy
GFSSP	generalized fluid system simulation program
H	hydrogen
HCl	hydrochloric acid
He	helium

LIST OF ACRONYMS AND SYMBOLS (Continued)

HTPIPE	steady-state heat pipe code analysis program developed by LANL
H_2O	water
ID	inside diameter
IFMP	Integrated Financial Management Program
ISO	International Organization for Standardization
K	potassium
LANL	Los Alamos National Laboratory
LECO	LECO corporation builds combustion analyzers to determine compositions in inorganic samples
Mg	magnesium
Mn	manganese
Mo	molybdenum
MSFC	Marshall Space Flight Center
N	nitrogen
Na	sodium
Nb	niobium
NDE	nondestructive evaluation
Ni	nickel
O	oxygen
OD	outside diameter
Re	rhenium
RF	radio frequency
SAES	SAES Getters Group
Si	silicon

LIST OF ACRONYMS AND SYMBOLS (Continued)

Sn	tin
SPAR	space power advanced reactor
SP–100	Space Power 100 kW (program)
TIG	tungsten inert gas
TP	Technical Publication
UHP	ultrahigh purity
V	vanadium
VTASC	visual thermofluid analyzer of systems and components
V&V	validation and verification
W	tungsten
WASP	water and steam properties
Zr	zirconium

NOMENCLATURE

A	channel dimension; area
A_c	surface area calorimeter shell outer wall diameter
A_f	coolant flow area
A_i	surface area inner wall
A_o	surface area outer wall
C	impurity concentration
C_p	specific heat
CTE	coefficient of thermal expansion
D_i	initial diameter
d	heat pipe diameter
d_{ci}	calorimeter channel wall inner diameter
d_{co}	calorimeter channel wall outer diameter
d_h	hydraulic diameter
d_i	inner diameter
d_o	outer diameter
d_{si}	calorimeter shell wall inner diameter
f	friction factor
f_R	material fraction of complete recrystallization
g	acceleration due to gravity
h	convective heat transfer coefficient

NOMENCLATURE (Continued)

h_{fg}	latent heat of vaporization
I	irradiation tests
k	thermal conductivity
k_e	effective thermal conductivity
L	calorimeter full length
L_a	adiabatic length
L_c	heat pipe condenser length
L_e	heat pipe evaporator length
l	width
l_{gg}	gas gap width
M''	mass fluence
MW	molecular weight of component
m	mass of component
$\dot{m}$	mass flow rate
m^o	stochiometric mass of getter
N	baseline life
Nu	Nusselt number
n	nucleation site radius
P	pressure
Pr	Prandtl number
$\dot{Q}$	heat transfer rate

NOMENCLATURE (Continued)

$\dot{Q}_{cond}$	conductive heat transfer rate
$\dot{Q}_{conv}$	convective heat transfer rate
$\dot{Q}_{fluid}$	fluid heat transfer rate
$\dot{Q}_{gas\ cond}$	gas conductive heat transfer rate
$\dot{Q}_{rad}$	radiation heat transfer rate
$\dot{Q}_{solid\ cond}$	solid condition heat transfer rate
$\dot{Q}_{total}$	total heat transfer rate
$\dot{q}$	applied evaporator power
$\dot{q}_{rad}$	radial heat flux
R	universal gas constant
Ra	Raleigh number
Re	Reynolds number
r	maximum pore radius
T	temperature
T_0	design temperature
T_a	ambient temperature
T_{avg}	average temperature
T_{cw}	calorimeter wall temperature
T_{cwi}	calorimeter channel inner wall temperature
T_{cwo}	calorimeter channel outer wall temperature
T_f	flow annulus fluid temperature

NOMENCLATURE (Continued)

T_h	radiating surface temperature
T_{hp}	heat pipe temperature
T_i	inner surface temperature
T_{in}	coolant inlet temperature
T_o	outer surface temperature
T_o	1-hr recrystallization temperature
T_{out}	coolant outlet temperature
T_∞	ambient temperature
t	time
V	fluid velocity
V_{disk}	getter volume
α	thermal diffusivity
α_{CTE}	thermal expansion coefficient
$\alpha(T)$	normalized Arrhenius diffusion rate
β	gas thermal expansion coefficient
Γ	viscosity ratio
ΔD	change in diameter
ΔE	work function
ΔH	activation energy
Δp	delta pressure
ΔT	delta temperature

NOMENCLATURE (Continued)

ΔT_{LM}	log mean temperature difference
δ	gap spacing
ε	total hemispherical emissivity
ε_i	inner surface emissivity
ε_o	outer surface emissivity
μ	absolute viscosity
μ_{bulk}	bulk fluid viscosity at average temperature
μ_{wall}	fluid viscosity at wall temperature
v	kinematic viscosity
ρ	density
σ	Stefan-Boltzmann constant
τ	time
τ_i	time at temperature
τ_{max}	maximum time
τ_o	recrystallization time at T_o
ϕ	flow annulus diameter ratio
ψ	flow annulus gap adjustment parameter

TECHNICAL PUBLICATION

DESIGN OF REFRACTORY METAL LIFE TEST HEAT PIPE AND CALORIMETER

1. INTRODUCTION

In the 1980s, a group at Los Alamos National Laboratory (LANL) began to approach heat pipe life testing using science-based methods. Tests were conducted on various alkali metal heat pipes for extended periods at elevated temperature and power. Material examination and assay were often conducted before and after test. Techniques such as x-ray microanalysis, electron microprobe, x-ray fluorescence, and Auger electron spectroscopy for chemical analysis (ESCA) were used in characterization. High-temperature corrosion modes were proposed from forensic examination of failed and nonfailed heat pipes. Attempts were made to understand complex chemical equilibrium mechanisms using free-energy minimization techniques with data supplied or extrapolated from the literature. One such thermal chemical simulation of the niobium (Nb)/potassium (K) system with typical contaminant levels found no life-limiting corrosion after 7 yr of operation at 875 K.[1]

During the Space Power 100 kW (SP–100) program, work was also done at LANL to systematically test heat pipes at several temperatures and mass fluences. Sena reported results for eight K-filled Nb-1%zirconium (Zr) heat pipes that were tested for 7,000–14,000 hr in the 850–950 K range.[2] One of the pipes developed a small evaporator leak at 13,000 hr that did not affect the operation of the heat pipe and was not detected by the vacuum system monitor. Tests on the other heat pipes concluded with no apparent problems. It is believed that Zr in an Nb-1%Zr centering wire touched the quartz tube during test. A wire-quartz contact point on the failed heat pipe surface was discovered after 13,000 hr of test. Zirconium, being more stable than quartz partitioned the oxygen, causing the oxygen (O) to diffuse from the quartz to the condenser wall. Oxygen from the quartz appears to have migrated to the heat pipe and saturated the Zr in the evaporator. Conditions for these eight Nb-1%Zr/K heat pipe tests approximated a 3^2 factorial configuration with temperature and radial heat flux to the evaporator as the two controlled factors. As far as it is known, this test was one of the first attempts to develop a multifactor response surface in a heat pipe corrosion test. In this case, results from the partial two-level factorial test series could have identified first-order effects and interactions between the two factors.[3]

2. ACCELERATED LIFE TEST HEAT PIPE APPROACH

There are several ways to establish heat pipe material system life without a full-term test. One approach is to hasten life-limiting effects. This can be accomplished, for instance, by testing at higher than the proposed operating temperature and mass fluence. Acceleration testing is intuitively appealing. The impurity corrosion rate is proportional to the accumulation of nonmetallic impurities such as oxygen, silicon, and carbon in the heat pipe evaporator. As the working fluid flows into the evaporator it vaporizes, concentrating the impurities and making the corrosion rate appear dependent on mass fluence. The radial heat flux ($\dot{q}_{rad}$) applied to the evaporator is given by

$$\dot{q}_{rad} = \dot{q}\left(\pi\ d\ L_e\right)^{-1} \ , \tag{1}$$

where $\dot{q}$ is the applied evaporator power, d is the heat pipe diameter, and L_e is the length of the evaporator section. Mass flux (G) through the evaporator is a function of the radial heat flux as

$$G = \dot{q}_{rad}\left(h_{fg}\right)^{-1} \ , \tag{2}$$

where h_{fg} is the latent heat of vaporization. Mass fluence (M'') through the evaporator is then given by

$$M'' = G\,\tau \ , \tag{3}$$

where τ is the operational time. Mass fluence can easily be increased by applying power along a shortened heat pipe evaporator length. Mass fluence can be used as a metric to accelerate heat pipe life or to affordably test subscale versions of a flight unit.

Mass diffusion transfers impurities from the heat pipe structure to the working fluid. The Arrhenius equation relates impurity diffusion rates to heat pipe temperature. Test conditions can be normalized using an expression such as

$$\alpha(T) = \exp\left[(\Delta H/R)\left(T_0^{-1} - T^{-1}\right)\right] \ , \tag{4}$$

where ΔH is activation energy, R is the universal gas constant, T_0 is the design temperature, and T is the heat pipe test temperature. It can be argued that since testing at high temperature accelerates the Arrhenius-governed diffusion rate, this same acceleration applies to heat pipe life. Such simplistic views must be approached with caution. The nature of chemical reactions and their kinetics can change dramatically with absolute temperature. Conditions that apply at one temperature do not necessarily hold true for others. Without deeper understanding of the underlying reaction mechanisms, conclusions drawn from such tests may be misleading.

Another approach to heat pipe life prediction involves extrapolation of corrosion effects of a reference design from separate tests conducted over different durations. Corrosion or reaction metrics

are taken for each test specimen and the results are plotted versus time. Appropriate metrics include changes in fluid composition, wall and wick integrity as determined by three-dimensional x-ray computed tomography, species distribution, and grain boundary condition as well as noncondensable gas production measured by residual gas analysis. For the corrosion rate, a curve can be generated with a slope that normally decreases with time. The long-term corrosion rate is extrapolated from the slope near the longest test time. This method is outlined in ASTM G 68–80.[4] Conditions of an extrapolated test series can closely match those of a proposed reference. Extrapolation tests conducted at prototypic temperatures avoid possible problems with elevated temperature acceleration.

Since the extrapolation method, outlined in ASTM G 68–80, is an accepted and defendable test practice, serious consideration has been given to following its guidelines for initial screening of life test heat pipes for potential material systems. Certainly, if time and budget constraints limit the number of life heat pipe tests, extrapolation should be favored over other test methods.

One or more experiments from an extrapolation test series can be used as the center point conditions for a later multifactor star design test series. Life tests that establish corrosion trends as a function of temperature, mass fluence, and contamination level are consistent with a test-to-failure design philosophy.

A heat pipe life test matrix is proposed for a molybdenum (Mo)-44.5% rhenium (Re)/sodium (Na) material combination as a function of operating temperature and mass fluence. Impurity levels in the heat pipe wall and working fluid are to be controlled at constant values. A series of accelerated life heat pipes permits compression of life-limiting mechanisms from the mission duration to a period consistent with the schedule of a flight program. The target of the proposed test program is to compress 12-yr operational life in about 3 yr of actual operation. Condenser calorimetry using forced convection of a cooling fluid is necessary to achieve the target power density and to provide realistic boundary conditions of a flight system.

Life test interpretation will require the initiation of a science-based program to pursue an understanding of mechanisms relevant to heat pipe life. This effort should provide insight into the effects that will be observed during periodic removal of life test heat pipes for nondestructive evaluation. Destructive evaluation will be planned for preselected heat pipes and for heat pipes that show early evidence of corrosion.

2.1 Proposed Test Matrix

The proposed test matrix conserves available material, eases fabrication, provides relevant data, and permits the use of compact test fixtures. A series of ≈16 short heat pipes with thick-walled condensers will be constructed. These short heat pipes will have similar condenser-to-evaporator area ratios relative to the reference design. The boiling limit for the baseline design is invariant with condenser length, so the short heat pipes should perform identically to the longer baseline versions.

A series of accelerated life heat pipes permits extrapolation of corrosion effects of a reference design from separate tests conducted over different durations. Destructive examination of the first life test heat pipe can begin within 6 mo of test initiation. Testing a series of heat pipes allows identification of random manufacturing and processing defects.

Tables 1 and 2 show a proposed test series consisting of ≈16 short heat pipes (ASTM G 68–80 G-series and Fisher multifactor star F-series). One or more experiments from an extrapolation test series is used to cross-correlate fluence conditions with a Fisher multifactor star design test series conducted at various temperatures and fluences.[3] Such life tests can establish and isolate corrosion trends as a function of temperature and mass fluence. Figure 1 plots the fluence and temperature relations for the combined test series.

Table 1. Option A life tests, Fisher series (F-series).

Heat Pipe	Wall/Wick Material/ Fluid	L_c/L_e	D_i (cm)	T (K)	$\alpha(T)$	$\dot{q}$ (W)	$\dot{Q}_{rad}$ (W/cm^2)	G (kg/cm^2–s)	t (hr)	M'' (kg/cm^2)
Design	Mo-Re/Na	2	1.41	1,250	1.00	5,752	22	0.059	105,120	2,233
F(–4)	**Mo-Re/Na**	**3**	**1.41**	**1,273**	**1.30**	**5,000**	**226**	**0.599**	**26,280**	**5,669**
F(–3)	Mo-Re/Na	3	1.41	1,273	1.30	1,000	45	0.120	26,280	1,134
F(–2)	**Mo-Re/Na**	**3**	**1.41**	**1,373**	**3.74**	**3,000**	**136**	**0.368**	**26,280**	**3,483**
F(–1)	Mo-Re/Na	3	1.41	1,173	0.38	3,000	136	0.351	26,280	3,321
F(0)	**Mo-Re/Na**	**3**	**1.41**	**1,273**	**1.30**	**3,000**	**136**	**0.360**	**26,280**	**3,401**
F(1)	Mo-Re/Na	3	1.41	1,223	0.72	2,000	90	0.237	26,280	2,241
F(2)	Mo-Re/Na	3	1.41	1,223	0.72	4,000	181	0.474	26,280	4,481
F(3)	Mo-Re/Na	3	1.41	1,323	2.25	2,000	90	0.243	26,280	2,295
F(4)	**Mo-Re/Na**	**3**	**1.41**	**1,323**	**2.25**	**4,000**	**181**	**0.485**	**26,280**	**4,589**

Table 2. Option A life tests, G68–80 series (G-series).

Heat Pipe	Wall/Wick Material/ Fluid	L_c/L_e	D_i (cm)	T (K)	$\alpha(T)$	$\dot{q}$ (W)	$\dot{Q}_{rad}$ (W/cm^2)	G (kg/cm^2–s)	t (hr)	M'' (kg/cm^2)
Design	Mo-Re/Na	2	1.41	1,250	1.0	5,752	22	0.059	105,120	2,233
G–1	Mo-Re/Na	3	1.41	1,273	1.3	3,000	136	0.36	4,380	567
G–2	Mo-Re/Na	3	1.41	1,273	1.3	3,000	136	0.36	8,760	1,134
G–3	Mo-Re/Na	3	1.41	1,273	1.3	3,000	136	0.36	13,140	1,701
G–4	Mo-Re/Na	3	1.41	1,273	1.3	3,000	136	0.36	17,520	2,267
G–5	Mo-Re/Na	3	1.41	1,273	1.3	3,000	136	0.36	21,900	2,834
G–6	Mo-Re/Na	3	1.41	1,273	1.3	3,000	136	0.36	26,280	3,401
G–7	Mo-Re/Na	3	1.41	1,273	1.3	3,000	136	0.36	30,660	3,968

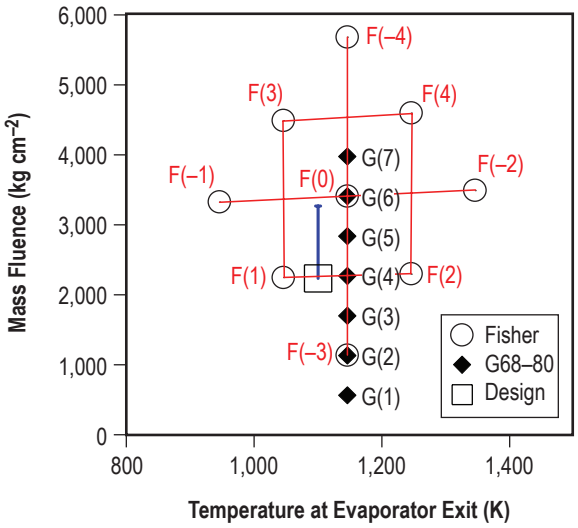

Figure 1. Life test matrix assuming a maximum 1-μm nucleation site radius for F- and G-test series.

These test series attempt to systematically correlate heat pipe corrosion behavior at several temperatures and mass fluences. Conditions for the Fisher test (table 1) represent a two-factor ($2^2+2\times2+1$) central composite configuration, with temperature and radial heat flux to the evaporator as the two controlled factors. Assuming corrosion is measurable, forensics are conducted and a multifactor response surface can be developed from this heat pipe corrosion test. In this case, results from the partial two-level factorial test series can identify first-order effects and interactions between the two factors, and can estimate second-order curvature effects in the data.[3]

It must be emphasized that the target radial heat fluxes in tables 1 and 2 are quite high, up to 10× that of a flight heat pipe design. Every attempt will be made to approach these target values by controlling surface roughness and noncondensable gas in the heat pipe. These measures should inhibit boiling. An initial test will include a performance test of the first pipe to show what radial heat fluxes and temperatures can be achieved. It may be necessary at this point to reduce the operating power by some factor to avoid a performance limit. Such reductions will necessarily lengthen the test time required to achieve a given mass fluence (app. A).

3. HEAT PIPE DESCRIPTION

There are several options that will allow a quick start to life tests of a refractory metal heat pipe. In the near term, materials availability will dictate the options and schedule of any heat pipe performance test. Unfortunately, a supply of 400-mesh Mo-41%Re cloth produced in 1982 for the space power advanced reactor (SPAR) reactor project has been depleted. A few remnants of this cloth remain, mostly in small pieces suited only for short wicks. However, other materials exist that could make suitable refractory metal pipes. For our immediate purposes, a heat pipe will be made at Marshall Space Flight Center (MSFC) from readily available refractory metals, such as Mo-44.5%Re, and filled with distilled Na stock produced by LANL. This Na stock was used to support a previous test program.[5,6]

A limited supply of fine wire mesh of Mo-5%Re is available to the program, courtesy of David Glass at NASA Langley Research Center (R. Reid, Private Communication, June 2004).There is enough 400-mesh Mo-5%Re wire cloth on hand to make several heat pipe wicks. Forming wicks from brittle Mo-5%Re is not easy. Several techniques have been developed to produce satisfactory porous tubes from this material. Making annular or arterial wicks from Mo-5%Re now appears possible and could be completed in approximately 16–22 wk. Wick fabrication will be easier once Mo-41%Re or Mo-44.5%Re screen material becomes available that has room temperature ductility after recrystallization. Rhenium has low solubility to nonmetallic impurities and alloys with higher Re content should exhibit similar or superior corrosion resistance compared to Mo-5%Re.

Closure plugs can be attached to long Mo porous annular or artery tubes with Zr or palladium-cobalt brazes. Unfortunately, such brazes induce recrystallization and room temperature brittleness. Brittle wicks are prone to shipping damage; therefore, they were fabricated and shipped in the ductile condition. Closure plugs will be attached to the wick body at room temperature by mechanical crimping (no brazing is planned for the test units). The manufacturer will clean the wick chemically and by firing in a dry-hydrogen furnace (hydrogen dewpoint of less than –77 °C) at a temperature that avoids recrystallization.

3.1 Heat Pipe Sizing and Performance

Table 3 shows an accelerated life heat pipe design. The heat pipe will be operated horizontally to mimic the neutral gravity conditions of space. An annular gap wick is selected for the life heat pipe because it is simple, robust, and performs well under ground test. Properly designed short heat pipes tested at relevant temperatures and mass fluence are made geometrically similar (L_c/L_e) to the flight heat pipes. Such similarity in heat pipe designs form the basis for virtually all long-term heat pipe corrosion testing to date.[7] The length of the heated region is 7.5 cm and the cooled region is 25 cm, reflecting approximate geometric similitude with a flight heat pipe. For the case of an annular gap wick, the channel dimension (A) is the concentric distance from the wick's outer and the pipe's inner surfaces. The value for A is chosen to optimize life test heat pipe performance at the reference temperature. A wick's maximum pore radius (r) most directly influences its capillary pumping capacity. A 45-μm effective pore radius has been assumed

Table 3. Life heat pipe design and conditions (neutral gravity).

Scale	Value
Wick shape	Annular gap
Evaporator length	$L_e = 0.075$ m
Adiabatic length	$L_a = \approx 0$ m
Condenser length	$L_c = 0.25$ m
Container inside radius	$R = 0.705$ cm
Channel dimension	$A = \approx 0.056$ cm
Wick pore radius	$r = 35$ μm nominal
Nucleation site radius	$n = \approx 1$ μm
Solid thermal conductivity	$k = 60$ W·m^{-1}K^{-1}
Working fluid	$f =$ Na
Temperature	$T =$ range 1,173 to 1,373 K
Design heat pipe power	$Q = 3$ kW

for the life heat pipe design. This value reflects bubble-point measurements taken with highly compressed 400-mesh screen wicks manufactured by Advanced Methods and Materials from February 2002 to the present. Radial power densities applied to the evaporator, operating temperature, and nucleation site radii are key variables in boiling limit calculations. Nucleation site radii of 1–3 μm are typical for many engineering surfaces and will be assumed for the life heat pipe. For the life test heat pipes designed here, an attempt was made to produce surfaces with ≈1-μm nucleation site radius. Section 3.1.1 discusses the nucleation site radius sensitivity.

3.1.1 Performance Envelope

A steady state heat pipe analysis computer program, HTPIPE, predicts heat pipe performance limits as a function of evaporator exit temperature and calculates axial temperature and pressure profiles.[8] The computational routines in HTPIPE have been validated on numerous occasions using alkali metal heat pipe test data.[9,10] The HTPIPE code uses a pressure balance in the flow direction for both the liquid and vapor to define the wicking limit or the viscous limit, depending upon whether the wick pumping capacity or the stagnation pressure defines the limiting available pressure. Other heat pipe performance limits calculated by the program are the sonic limit, the entrainment limit, and the boiling limit. Figure 2 superimposes the proposed life test matrix on a performance map calculated with HTPIPE. The heavy red line shows the boiling limit assuming a 1-μm nucleation site radius. The lighter line shows the boiling limit for a 3-μm radius. This plot emphasizes the importance of producing heat pipes with honed heated regions. Failure to achieve a high boiling limit will require that certain set points be rescoped or the possible shifting of the entire test matrix.

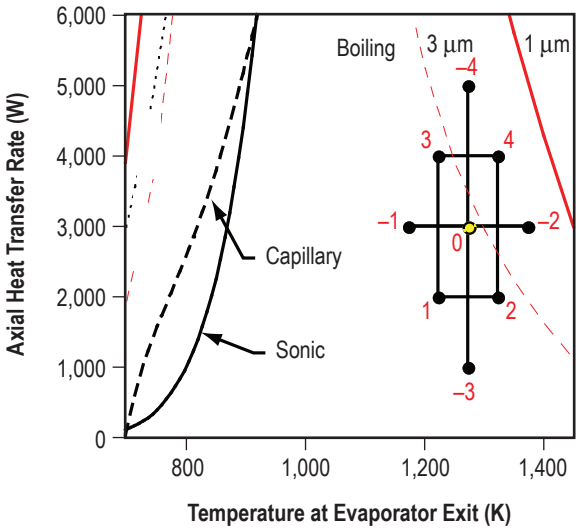

Figure 2. Proposed life test matrix compared to operating limits at two-nucleation site radii.

3.1.2 Wick Assembly Description

During cleaning, the wire cloth material will be vacuum fired and/or hydrogen heat treated, with the hydrogen dewpoint less than –77 °C, the nature of which will be discussed with and approved by MSFC. During these heat treatments the material will be kept within the following time-temperature envelope:

$$\tau_{max}(T) < \tau_o \, f_R \exp\left[\left(-\Delta E/R\right)\left(1/T_o - 1/T\right)\right] , \tag{5}$$

where f_R is the material fraction recrystallized, τ_o is the recrystallization time at T_o (1 hr), R is the universal gas constant, and ΔE is the work function. One-hour recrystallization times for pure Mo and activation energy data, shown in figure 3, is used to prevent recrystallization of the Mo-5%Re material.[11,12] For multiple heat-treat steps at different temperatures, the relation

$$\sum_{i=1}^{N}\left[\tau_i\left(T_i\right)/\tau_{max}\left(T_i\right)\right] < 1 , \tag{6}$$

applies where τ_i is the time at temperature T_i for a given step and τ_{max} is the maximum time at temperature for a given processing step. Figure 3 shows the not-to-exceed time proposed for wick material as a function of temperature at various percent recrystallization.

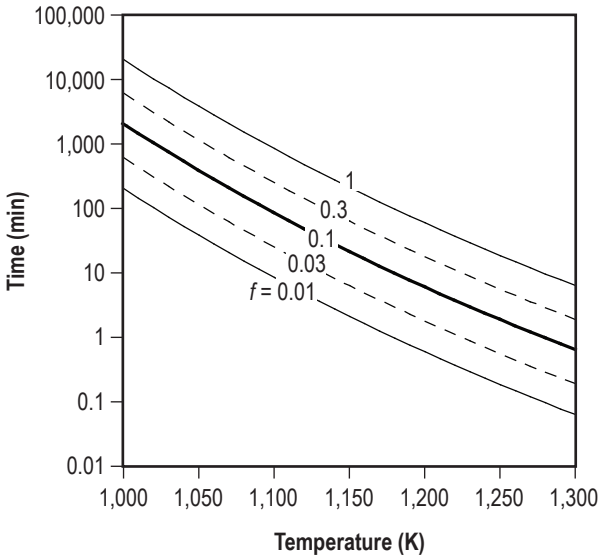

Figure 3. Not-to-exceed time-temperature relation for Mo-5%Re material.

3.1.3 Getter Pack Description

Corrosion in high-temperature heat pipes can be inhibited with nonsoluble getters that trap impurities during operation. Such getters can be distributed to allow wetting by the condensate and can be part of the heat pipe container or placed in packs. Assuming a well-distributed getter, the potential for corrosion should relate to the total impurity concentration compared with the total stoichiometric impurity capacity in the getter and container as follows:

$$\Sigma \equiv (\text{impurity capacity of heat pipe getter}) \times (\text{impurity content of heat pipe})^{-1} \quad . \tag{7}$$

Getter material in high-temperature heat pipes should be hyperstoichiometric, compared with nonmetallic impurities from all sources. As a rule of thumb, the impurity capacity to impurity ratio should be at least several times stoichiometric proportions, shown as follows:

$$m_{\mathrm{Zr}} = \rho_{\mathrm{Zr}} V_{disks} \quad , \tag{8}$$

$$m^{o}_{\mathrm{Zr}} = m_{\mathrm{Mo}} MW_{\mathrm{Zr}} \left[\frac{C^{\mathrm{Mo}}_{\mathrm{O}}}{MW_{\mathrm{O}}} + \frac{C^{\mathrm{Mo}}_{\mathrm{N}}}{MW_{\mathrm{N}}} + \frac{C^{\mathrm{Mo}}_{\mathrm{C}}}{MW_{\mathrm{C}}} + \frac{C^{\mathrm{Mo}}_{\mathrm{Si}}}{MW_{\mathrm{Si}}} + \frac{C^{\mathrm{Mo}}_{\mathrm{B}}}{MW_{\mathrm{B}}} \right] + m_{\mathrm{Na}} MW_{\mathrm{Zr}} \left[\frac{C^{\mathrm{Na}}_{\mathrm{O}}}{MW_{\mathrm{O}}} + \frac{C^{\mathrm{Na}}_{\mathrm{N}}}{MW_{\mathrm{N}}} + \frac{C^{\mathrm{Na}}_{\mathrm{C}}}{MW_{\mathrm{C}}} \right] \quad , \tag{9}$$

and

$$\Sigma = \frac{m_{\mathrm{Zr}}}{m^{o}_{\mathrm{Zr}}} \quad . \tag{10}$$

Using these relations, a getter pack consisting of 1.5 g of Zr foil provides a factor of 6.4 margin for a 0.3-kg tube with 20 ppm oxygen (O), 20 ppm carbon (C), 30 ppm nitrogen (N), 30 ppm silicon (Si), and

20 ppm boron (B) filled with 10 g of Na containing 10 ppm oxygen. Hafnium and vanadium (V) getters can also be used as in Na heat pipes. Titanium is appropriate at a slightly lower temperature.

3.1.4 Heat Pipe Material/Envelope

The heat pipe envelope will be manufactured from an Mo/Re-based alloy with the two leading candidates having blends of 44.5% and 47.5% Re (by weight) to improve low-temperature ductility, supplied in a recrystallized state annealed at 1,775 K. The components (tubing and rod stock) will be drawn/swaged (or another acceptable technique) from raw material formed by either powder metallurgy or arc cast techniques. There have been a series of discussions between Ross Luther (Bechtel Bettis) and MSFC personnel regarding composition, material forming, chemical composition, and other metallurgical considerations pertinent to the process. Details are listed in the specification statement submitted for procurement, as provided in section 3.3. Current vendor estimates indicate delivery time of the required Mo-Re alloy components is 16–20 wk after receipt of order (ARO).

A key element of these specifications is the chemical composition of the bulk materials used in fabricating hardware components. Test methods to verify the composition can include a LECO Corporation elemental analyzer and glow discharge mass spectroscopy (GDMS) to examine both bulk and surface compositions. A list of the maximum and targeted impurity concentrations is provided in table 4.

Table 4. Impurity chemical composition (acceptable) final heat Mo-Re alloy material (powder metallurgy).

Element	Maximum (wppm)	Target (wppm)
O	20	<10
C	20	<10
N	30	<3
H	25	<1
Ca	7	<5
Fe	75	<20
Ni	50	<20
W	300	<100
Si	30	<10
Mg	10	<10
Mn	4	<4
Co	30	<30
Sn	20	<20
B	20	<10

A significant area of concern involves the electron beam (EB) welding process for the Mo-Re alloy that will be employed to assemble the heat pipe units. Based on information gathered from Ross Luther (Bechtel Bettis), the oxygen and carbon content in the alloy are critical to the success of the welding process. Luther recommends that the maximum oxygen and carbon content concentration should be set to 20 ppm for powder metallurgy material, and for arc cast material, the maximum oxygen concentration should be set to 20 ppm with a carbon range of 40 to 80 ppm. During further discussions, it has become apparent that some welding tests of appropriate sample coupon materials should be performed to investigate

and document the operations (examine weld ductility, shock resistance, and porosity). Testing could potentially be performed at MSFC, LANL, and subcontractor sites such as Advanced Methods and Materials. These tests can help resolve any critical surface preparation and welding parameters. Cleaning of material can consist of chemical cleaning and vacuum/hydrogen firing. A proposed general chemical cleaning procedure for all Mo-Re parts includes the following:

(1) Wash the piece in PF® solvent, an R113 substitute, until all signs of grease have been removed.

(2) Soak the piece for 1–2 min in one part by volume HCl and one part by volume deionized water (target of 10 MΩ cm or better) to remove residual iron surface impurities.

(3) Soak the piece in caustic cleaning solution consisting of 11 parts by volume deionized water (target of 10 MΩ cm or better), 1 part by volume NaOH, and 1 part by volume H_2O_2 for 5 min. Remove piece from caustic bath. Replenish or replace solution as required.

(4) Wash the part in hot deionized water (target of 10 MΩ cm or better) for at least 5 min.

(5) Repeat steps (3) and (4) three times.

(6) Rinse piece in ethanol inside an ultrasonic cleaner for 5 min.

(7) Vacuum-fire or hydrogen-fire part as appropriate, not exceeding specific time-temperature requirements associated with recrystallization of low-Re content Mo materials. Hydrogen used in firing will have a dewpoint of less than –77 °C.

The heat pipe wick structure will be produced from existing Mo-5%Re mesh material, a 400 × 400 weave with a wire diameter of 0.001 in. This material is in the uncrystallized condition, so it is sufficiently ductile for the wick-forming process. During subsequent vendor processing, the cumulative time-at-temperature must be monitored for all expected heat treatments to ensure that the material has not significantly recrystallized, becoming brittle at room temperature and increasing the chance of damage during shipping and handling. A proposed time-temperature relationship is provided in table 5. For multiple heat-treat steps at different temperatures, the relation given in equation (6) will apply.

Table 5. Time-temperature relationship for Mo-5%Re material.

Temperature (K)	Maximum Time at Temperature (min)
T_i	$\tau_{max}(T_i)$
1,000	2,049
1,010	1,448.9
1,020	1,031.6
1,030	739.3
1,040	533.2
1,050	387.0
1,060	282.6
1,070	207.6
1,080	153.3
1,090	113.9
1,100	85.1
1,110	63.9
1,120	48.2
1,130	36.5
1,140	27.9
1,150	21.3
1,160	16.4
1,170	12.7
1,180	9.8
1,190	7.7
1,200	6.0
1,210	4.7
1,220	3.7
1,230	2.9
1,240	2.3
1,250	1.9
1,260	1.5
1,270	1.2
1,280	1.0
1,290	0.8
1,300	0.6

3.2 Heat Pipe Engineering Drawings

Required heat pipe performance specifications were translated into an engineering design and drawing generated for the wick structure, getter pack, and envelope. A computer-aided design (CAD) software package called Autodesk Inventor Series Version 8 was used to create the engineering drawing set. Three drawings were created to describe the complete heat pipe unit. Figure 4 shows the wick assembly with the evaporator end plug that provides sealing of the capillary channel. The current approach is to mechanically crimp the end plug to the wick for the final test units with a vendor-developed process that eliminates a high-temperature braze resulting in a brittle wick assembly. The sealing integrity of this crimp and of the wick material will be checked during bubble-point testing of the assembly.

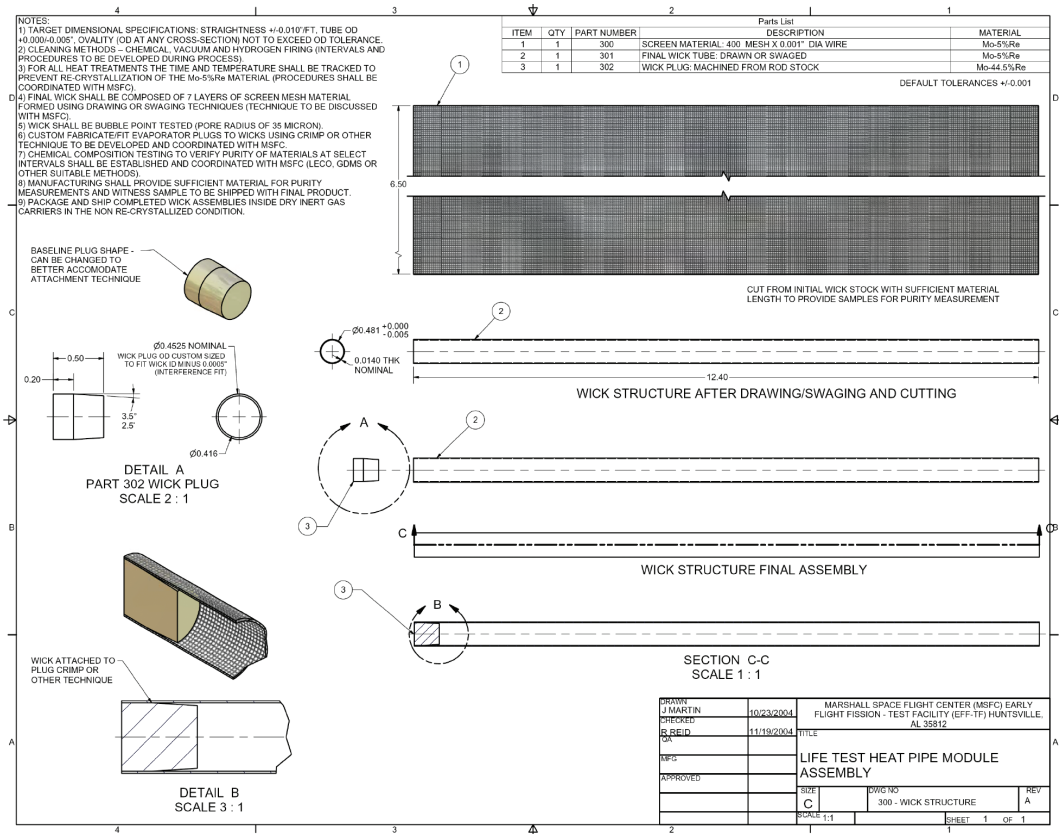

Figure 4. Wick assembly engineering drawing.

Figure 5 shows details of the getter unit and its assembly. The getter is an integral part of the heat pipe evaporator end plug assembly. The getter is comprised of 31-Zr disks stacked and held in place with a tack-welded cover plate and support rod. Figure 6 shows details of the heat pipe envelope components and final assembly of the unit. Electron beam welding is used exclusively during assembly of the hardware. This information, with specifications, is contained in the heat pipe procurement solicitation provided in section 3.3.

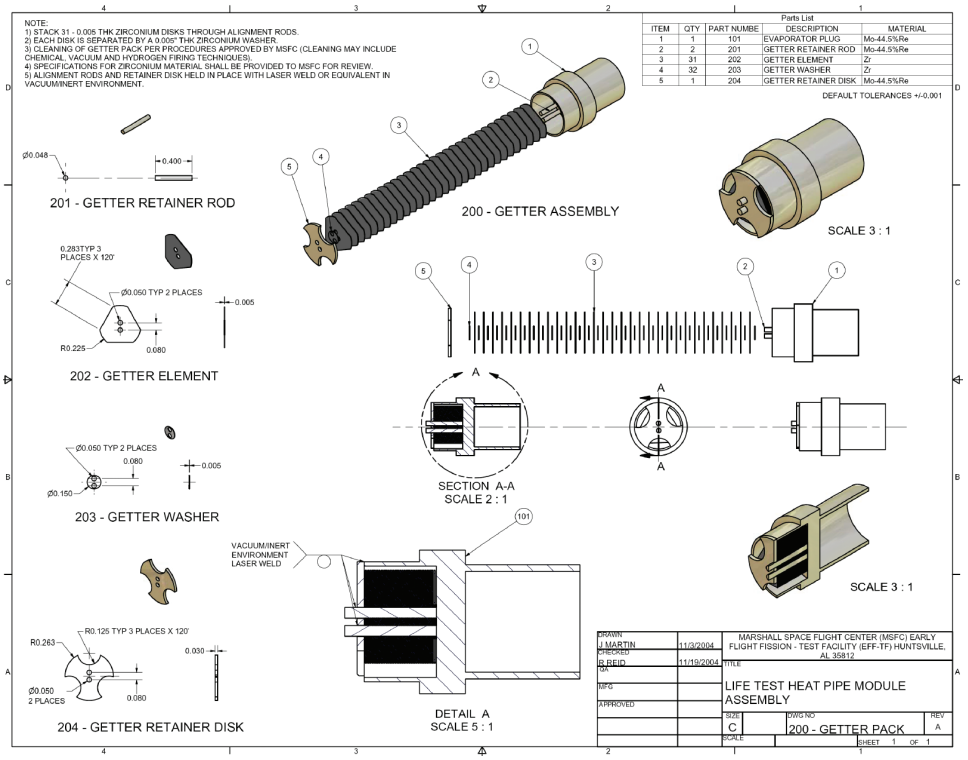

Figure 5. Getter pack design and assembly engineering drawing.

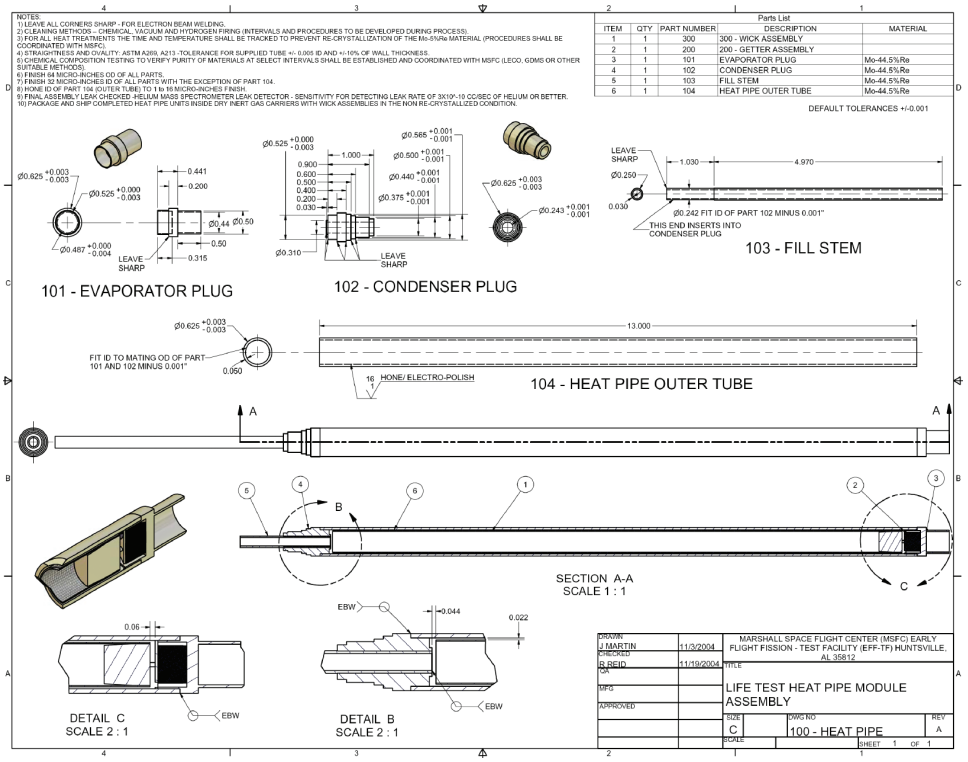

Figure 6. Heat pipe envelope and assembly engineering drawing.

3.3 Heat Pipe Procurement Specifications

Procurement specifications have been generated to cover fabrication of the heat pipe units. These procurements will be issued by MSFC using full and open competition. The final evaluation of vendor quotes will be based on the lowest cost, technically acceptable approach. Three procurement specifications were developed covering each of the primary requirement areas as follows:

(1) Wick assembly fabrication for heat pipe units using existing Mo-5%Re 400×400 mesh material and an Mo-Re evaporator plug from the material type selected for the heat pipe envelope. Wicks will be fabricated by drawing, or another acceptable technique, to produce average 35-μm pores. The completed wicks will have documentation that details the process and the results of cleaning, bubble-point testing, and material chemical composition testing. Appendix B contains the detailed wick assembly procurement specification. The current vendor estimate is 16–22 wk for delivery.

(2) Basic materials for the heat pipe envelope are composed of an Mo-Re alloy with a blend of 44.5%Re by weight (44.5%Re is a Rhenium Alloys Inc. specific material that has no sigma phase-brittle intermetallic) or 47.5%Re by weight. The material quoted can be formed by either powder metallurgy or arc cast techniques. The required component shapes include tube, rod, and plate stock of various diameter and lengths that have material data sheets detailing chemical composition, ductility, grain size, etc. Appendix C contains the detailed material procurement specification. The current vendor estimate is 16–20 wk for delivery.

(3) Heat pipe fabrication and assembly use the tube, rod, and plate stock with wick assemblies detailed under the previous two specifications. This will include machining of component pieces and getter pack, followed by EB welding to assemble the units. Machining and assembly processes will be documented and documentation will be provided, as necessary, for material chemical composition, welding technique, leak check, ductility, etc. Appendix D contains the detailed heat pipe fabrication procurement specification. The current vendor estimate is 16–20 wk for delivery.

These specifications do not include the engineering requirements needed for final closeout of the heat pipe units after Na loading at MSFC. These requirements will be developed once the details pertaining to the heat pipe final mounting method and Na-sampling technique have been determined.

4. CALORIMETER UNIT

A calorimetry system is required to extract heat from the condenser section of the heat pipe and transfer it to a media that can be measured to quantify the power being removed from the heat pipe. There are two primary techniques for removing energy from the heat pipe condenser section: (1) Pure radiation to the surroundings and (2) conductive/forced convective coupling to a working fluid.[13,14] In the case of radiation calorimetry, the heat transfer is controlled by the Stefan-Boltzmann relationship, $\dot{Q}=\varepsilon\sigma A(T_h^4-T_a^4)$, where $\dot{Q}$ is the total transferred power, ε is the total hemispherical emissivity, σ is the Boltzmann constant, A is the radiation surface area, T_h is the radiating surface temperature, and T_a is the ambient temperature. This is the simplest configuration, requiring only that the surrounding chamber be kept cool and a method employed to monitor the surface temperature of the heat pipe condenser. Radiation heat transfer can be high at the expected heat pipe test temperatures; however, for Mo-based alloys, the total hemispherical emissivity of the surface is typically very low ($\approx$0.15), resulting in poor overall heat transfer, with an approximate range of 200–300 W at proposed test temperatures. The second calorimetric technique relies on a conductive/forced convective combination to remove energy from the heat pipe condenser. This system is more complex, as it requires additional hardware and a working fluid to absorb and transport the energy. The typical approach is a two-step process making use of a static gas conduction gap between the heat pipe condenser section and the inner wall of the calorimeter, followed by a flowing fluid contained in the calorimeter annulus. The heat transfer rate across the static gas gap is governed by a combination of the radiation heat transfer rate, the Stefan-Boltzmann relationship, and the Fourier heat transfer rate relation, $\dot{Q}=kA(T_{hp}-T_{cw})/l$, where k is the thermal conductivity, T_{hp} is the heat pipe temperature, T_{cw} is the calorimeter wall temperature, and l is the gap width with typical gap widths ranging from 0.02 to 0.10 in, depending on the magnitude of energy to be transferred. The gas gap can either be sealed, if the calorimeter system is physically attached to the heat pipe condenser with a seal weld, or open, if the heat pipe and calorimeter are contained in a test chamber with the desired gas constituents. The calorimeter coolant (gas, water, or other fluid contained in the flow annulus) absorbs and transports the energy to an external heat exchanger where it is removed. Heat transfer into the calorimeter fluid is governed by the convective heat transfer rates, $\dot{Q}=hA(T_{cw}-T_f)$, where h is the convective heat transfer coefficient, T_f is the flow annulus fluid temperature, and the difference $(T_{cw}-T_f)$ is commonly evaluated as the log mean temperature difference (ΔT_{LM}).

In general, sealing the static gas gap to the heat pipe condenser results in a more complex system (calorimeter is designed and fabricated as part of the heat pipe condenser) when compared to the noncontact approach with a gas-flooded test chamber. This complexity is compounded when fabricating heat pipe units from refractory alloys, requiring the calorimeter to be fabricated from the same material and limiting the types of coolant that can be used to maintain compatibility. For Mo-Re, this becomes a very expensive endeavor. In addition, there is little experience in fabricating and welding the structural shapes and fittings required to make an Mo-Re alloy calorimeter assembly, making it a high-risk undertaking. In contrast, the noncontact calorimeter can be manufactured from more common materials, such as stainless steel or copper, and supported so the heat pipe and inner diameter of the calorimeter remain nearly concentric. The final design will incorporate provisions, such as bumpers or foils, to prevent the heat pipe and calorimeter from touching. Such isolation also avoids uncontrolled mass-transfer conditions believed to have been experienced in previous tests.[2]

Selection of the coolant flow system to be used in the calorimeter flow annulus can again be addressed based on complexity. The most complex arrangement would make use of a gas flow system (helium (He) or He/argon (Ar) mixture) requiring a single, high-power gas compressor, or a series of lower power units providing sufficient system lift (order of several psia) to account for flow pressure drop with a plumbing system capable of operating in the 50–150 psia range. These components are available commercially; however, they are expensive and often require lead times or modifications. A simpler calorimeter cooling technique would consist of a pressurized water loop operating at 50–75 psia (to increase the water boiling point) with a pump providing up to 20 psi of lift (compensating for system losses). Components for this system are commercially available and are typically off-the-shelf items. The downside to a water-based system is that there is a risk associated with the potential leakage of water into the test chamber and its potentially catastrophic interaction with refractory metals at high temperatures. To minimize this potential, all water feed lines should be welded/brazed and mechanical connections should be avoided.

Based on these considerations, the selected approach was a noncontact calorimeter design using water as the cooling fluid and He/He-Ar gas mixture as the test chamber gas species. The test chamber gas pressure would be maintained in the 50–100 torr range to minimize convective losses while providing margin above the potential Paschen minimum pressure for ionization.[15] The heat pipe power source will be a radio frequency (RF) inductive coil that will operate at 100–450 kHz and up to 500 V.

4.1 Water Calorimeter Description

The selected baseline calorimeter was a smooth tube laminar design lending itself to simple performance estimates supporting initial concept feasibility assessment. The initial configuration layout is illustrated in figure 7. It is comprised of three concentric tube shells referred to as: (1) Channel tube, separating the gas gap and water film annulus; (2) shell tube, separating the water film annulus and water return annulus; and (3) cover tube, separating the water return annulus and test chamber environment. The inlet end of the calorimeter makes use of a double wall to create an inlet plenum to distribute water to the film annulus. The cooling water passes along this annulus to the end of the calorimeter, where it passes through a series of holes/slots into the return path annulus.

The typical film flow annulus width is 0.01–0.02 in and the return path is sized at 0.125-in width; the majority of the system pressure drop is expected in the film flow annulus. The calorimeter would be an all-welded construction to minimize the potential for leakage. The overall length of the calorimeter body could range from 11 to 13 in, depending on the final heat pipe attachment technique.

Currently, the proposed method for holding the calorimeter and heat pipe unit uses a concentric support/mounting bracket, as illustrated in figure 8. The mounting bracket uses a radial slot to capture and clamp the calorimeter, while the heat pipe is held in the central bore clamp. Both the calorimeter and heat pipe are cantilevered from the mounting bracket, minimizing heat pipe contact and restricting contact location to the coolest heat pipe element—the closeout stem. It is believed that the proposed mounting technique, that holds radial dimensional tolerance on a single-mounting element, would be the easiest to fabricate and would result in the most accurate approach to align both the calorimeter and heat pipe. A Mo or Mo-Re bumper foil may still be required, or desired, at the ends of the calorimeter to prevent unanticipated touching of the two components. If required, additional support can be provided at the very end of the evaporator plug tube extension which is 0.5 in long (0.5 in diameter by 0.03 in wall material).

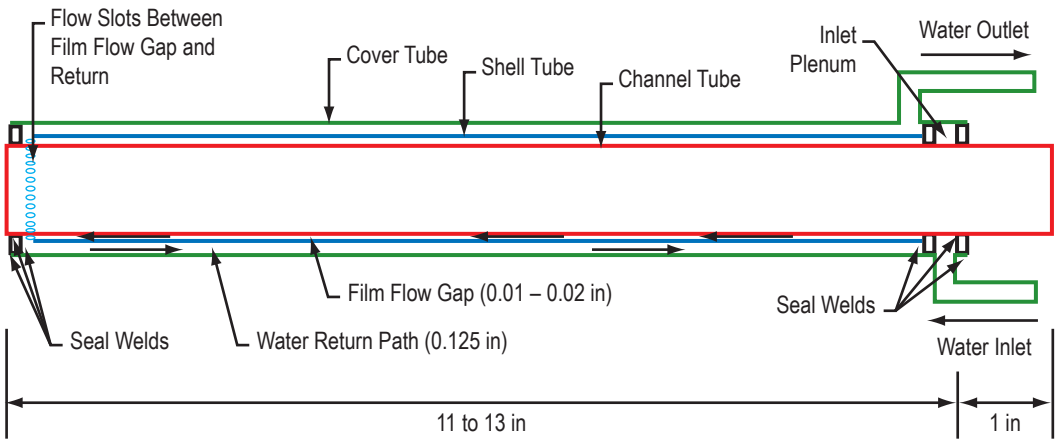

Figure 7. Calorimeter conceptual design.

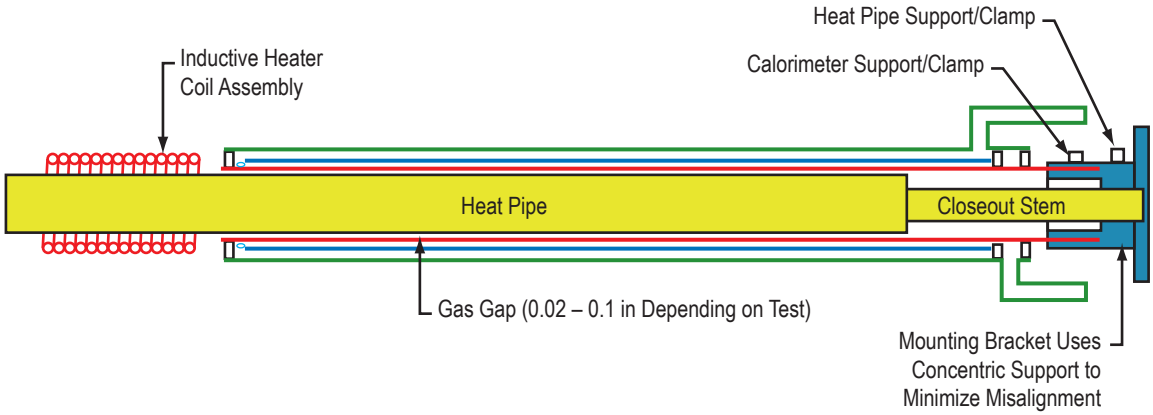

Figure 8. Conceptual heat pipe/calorimeter mounting setup.

Material selection for the calorimeter includes either 316 stainless steel or copper alloy. Stainless steel is easy to work with during fabrication and assembly (significant shop and laboratory experience), although the tight tolerance (±0.002 in on dimensions of 0.01 in over the full length) would prove challenging. On the other hand, stainless steel has several problem areas. First, it is available as tubing in a set division of diameters and wall thickness; therefore, any design would have to be tailored to the available sizes and then drawn or machined as necessary, potentially increasing tolerance variability. Second, it has a low-thermal conductivity (≈15 W/m-K) resulting in an appreciable temperature gradient across its thickness necessitating higher material surface temperatures to achieve required heat transfer rates into the calorimeter; however, the gas gap is still the limiting thermal resistance.

Copper is a better alternative for the calorimeter construction. The copper alloy C122 deoxidized high-residual phosphorus, commonly used in heat transfer tubing and heat exchangers, is 99.9% copper and 0.02% phosphorus and has a thermal conductivity of 339 W/m-K at 300 K (value provided by Wolverine Tube, Inc.). This is a factor of 20 better than stainless steel and essentially eliminates any material thermal

gradient by placing the hot-side material temperature at the coolant interface where it provides the most benefit. Discussions with Wolverine Tube, Inc. indicate that with their precision tubing process, their dies can be adjusted to draw tubing to virtually any diameter from 0.1 to 2 in, with a tolerance of 0.001–0.002 in. In this fabrication process, the tube wall thickness would be held constant for all diameters at one of several available wall thicknesses, the most attractive for our purposes being 0.058 in. This simplifies design, fabrication, assembly, and performance calculation processes since minimal machining will be required, introducing less variability in the final product.

Cost estimates for the calorimeter will be solicited once the final engineering drawings are completed. The initial design is shown in figures 9 and 10. The current material baseline for the calorimeter design is copper C122, as suggested by Wolverine Tube, Inc. The following sections provide a detailed summary of the calorimeter film flow gap sizing and its sensitivity to parameters such as coolant flow rate, pressure drop, calorimeter channel wall temperature, and film flow temperature rise (outlet-inlet).

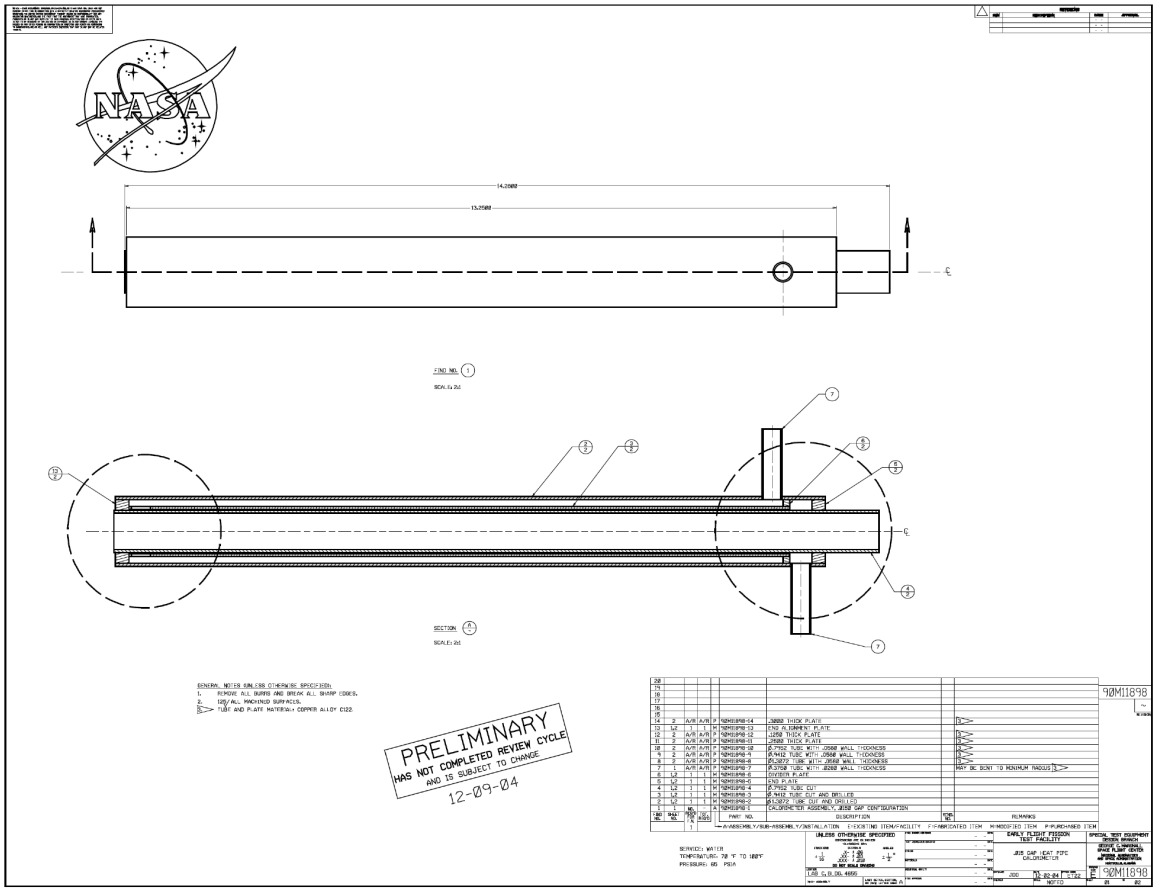

Figure 9. Initial calorimeter concept engineering design layout.

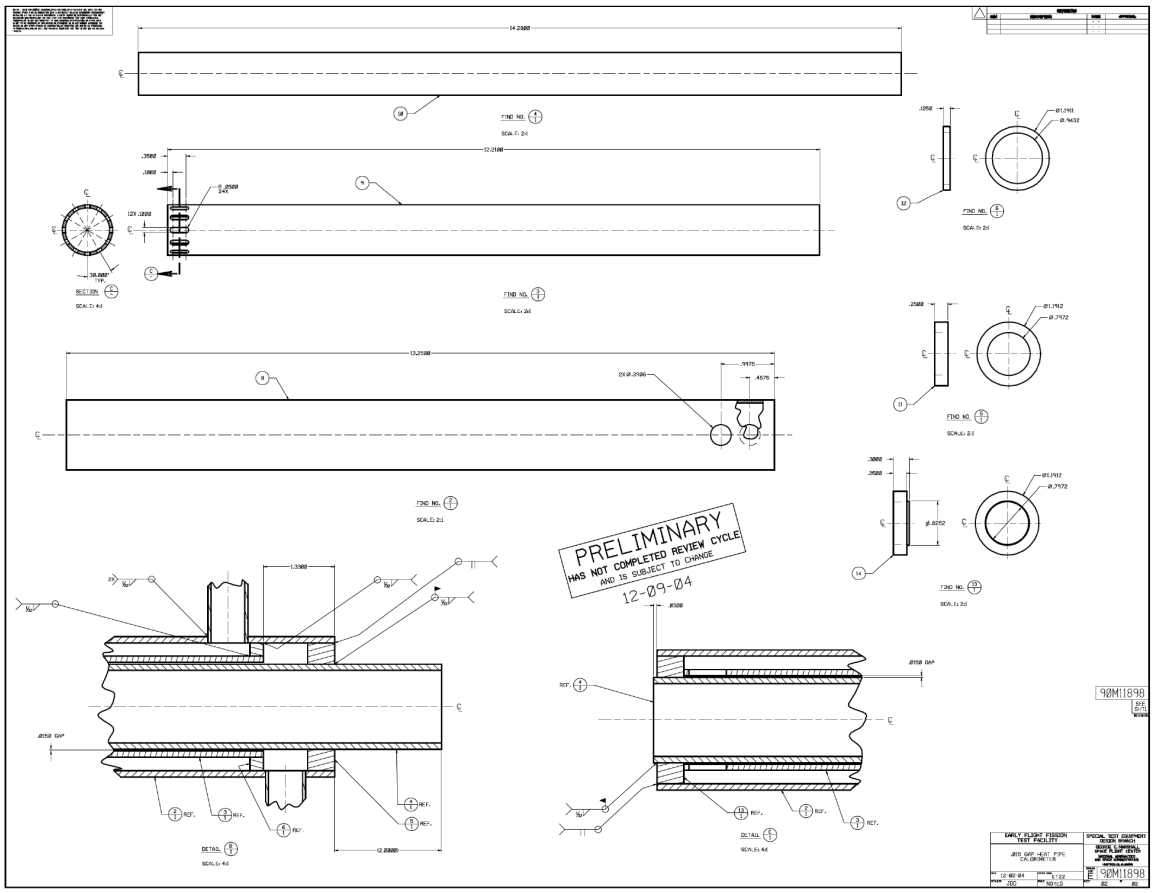

Figure 10. Initial calorimeter concept engineering design parts detail.

4.2 Heat Pipe/Calorimeter Performance

Determination of the size and performance of the calorimeter system to meet the requirements for each heat pipe test case was accomplished using a simple spreadsheet-based model. A more detailed flow network model is also currently being built using the generalized fluid system simulation program (GFSSP); however, it was not completed in time to support the initial design work described in this Technical Publication (TP). The GFSSP model will be used later in the program to reassess the current findings and to provide pretest performance predictions.

The spreadsheet model assumes radial heat flow (heat pipe wall to calorimeter) and assumes average properties across the length of the assembly. This is a reasonable approach for steady state operation and provides an established set of operating test conditions. The selection of a pressurized water calorimeter, copper construction materials, and the use of the in-house water-cooling system provide additional constraints to the analysis. The approach taken was to divide the heat transfer path into two component elements including: (1) Heat flux from the heat pipe external wall across the gas gap to the calorimeter wall and (2) heat flux through the calorimeter wall into the coolant flow. The common factor coupling these elements, maintaining a balanced heat flux, is the calorimeter wall temperature. This temperature can be adjusted to obtain an acceptable solution for flow and pressure drop while meeting the

required power transfer. For all model calculations, temperature-dependent material properties were used (evaluated at average conditions). Property information is provided in appendix E.

4.2.1 Static Gas Gap Conduction and Radiation Heat Transfer

The limiting thermal resistance in the heat transfer path between the heat pipe surface and the calorimeter coolant flow is conduction across the static gas gap. This is an important feature allowing the inside diameter of the calorimeter channel to be sized for the expected heat pipe operating condition. The conductivity across the gap can then be tuned up or down using the gas composition as a knob to provide coarse adjustment in the overall heat flux. In addition, the maximum calorimeter channel wall temperature is set by the boiling limit of the pressurized water system. Figure 11 shows the variation in the water boiling point with pressure. For a cooling system operating pressure of 65 psia, the boiling point of water is ≈ 420 K. To maintain margin in the calorimeter design, a maximum calorimeter surface temperature should be in the 375–390 K range.

Another consideration is the increase in heat pipe diameter due to its thermal growth over the expected operating temperature range; this will influence the final width of the gas gap. For the Mo-44.5%Re alloy heat pipe, the change in diameter can be assessed using

$$\Delta D = \alpha_{CTE} \Delta T D_{initial} \quad , \tag{11}$$

where ΔD is the change in diameter, α_{CTE} is the coefficient of thermal expansion, ΔT is the temperature difference between the two conditions, and $D_{initial}$ is the initial material diameter. The final result is an increase in heat pipe outer diameter of ≈ 0.004 in over the temperature range of 300 to 1,400 K, as illustrated in figure 12. A curve fit describing the heat pipe unit outer diameter as a function of temperature was used in the model to account for heat pipe radial growth at each operating condition.

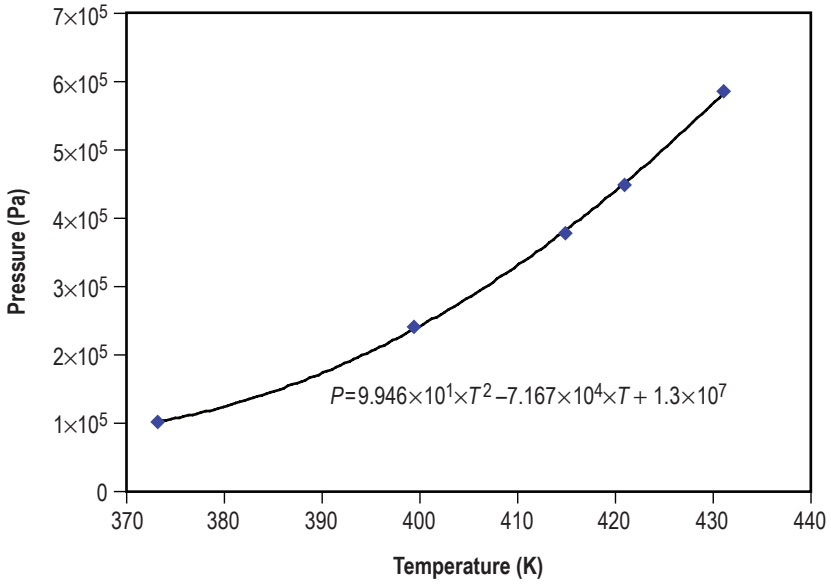

Figure 11. Water boiling point as a function of pressure.

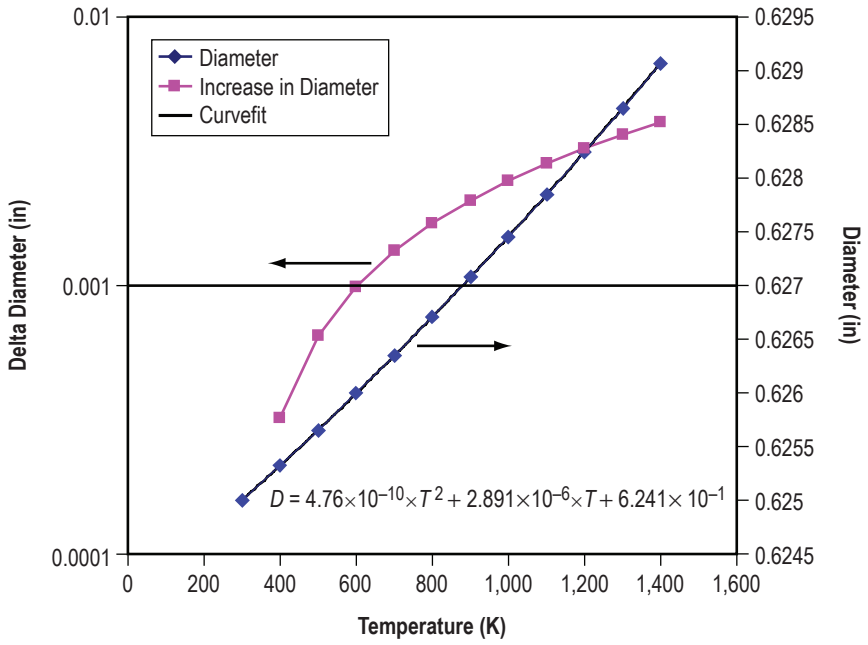

Figure 12. Mo-44%Re heat pipe diameter growth as a function of temperature.

The heat flux balance across the static gas gap is a summation of the radiation and conduction heat transfer components. The radiation component can be assessed assuming the operating temperatures of both the heat pipe and calorimeter. As expected, radiation accounts for a small portion of the total heat transfer (due to the low emissivity, ≈0.15, of the Mo-Re alloy at the operating temperature). The total heat flux rate ($\dot{Q}_{total}$) is given by

$$\dot{Q}_{total} = \dot{Q}_{rad} + \dot{Q}_{cond} \quad , \tag{12}$$

where $\dot{Q}_{rad}$ is the radiation component rate and $\dot{Q}_{cond}$ is the conductive heat transfer load rate. Figure 13 illustrates the static gap and calorimeter layout with relevant parameter identified. The radiative component of the heat flux can be calculated using the Stefan-Boltzmann relationship and the emittance and area of each of the relevant surfaces as

$$\dot{Q}_{rad} = \frac{\sigma A_i \left(T_{hp}^4 - T_{cwi}^4 \right)}{1/\varepsilon_i + \left(A_i / A_o \right)\left(1/\varepsilon_o - 1 \right)} \quad . \tag{13}$$

With the known conductive heat-flux component and the Fourier conduction heat transfer relationship for concentric cylinders,

$$\dot{Q}_{cond} = \frac{2\pi L_c k \left(T_{hp} - T_{cwi} \right)}{\ln\left(d_o / d_i \right)} \quad , \tag{14}$$

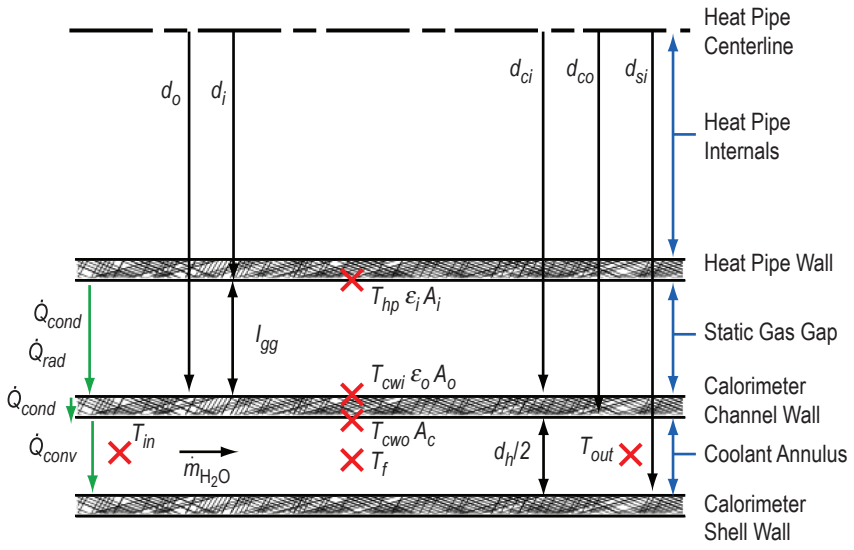

Figure 13. Static gap and calorimeter layout.

where d_o and d_i are the outer and inner diameters, respectively. The static gas gap width (l_{gg}) can be solved as follows:

$$l_{gg} = \frac{1}{2}\left(d_o - d_i\right) . \tag{15}$$

Following this approach, the model was used to calculate the calorimeter sizing parameters for all heat pipe test conditions (condenser radial heat flux ranging from 8.5 W/cm^2 at 1,000 W throughput to 42 W/cm^2 at 5,000 W throughput). The results for two static gas gap compositions (pure He and He-32%Ar by mass) with an assumed calorimeter wall temperature of 390 K are illustrated in figure 14. As expected, the pure He condition requires use of a much larger gas gap width because its thermal conductivity is approximately twice that of the He-32%Ar mixture.

The use of a reduced gas thermal conductivity in the layout provides for some upward margin in the design, making up for variability in the final width of the gas gap in the as-built hardware (e.g., more or less, Ar can be added to compensate for geometric variations to reach the required heat flux). The most difficult case is F(−4) that has the highest heat flux of 5,000 W, requiring an approximate gap width of 0.014 in. This condition is followed closely by the 4,000-W cases, F(2) and F(4), with gas gap widths of approximately 0.0165 in and 0.019 in, respectively. To maintain a design that can be manufactured and assembled, a minimum gap width of 0.02 in should be used. Adhering to this gap limit drives the 5,000-W case Ar concentration to be reduced from 32% to 6%, which still provides some limited upward margin in the design.

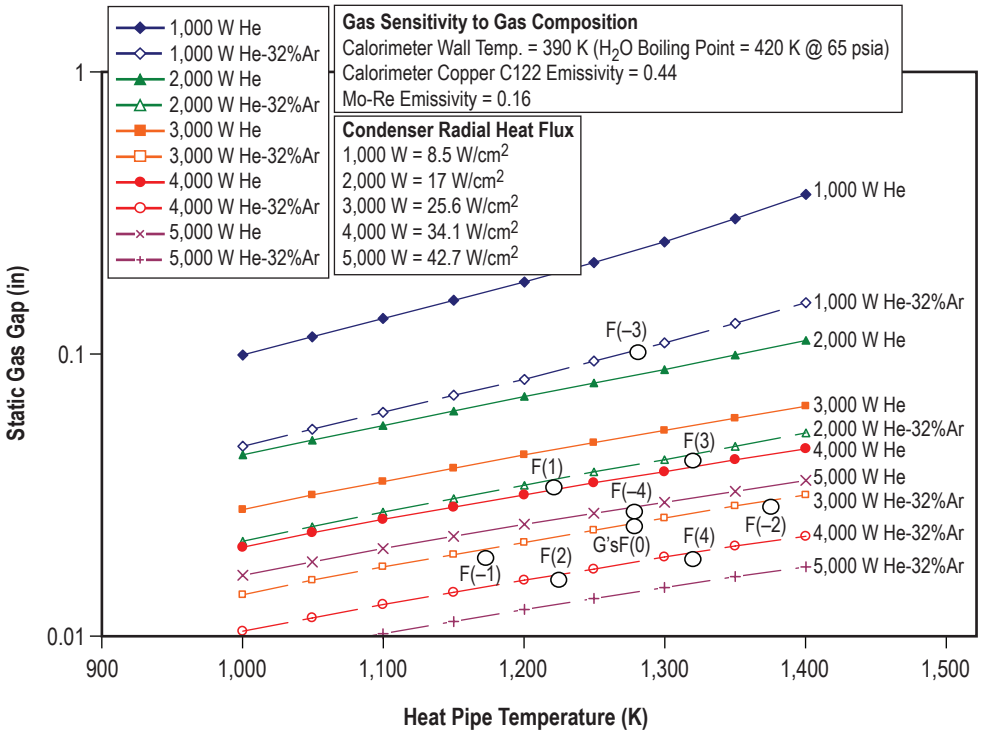

Figure 14. Sensitivity of the static conduction gap with gas composition.

An additional consideration is the sensitivity of the calorimeter channel wall temperature on the static gas gap width. As expected, it has as small effect for the F(2) test case at a power setting of 4,000 W, as shown in figure 15. The wall temperature was varied over a range from 320 to 420 K, capturing the maximum extent of available water temperature. The resulting gap width variation is 0.001 in for the He-32%Ar mixture and 0.002 in for the pure He mixture. Therefore, the assumption of a maximum calorimeter channel wall temperature of 390 K in the original assessment, used to produce figure 14, should be acceptable for the range of actual calorimeter temperatures expected.

The next step in the sequence is to link the calorimeter cooling film flow to the total heat transfer though the calorimeter channel wall. This step will require calculation of the convective heat transfer coefficient and coupling this to the coolant flow and pressure drop.

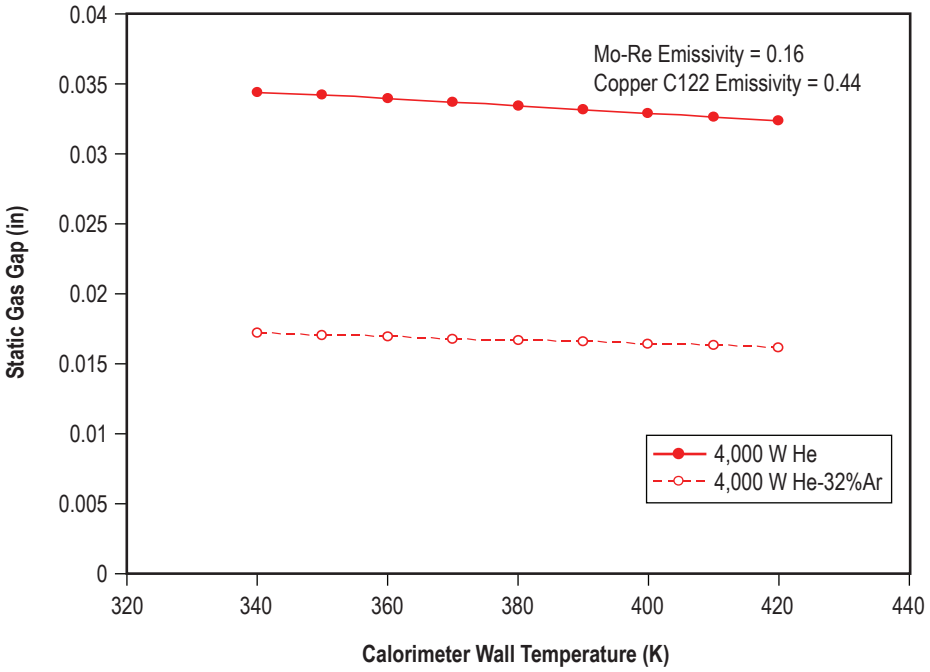

Figure 15. Sensitivity of static gas gap with calorimeter wall temperature.

4.2.2 Calorimeter Coolant Flow Heat Transfer

The power absorbed by the calorimeter is described by the solid conduction heat transfer through the calorimeter channel wall thickness and convective heat transfer into the coolant flow. The temperature drop across the calorimeter channel wall is assessed using Fourier conduction for concentric cylinders, equation (16), where T_{cwi} and T_{cwo} are wall temperatures and d_{ci} and d_{co} are the inner and outer diameters. Results show temperature drops of ≈1 K due to the high thermal conductivity of copper. Heat flux is then absorbed by the flowing coolant using convective heat transfer equation (17), where h is the convective heat transfer coefficient and T_f is a mean film temperature as follows:

$$\dot{Q}_{cond} = \frac{2\pi L_c k\left(T_{cwi} - T_{cwo}\right)}{\ln\left(d_{co}/d_{ci}\right)} \tag{16}$$

and

$$\dot{Q}_{conv} = hA_c\left(T_{cwo} - T_f\right) = hA_c\Delta T_{LM} \quad . \tag{17}$$

The temperature delta $(T_{cwo}–T_f) = \Delta T_{LM}$ is the log mean temperature difference and is given by the following expression:

$$\Delta T_{LM} = \frac{\left(T_{out} - T_{in}\right)}{\ln\left[\left(T_{cwo} - T_{in}\right)/\left(T_{cwo} - T_{out}\right)\right]} \quad , \tag{18}$$

where T_{in} and T_{out} are the inlet and outlet temperature of the coolant flow. The power transferred to the coolant flow results in a temperature increase ($T_{out} - T_{in}$) as given by

$$\dot{Q}_{fluid} = \dot{m} C_p \left(T_{out} - T_{in} \right) \tag{19}$$

and

$$\dot{m} = \rho V A_f \ , \tag{20}$$

where C_p is the specific heat of water, $\dot{m}$ is the mass flow rate, ρ is the density, V is the velocity, and A_f is the coolant film flow area. The convective heat transfer is calculated from a laminar form (Reynolds number (Re) <2,300) of the Nusselt number (Nu) and the hydraulic diameter (d_h) as

$$\frac{h d_h}{k} = Nu = 3.66 + 1.2 \left(\frac{d_{co}}{d_{si}} \right)^{-0.8} \quad Re \le 2{,}300 \ , \tag{21}$$

and

$$d_h = d_{si} - d_{co} \ . \tag{22}$$

The flow regime (laminar in all cases for this assessment) is determined by the Reynolds number, which is a function of the hydraulic diameter and the average properties of the water coolant flow:

$$Re = \frac{\rho V d_h}{\mu} \ . \tag{23}$$

The pressure drop (Δp) is also assessed using a laminar Reynolds number correlation to estimate the friction factor (f), where ψ is an adjustment factor for annular gap size and Γ is a fluid viscosity correction for nonisothermal flow conditions.[16] It is assumed that the flow through the film annulus is fully developed due to the high aspect (total length-to-width) as follows:

$$f = \psi (64/Re) \Gamma^{-0.25} \quad Re \le 2{,}300 \ , \tag{24}$$

$$\psi = \left(1 - \phi\right)^2 \Big/ 1 + \phi^2 + \left(1 - \phi^2\right) \Big/ \ln(\phi) \ , \tag{25}$$

$$\phi = d_{co} / d_{si} \ , \tag{26}$$

$$\Gamma = \mu_{bulk} / \mu_{wall} \ , \tag{27}$$

and

$$\Delta p = \frac{f L \rho V^2}{2 d_h} \ . \tag{28}$$

For the basic calorimeter design, discussed previously, figure 16 shows the power that can be removed by the calorimeter ($\dot{Q}_{fluid}$) as a function of flow rate for a series of ΔTs (where $\Delta T = T_{out} - T_{in}$) for the coolant film channel.

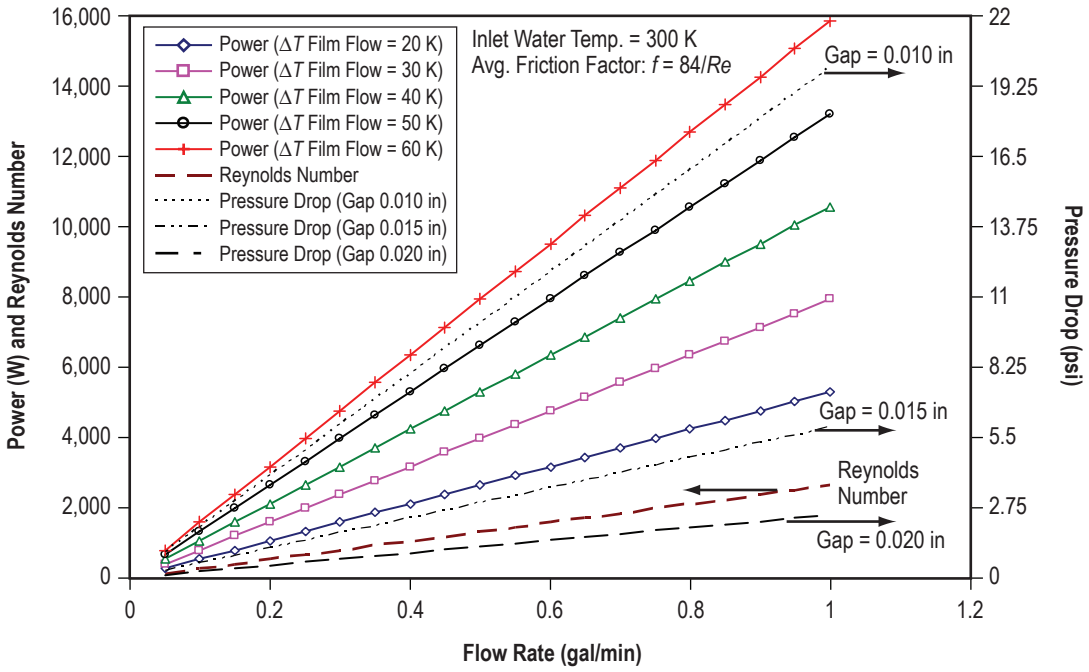

Figure 16. Calorimeter power and pressure drop variation with flow rate.

In this figure, both the heat transfer rate ($\dot{m} C_p \Delta T$) and pressure drop (Δp) are independent of the convective coupling of the calorimeter channel wall, as the figure is intended to illustrate the power capability and regime of the flowing water in the film annulus over a wide operating range. Three film flow gap sizes are analyzed as a function of water flow rate, showing the pressure loss penalty for smaller gaps. The calorimeter pressure drop is a function of fluid properties, Reynolds number, and calorimeter flow path geometry and is reduced by a factor of ≈ 8 by doubling the film gap width.

The desired operating condition for the heat pipe calorimeter is a combination of low-film flow (ΔT) avoiding boiling point limits and low-pressure drop minimizing water system pumping requirements; however, these conditions must be balanced with the forced convection heat transfer coupling of the calorimeter channel wall temperature to water film flow. This coupling is governed by two primary factors. First, the coupling is affected by the convective heat transfer coefficient (h) that is a strong function of the film gap width, equations (17) and (21) as the heat transfer coefficient benefits from the smallest gap size possible (the opposite of pressure drop). Second, the coupling is affected by the temperature difference between the calorimeter channel wall, high-temperature source, and a mean film flow temperature, the low-temperature sink, used in evaluation of the overall convective heat transfer.

To examine this sensitivity, figures 17 and 18 illustrate the required calorimeter channel wall temperatures for three film gap widths at three fixed cooling film flow ΔTs. The cooling system in the planned heat pipe tests will use pressurized water at 65 psia. At this pressure, the boiling point of water is 420 K. Figures 17 and 18 clearly show that for a given film flow rate and power transfer combination, the smaller film flow gap provides a lower required calorimeter channel wall temperature, but has a corresponding increase in pressure drop. For case F(−4), which is the most demanding of the heat pipe tests and requires that 5,000 W be transferred to the fluid, the following is observed:

- For a small film flow gap width of 0.01 in, film flow (ΔT) of 20 K and a flow rate of 0.95 gal/min, at a pressure drop of 19 psi (fig. 16), the calorimeter wall temperature is 356 K (fig. 17), with a cooling film flow outlet temperature of 320 K. This condition requires a large coolant driving pressure.

- Increasing the film flow (ΔT) to 60 K with the same 0.01-in film gap width and a corresponding flow rate of 0.32 gal/min, at a pressure drop of 6.3 psi (fig. 16) the calorimeter wall temperature is 395 K (fig. 18), with a cooling film flow outlet temperature of 360 K. This condition yields an acceptable pressure loss for the water-cooling system, however, it is approaching the boiling limit.

The tradeoff in selecting the width of the flow gap is an increase in calorimeter pressure drop for a reduction in calorimeter channel wall temperature. The final calorimeter geometry that is selected will balance the pumping system requirements with sufficient margin on the hot-side temperature to maintain a condition that is comfortably below the water boiling point. The effect of increasing the calorimeter film annulus reduces the calorimeter pressure drop; opening up the channel improves the ability to machine and assemble the unit. However, it also reduces the overall convective heat transfer coefficient (h), which in turn requires a higher calorimeter channel-wall temperature. For the case F(−4) with a larger film flow gap, the following is observed:

- For an intermediate film flow annulus of 0.015 in, film flow (ΔT) of 20 K and flow rate of 0.95 gal/min, the required calorimeter wall temperature is 375 K (fig. 17), nearly 20 K higher than with the smaller film annulus. This temperature increase is due to the lower convective heat transfer coefficient of 4,174 W/m-K; however, the pressure drop falls to 5.6 psi, which is now in an acceptable range.

- Increasing the film flow (ΔT) to 60 K for the same 0.015-in film gap (fig. 18) results in a calorimeter channel-wall temperature of 416 K, which is unacceptably high and nearly at the boiling point of the pressurized water system (420 K). The calorimeter pressure drop, however, falls to 2.1 psi.

- Increasing the film flow annulus to a 0.02-in width with a film flow (ΔT) of 20 K (fig. 17) results in a calorimeter channel-wall temperature of 390 K and a corresponding pressure drop of 1.9 psi. This is an acceptable pressure drop while still allowing some margin on the boiling point.

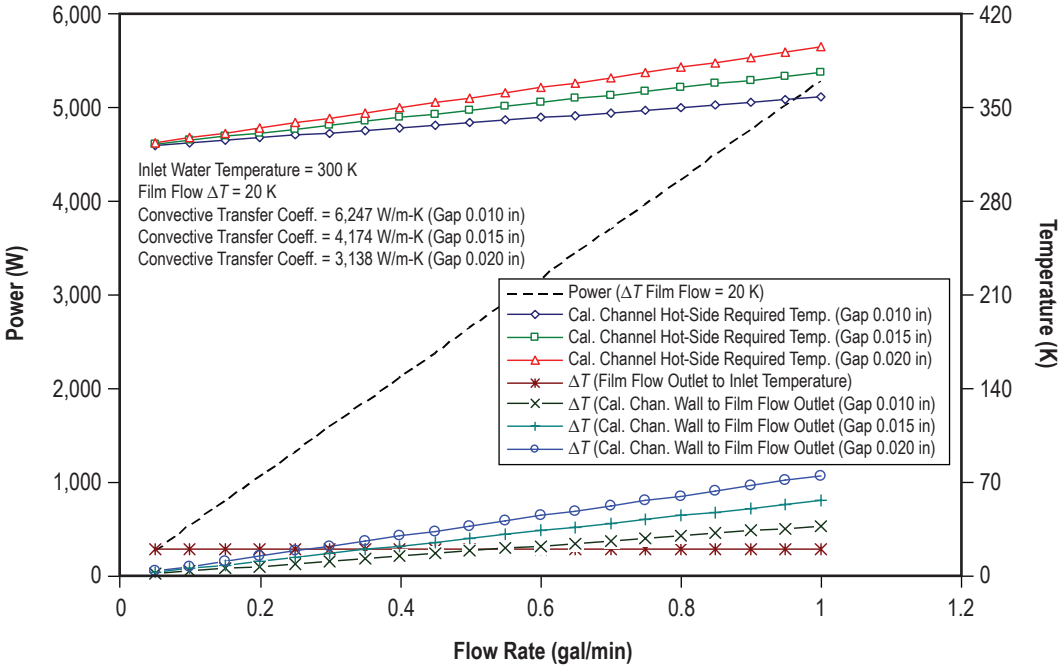

Figure 17. Calorimeter temperatures and film annulus sensitivities (ΔT=20 K).

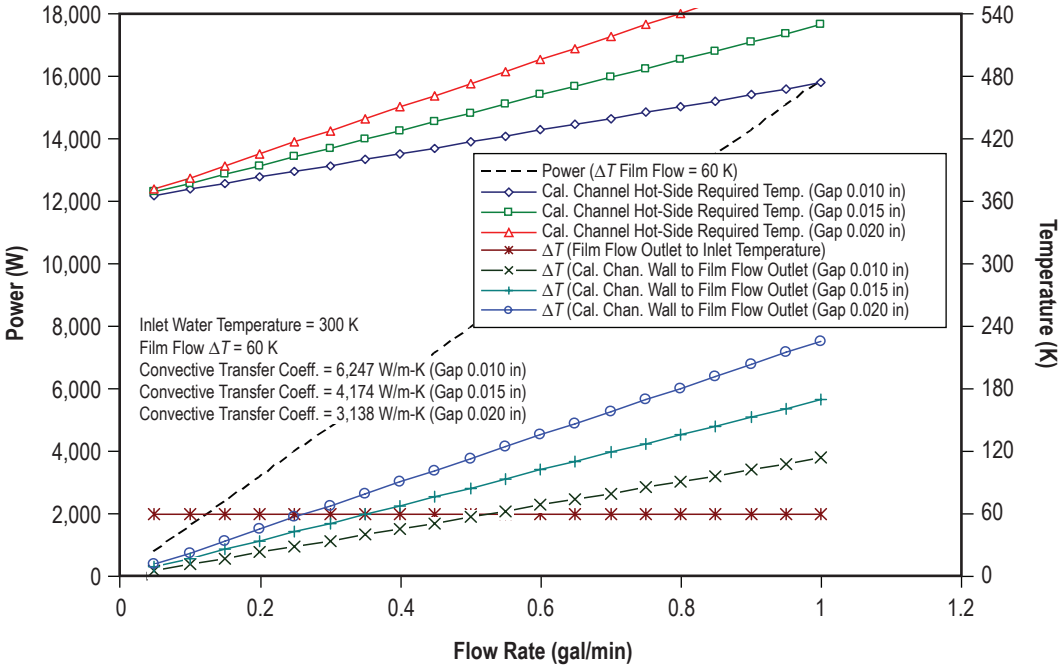

Figure 18. Calorimeter temperatures and film annulus sensitivities (ΔT=60 K).

The estimation model applied target calorimeter channel temperatures to provide overall performance given the cooling film flow gap width and water inlet temperature. Specific calorimeter results producing feasible designs for the three film flow gap widths of 0.010, 0.015, and 0.020 in are shown in tables 6–8. To ease manufacturing and assembly, the 0.015-in gap width is strongly recommended. It is noted that there is a workable 0.020-in gap design for all tests cases, with the exception of case F(−4), if the Reynolds number is to be maintained below 2,300. The results of the spreadsheet model for each test case are provided in appendix F. The calorimeter coolant return annulus is sized with a 0.125-in width to minimize pressure loss and to simplify fabrication and assembly; it is not analyzed by this model.

Table 6. Calorimeter parameters for a film gap width of 0.010 in.

Film cooling water inlet temperature		300 K									
Film gap width		0.010 in									
Calorimeter heat extraction length		9.25 in									
Calorimeter total length		13 in									
Test Condition	**Units**	**G Series**	**F(–4)**	**F(–3)**	**F(–2)**	**F(–1)**	**F(1)**	**F(2)**	**F(3)**	**F(4)**	**F(0)**
Power	W	3,000	5,000	1,000	3,000	3,000	2,000	4,000	2,000	4,000	3,000
Heat pipe to calorimeter gas gap width	in	0.026	0.025	0.104	0.031	0.021	0.037	0.017	0.046	0.02	0.026
Heat pipe temperature	K	1,273	1,273	1,273	1,373	1,173	1,223	1,223	1,323	1,323	1,273
Calorimeter channel wall temp.	K	350	385	328	350	350	335	365	335	365	350
Log mean temp. diff. (wall to fluid)	K	33.1	54.1	9.3	32.7	33.6	21.6	44.9	21.2	44.5	33.1
Cooling film flow ΔT (outlet-Inlet)	K	29.7	53.5	26.6	30.4	29.1	23.1	35.8	23.7	36.5	29.7
Cooling flow outlet temperature	K	329.5	353.3	326.4	330.2	328.9	322.9	335.6	323.5	336.3	329.5
Cal. film flow ID	in	0.796	0.794	0.953	0.807	0.786	0.819	0.778	0.837	0.785	0.796
Cal. film flow OD	in	0.816	0.814	0.973	0.827	0.806	0.839	0.796	0.857	0.805	0.816
Water film flow rate	gal/min	0.38	0.35	0.14	0.37	0.39	0.33	0.42	0.32	0.42	0.38
Heat transfer coefficient	W/m^2-K	6,071	6,211	6,046	6,075	6,067	6,027	6,110	6,030	6,113	6,071
Reynolds No.	–	1,174	1,345	354.6	1,139	1,205	916.26	1,407	878	1,378	1,174
Calorimeter pressure drop	psi	7.5	5.3	2.6	7.2	7.8	6.9	7.8	6.5	7.5	7.5

Table 7. Calorimeter parameters for a film gap width of 0.015 in.

Film cooling water inlet temperature		300 K									
Film gap width		0.015 in									
Calorimeter heat extraction length		9.25 in									
Calorimeter total length		13 in									
Test Condition	**Units**	**G Series**	**F(–4)**	**F(–3)**	**F(–2)**	**F(–1)**	**F(1)**	**F(2)**	**F(3)**	**F(4)**	**F(0)**
Power	W	3,000	5,000	1,000	3,000	3,000	2,000	4,000	2,000	4,000	3,000
Heat pipe to calorimeter gas gap width	in	0.025	0.025	0.103	0.031	0.021	0.037	0.017	0.046	0.02	0.025
Heat pipe temperature	K	1,273	1,273	1,273	1,373	1,173	1,223	1,223	1,323	1,323	1,273
Calorimeter channel wall temp.	K	360	396	338	360	360	340	380	340	380	360
Log mean temp. diff. (wall to fluid)	K	50.2	83.3	13.8	49.5	50.9	32.7	68.2	32	67.5	50.2
Cooling film flow ΔT (outlet-Inlet)	K	18.8	24.6	35.2	20.1	17.6	13.9	22.8	15.2	24	18.8
Cooling flow outlet temperature	K	318.6	324.4	335	319.9	317.4	313.8	322.6	315	323.8	318.6
Cal. film flow ID	in	0.795	0.794	0.951	0.806	0.786	0.818	0.777	0.836	0.785	0.795
Cal. film flow OD	in	0.825	0.824	0.981	0.836	0.816	0.848	0.807	0.866	0.815	0.825
Water film flow rate	gal/min	0.6	0.77	0.11	0.56	0.65	0.54	0.67	0.5	0.63	0.6
Heat transfer coefficient	W/m^2-K	4,009	4,035	4,075	4,015	4,004	3,986	4,028	3,991	4,033	4,009
Reynolds No.	–	1,652	2,234	290	1,543	1,760	1,369	1,936	1,244	1,842	1,652
Calorimeter pressure drop	psi	3.7	4	0.5	3.3	4	3.5	3.8	3.1	3.5	3.7

Table 8. Calorimeter parameters for a film gap width of 0.020 in.

Film cooling water inlet temperature		300 K									
Film gap width		0.020 in									
Calorimeter heat extraction length		9.25 in									
Calorimeter total length		13 in									
Test Condition	**Units**	**G Series**	**F(–4)**	**F(–3)**	**F(–2)**	**F(–1)**	**F(1)**	**F(2)**	**F(3)**	**F(4)**	**F(0)**
Power	W	3,000	5,000	1,000	3,000	3,000	2,000	4,000	2,000	4,000	3,000
Heat pipe to calorimeter gas gap width	in	0.025	0.024	0.103	0.03	0.021	0.037	0.016	0.046	0.02	0.025
Heat pipe temperature	K	1,273	1,273	1,273	1,373	1,173	1,223	1,223	1,323	1,323	1,273
Calorimeter channel wall temp.	K	375	420	337	375	375	360	401	350	400	375
Log mean temp. diff. (wall to fluid)	K	67.1	112	18.4	66	68	43.6	91.1	42.6	90.3	67.1
Cooling film flow ΔT (outlet-Inlet)	K	15.6	16.1	29.8	17.6	13.9	12.5	19.6	14.4	19.1	15.6
Cooling flow outlet temperature	K	315.4	315.9	329.6	317.4	313.7	312.3	319.4	314.2	319	315.4
Cal. film flow ID	in	0.795	0.793	0.951	0.806	0.785	0.818	0.777	0.836	0.784	0.795
Cal. film flow OD	in	0.835	0.833	0.991	0.846	0.825	0.858	0.817	0.876	0.824	0.835
Water film flow rate	gal/min	0.73	1.17	0.13	0.65	0.82	0.6	0.77	0.53	0.79	0.73
Heat transfer coefficient	W/m^2-K	3,003	3,005	3,046	3,010	2,998	2,992	3,018	2,998	3,016	3,003
Reynolds No.	–	1,909	3,106	324	1,710	2,132	1,492	2,166	1,299	2,185	1,909
Calorimeter pressure drop	psi	1.8	2.6	0.3	1.6	2.1	1.6	1.8	1.4	1.8	1.8

4.2.3 Environmental Losses

To establish good thermal coupling between the heat pipe and calorimeter assembly, the proposed test setup requires that the test chamber be flooded with an inert gas (He or He-Ar mixture). The downside is that the gas also provides better thermal coupling to the chamber wall, introducing additional losses that must be compensated for by the inductive heater system. Figure 19 illustrates the locations of heat loss to the environment and support system. At the evaporator section, there is a combination of radiation, conduction, and natural convection heat loss to the RF inductive coil and chamber walls. The surface of the calorimeter has a natural convection loss component to the test chamber environment (small, due to its low temperature, but it must be assessed). The condenser support has a combination of solid conduction along the length of the support tube and gas conduction and radiation between the surface of the support tube and calorimeter inner wall.

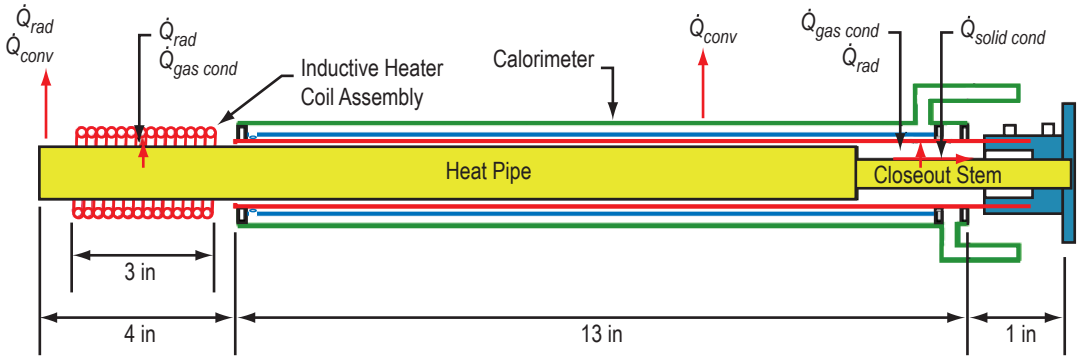

Figure 19. Heat pipe/calorimeter environmental heat loss.

A simple spreadsheet model was assembled to estimate the losses; these calculations will be incorporated into the final GFSSP model (sec. 4.3). The approach makes use of constant surface temperature for the heat pipe, calorimeter outer surface, mounting bracket, test chamber wall, and RF inductor coil (taken from the cases listed in table 7 for a 0.015-in film flow gap). The current assumption is that the test chamber wall will be water-cooled to maintain a temperature of ≈300 K. The RF inductor coil will also be water-cooled, and for this analysis, the coil temperature is assumed to be 350 K, due to its close proximity to the heat pipe evaporator. The heat pipe and calorimeter mounting bracket is assumed to operate at a temperature of 400 K—slightly above the test chamber wall temperature; no cooling of the bracket is currently planned. The test chamber is to be held at a pressure of ≈70 torr.

Radiation heat transfer is calculated using the same expression as equation (29) and gas-conduction heat transfer, equation (30), with the appropriate values to describe fluid/material properties and boundary temperatures. Free convection was assessed as natural convection from a long cylinder using equations (29–34), where Ra is the Raleigh number, Pr is the Prandtl number, d_o is the outer diameter of the component, β is the gas thermal expansion coefficient, α is the gas thermal diffusivity, ρ is the gas density, C_p is the gas specific heat, and ν is the gas kinematic viscosity as follows:

$$\dot{Q} = hA\left(T - T_\infty\right) \ , \tag{29}$$

$$h = \frac{k}{d_o} Nu = \frac{k}{d_o}\left[0.6 + \frac{0.387 \times Ra^{0.167}}{\left[1 + (0.559/Pr)^{0.562}\right]^{0.296}}\right]^2 \tag{30}$$

$$Ra = \frac{g\beta\left(T - T_\infty\right)d_o^3}{\nu\alpha}\left(10^{-5} < Ra < 10^{12}\right) \ , \tag{31}$$

$$Pr = \frac{\nu}{\alpha} \ , \tag{32}$$

$$\alpha = \frac{k}{\rho C_p} \ , \tag{33}$$

$$\beta \approx \frac{1}{T_{avg}} \ . \tag{34}$$

Material and fluid properties are assessed at an average temperature of the hot and cool surfaces involved. The results of the heat loss calculations for each of the heat pipe test conditions are provided in tables 9 and 10 for pure He and He-32%Ar, respectively. During nominal heat pipe operation, thermal loss rates are a function of the surface temperatures; at the maximum temperature of 1,373 K, test case F(–2), the heat loss is 890 W with pure He and 560 W with a He-32%Ar mixture. Appendix G shows a complete listing of the spreadsheet.

Table 9. Heat pipe and calorimeter thermal loss to environment for pure He (70 torr).

Test Condition	Units	G-Series	F(–4)	F(–3)	F(–2)	F(–1)	F(1)	F(2)	F(3)	F(4)	F(0)
Variables											
Heat pipe power level	W	3,000	5,000	1,000	3,000	3,000	2,000	4,000	2,000	4,000	3,000
Heat pipe temperature	K	1,273	1,273	1,273	1,373	1,173	1,223	1,223	1,323	1,323	1,273
Environment temperature	K	300	300	300	300	300	300	300	300	300	300
Avg. calorimeter temperature	K	360	398	338	360	360	340	380	380	340	360
Avg. RF inductive coil temp.	K	350	350	350	350	350	350	350	350	350	350
Support bracket temperature	K	400	400	400	400	400	400	400	400	400	400
Gas composition factor (1=pure He)	–	1	1	1	1	1	1	1	1	1	1
Condenser Support Losses											
Solid conduction loss	W	12	12	12	14	10	11	11	13	13	12
Radiation loss	W	14	14	14	19	11	12	12	16	17	14
Gas conduction loss	W	284	267	293	323	247	274	257	295	312	384
Calorimeter Surface Losses											
Natural convection	W	6	6	5	7	6	3	8	3	8	6
Evaporator Surface Losses											
Radiation loss	W	120	120	120	172	82	99	99	144	144	120
Gas conduction loss	W	233	233	233	270	199	216	216	252	252	233
Natural convection loss	W	74	74	74	85	65	70	70	79	79	74
Total Losses to Environment	W	745	728	753	890	619	685	673	803	825	745

Table 10. Heat pipe and calorimeter thermal loss to environment for He-32%Ar (70 torr).

Test Condition	Units	G-Series	F(–4)	F(–3)	F(–2)	F(–1)	F(1)	F(2)	F(3)	F(4)	F(0)
Variables											
Heat pipe power level	W	3,000	5,000	1,000	3,000	3,000	2,000	4,000	2,000	4,000	3,000
Heat pipe temperature	K	1,273	1,273	1,273	1,373	1,173	1,223	1,223	1,323	1,323	1,273
Environment temperature	K	300	300	300	300	300	300	300	300	300	300
Avg. calorimeter temperature	K	360	398	338	360	360	340	380	380	340	360
Avg. RF inductive coil temp.	K	350	350	350	350	350	350	350	350	350	350
Support bracket temperature	K	400	400	400	400	400	400	400	400	400	400
Gas composition factor (1=pure He)	–	0.51	0.51	0.51	0.51	0.51	0.51	0.51	0.51	0.51	0.51
Condenser Support Losses											
Solid conduction loss	W	12	12	12	14	10	11	11	13	13	12
Radiation loss	W	14	14	14	19	11	12	12	16	17	14
Gas conduction loss	W	145	136	150	165	126	140	131	150	159	145
Calorimeter Surface Losses											
Natural convection	W	4	3	3	4	4	2	5	2	5	4
Evaporator Surface Losses											
Radiation loss	W	120	120	120	172	82	99	99	144	144	120
Gas conduction loss	W	119	119	119	138	101	110	110	128	128	119
Natural convection loss	W	43	43	43	48	37	40	40	45	45	43
Total Losses to Environment	W	457	448	461	560	370	414	408	499	511	457

The gas gap at both the evaporator/RF coil and condenser closeout stem have a concentric arrangement; however, the gap diameter is small, minimizing the potential for natural convection currents. For natural convection in an annulus, the total heat transfer can be assessed using an effective thermal conductivity (k_e) in the following Fourier heat transfer equation:

$$\dot{Q} = \frac{2\pi k_e l}{\ln\left(d_o/d_i\right)}\left(T_i - T_o\right) \ . \tag{35}$$

The k_e term can be evaluated based on the annulus inside and outside dimensions and gap width (L) as follows:

$$k_e = k\left(0.386\left(\frac{Pr}{0.861+Pr}\right)^{1/4}\left(Ra^*_{cyl}\right)^{1/4}\right) , \tag{36}$$

$$Ra^*_{cyl} = \frac{\left[\ln\left(d_o/d_i\right)\right]^4}{\delta^3\left(d_i^{-3/5}+d_o^{-3/5}\right)^5} Ra_\delta \ \left(10^2 < Ra^*_{cyl} < 10^7\right) , \tag{37}$$

$$Ra_\delta = \frac{g\beta\left(T - T_\infty\right)\delta^3}{\nu\alpha} \ , \tag{38}$$

and

$$\delta = \frac{1}{2}\left(d_o - d_i\right) \ . \tag{39}$$

For the annular gap (δ) dimensions in the heat pipe calorimeter/RF inductor geometry, the calculated value of Ra_c* is two orders of magnitude below its valid range of $100 < Ra_c^* < 10^7$ and therefore not applicable. While equations (35) and (36) are not strictly applicable for the conditions here, they do indicate that considering gas conduction alone is an acceptable approach for the small concentric components proposed, since the natural convection heat transfer rate yielded by equation (35) produces a rate approximately one-fifth that of the gas condition.

4.3 The Generalized Fluid System Simulation Program Model

The GFSSP is a general-purpose computer program for analyzing steady state and time-dependent flow rates, pressures, temperatures, and concentrations in a complex flow network.[17] The program is capable of modeling phase changes, compressibility, mixture thermodynamics, conjugate heat transfer, pumps, compressors, and external body forces (e.g., gravity and centrifugal force). Three thermodynamic property programs, GASP, WASP, and GASPAK™ are integrated with GFSSP to provide real fluid thermodynamic and thermophysical properties for 35 fluids.[18–20] Eighteen different resistance and source options are available. The flexibility exists to add additional resistance/source options as well as fluid properties via user-defined subroutines and lookup tables. The user efficiency of GFSSP is enhanced through the incorporation of the visual thermofluid analyzer of systems and components (VTASC) graphical user interface. Code validation and verification (V&V) is described in appendix H.

A model, currently under development, will provide a tool to simulate the performance of the coupled heat pipe and calorimeter configuration. Due to time constraints and the preliminary nature of the design phase, the bulk of the analytical work was done via correlations incorporated into spread-sheets. The additional fidelity required for design verification and pretest performance predictions is currently being incorporated into a GFSSP model. A preliminary nodal layout, representing an earlier version of the calorimeter system, is illustrated in figure 20. The existing model treats the heat pipe as a collection of ambient nodes at constant temperature. Nodes 41, 1, 4, and 19 are the heat pipe nodes. Node 41 is located in the evaporator section, which loses heat to the chamber wall by radiation and natural convection. Nodes 1, 4, and 19 are located within the calorimeter and transfer heat to the incoming water through an annular gap of He and He-Ar mixture and calorimeter channel tube. The gas gap is modeled with two gas nodes in the radial direction at five axial stations. The calorimeter water flow path and shell assembly is also modeled with a similar series of nodes in both the radial and axial directions. The heat transfer coefficient at the surface of the calorimeter was calculated using the Dittus-Boelter equation.[21] The thermodynamic properties of water were supplied by the WASP computer program, while He properties were supplied by the GASPAK computer program. Properties for the calorimeter material were obtained from Incropera.[13]

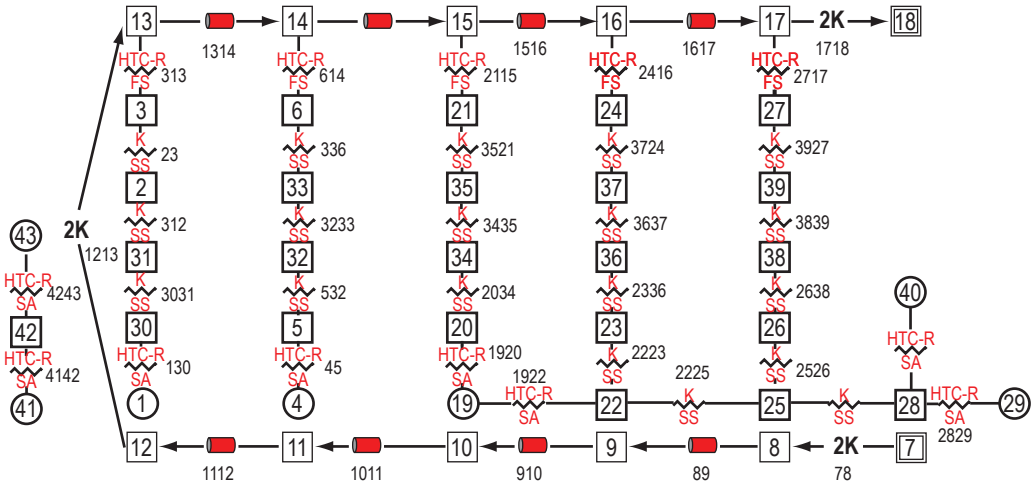

Figure 20. GFSSP model of heat pipe test setup.

As is typical with most analytical efforts, a series of iterations will be required to refine the model for efficient and accurate use in assessing the performance of the heat pipe and calorimeter assembly. Once the GFSSP model is completed and the output is checked against analytical and spreadsheet estimates, it should prove to be a useful tool in performing quick turnaround parametric computational analyses to support final system design and pretest operations. The model will be updated once test data become available.

5. OTHER CONSIDERATIONS

5.1 Sodium Working Fluid Sampling (Vanadium Wire Technique)

Interest has been expressed in sampling the Na working fluid after it has been transferred into the refractory metal heat pipe unit. This provides insight into the initial oxygen concentration within the unit—the sum of impurities in the dispensed Na and what is picked up from the heat pipe materials. A potential method to assess the oxygen concentration is based on a V wire equilibration technique (ASTM 997–83).[22] Details of this technique are covered in *NASA/TM—2005–213902*.[23] Prior to incorporating this technique into the heat pipe processing sequence, laboratory testing must be performed to confirm the accuracy of the method. Sample testing can be performed in the MSFC alkali metal handling glove box with the current Na supply that will be used to fill the heat pipes discussed in this TP. To validate the V wire technique, detailed engineering will be required to accommodate the sampling hardware in the heat pipe fill stem. The key in this design will be to devise an operation in which the V wire sample can be removed from the heat pipe without introducing impurities. Additional support hardware required for these operations, such as the equilibration furnace and valve cooling, will have to be incorporated into the glove box system.

The V wire technique was successfully applied in Na loops in the EBR–II Program.[24] A V wire, present in the heat pipe during processing, appears suitable to characterize oxygen levels in fully assembled and filled heat pipe modules. A method has been devised to remove the wire from the Na during closeout with negligible impurity introduction. The validity of this technique can be independently confirmed by analysis of sample heat pipe modules.

Figure 21 depicts one possible sequence of steps. Sodium is introduced into the heat pipe through a fill stem containing a 0.25-mm-diameter by 3-cm-long V wire (step A). The heat pipe is then closed and wetted over a 48-hr period at the core design temperature.

The heat pipe is then inverted and heated to immerse the V wire in the Na (step B). The assembly is then brought to temperature for a time sufficient to reach equilibrium oxygen concentration between the Na and the wire. Figure 22 shows a time-temperature relation for two wire diameters, assuming that oxygen diffusion through the V is the rate-limiting mechanism.

The heat pipe is cooled to room temperature and the fill stem containing the V wire is severed from the heat pipe inside an Ar dry box (step C). The wire and an Na sample are extracted from the fill stem for analysis. A cap is attached to the heat pipe fill stem using an EB welder connected to the dry box (step D). Since the V wire further purifies the Na during equilibration, some correction will be necessary to establish the true oxygen concentration in the working fluid before and after equilibration.

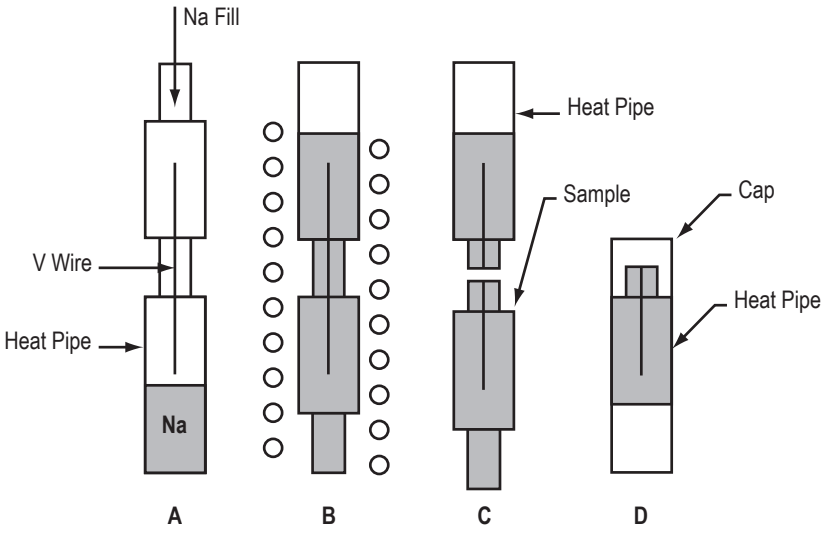

Figure 21. Concept to measure working fluid oxygen concentration in Na-filled heat pipes.

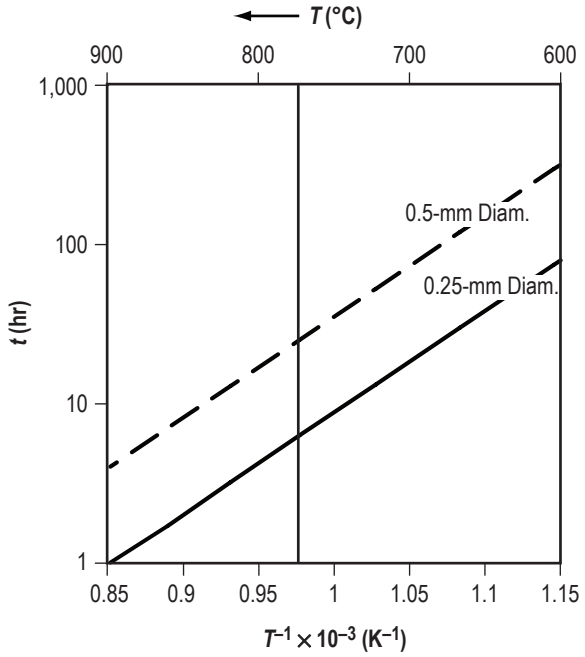

Figure 22. Estimated time required for equilibrium oxygen concentrations in static Na immersed for two V wire diameters.

5.2 Heat Pipe Closeout and Support Concept

Closeout of the heat pipe fill stem is required once Na loading and purity measurements are completed; this will require a number of welding operations to seal, protect, and provide a support mechanism for mounting the heat pipe to the calorimeter. One possible fill stem closeout concept, shown in figure 23, requires that the fill stem be crimped near the condenser plug and then sealed using a tungsten inert gas (TIG) welder to make a cut/weld pass across the center of the crimp. The sealed fill-stem stub can then be protected by placing a plug and tube cover over it and welding it to the condenser plug using an EB welder. The EB technique provides a vacuum in the sealed volume surrounding the crimped fill stem. The evacuated closeout tube provides a containment enclosure should the TIG seal weld leak; since it is evacuated, no external trapped purge gas would be introduced into the heat pipe volume affecting its operation. To support the heat pipe, an additional closeout support tube can be EB welded to the closeout plug. The length of the support tube will need to be sized to provide sufficient room for assembly and to minimize the heat loss through material conduction. Alignment fixtures will be required to assemble the closeout and support components so that straightness can be maintained, a key parameter for integrating the heat pipe with the calorimeter, so the two components do not touch.

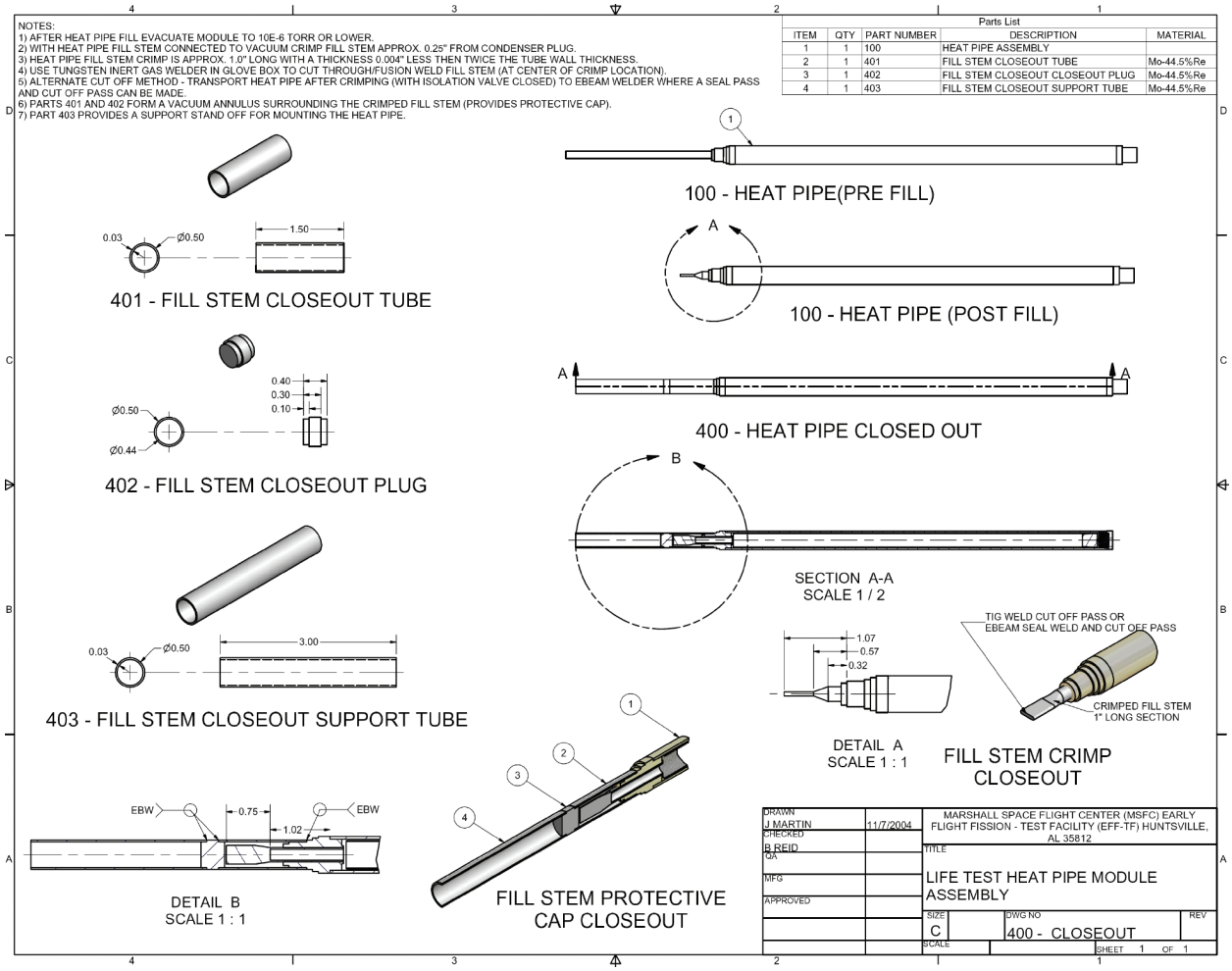

Figure 23. Method 1 to close out the heat pipe fill stem and provide mounting support.

Another possible method to close out the heat pipe fill stem is illustrated in figure 24. After the heat pipe is evacuated, it is heated to a temperature to melt all the Na and then positioned with the fill stem down, transferring the Na to fill the stem. The heat pipe is then cooled, solidifying the Na in the fill stem and creating a freeze plug. The fill stem is then severed using a cutting tool ≈0.25 in from the condenser plug; the freeze plug protects the heat pipe internal vacuum (prevents leakage of glove box inert gas into the heat pipe). The fill stub is deburred and a stem cap placed over the stub (tight tolerance so that it remains snug to the fill stem). The heat pipe unit is then placed in a welding fixture and bagged to maintain an inert environment around the unit while it is transported from the glove box to an EB welder. Welding is performed in a vacuum, thus removing any purge gas remaining in the stem cap. The capped fill stem stub is protected in a fashion similar to that described previously, making use of an evacuated plug and tube cover (welded to the condenser plug) to provide an additional containment enclosure. Mounting is accomplished by an additional support tube EB welded to the closeout plug, with a length sized to meet heat loss and support setup requirements.

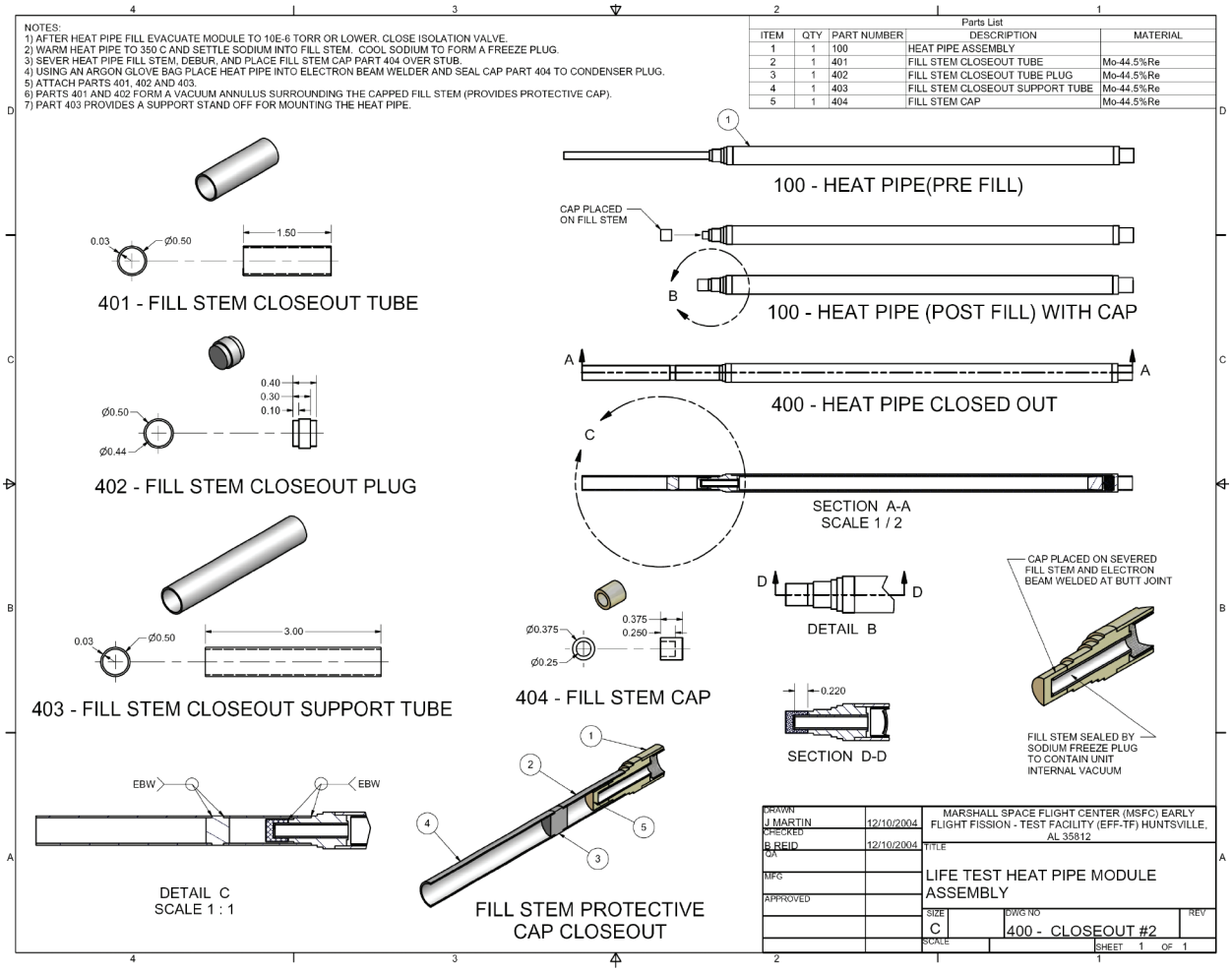

Figure 24. Method 2 to close out the heat pipe fill stem and provide mounting support.

5.3 Heat Pipe Radio Frequency Inductive Heating Coil

Induction heating has been selected to provide a well-characterized mass transfer boundary at the heat pipe evaporator. Fifteen of sixteen life test heat pipes are inductively heated in three clusters with each cluster containing five positions. Table 11 lists the heat pipes that will initially comprise each cluster. A water-cooled copper bus bar, shaped like an inverted patriarch cross, forms a pentagonal pattern around which each induction coil is mounted, as shown in figure 25. The cross arrangement minimizes inductive interference among positions. Each induction coil can be affixed to or removed from its bus bar with mounting pins or screws in a flexible modular fashion. Assessment of the final system design will require determination of the evaporator inductor coil RF coupling to the condenser calorimeter end plate. The objective is to minimize potential RF heating of the calorimeter, which would skew the power data. In addition, RF coupling to any metallic shielding placed around the evaporator section (serving as isolation shield) must be assessed.

Table 11. Initial life test heat pipe arrangement.

Position/Cluster	0	1	2	3
1	F5c	F1c	F3a	G1
2		F2b	F3c	G2
3		F2d	F3e	G3
4		F4b	G6	G4
5		F4d	G7	G5

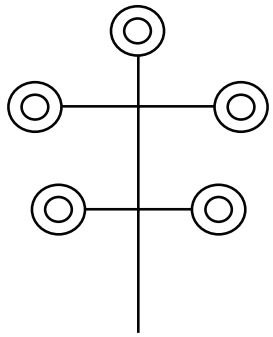

Figure 25. Induction coil cluster mounted on five-position bus bar (end view).

Clusters 0 and 1 hold only F-series heat pipes that operate for the duration of the test. The heat pipe on cluster 0 operates at 5 kW and is inductively heated on a separate electrical circuit. This single-position circuit also serves to determine the performance limits of individual heat pipes before the life test begins. Cluster 1 holds heat pipes that require power to be supplied at 1, 2, and 4 kW each (powers of two).

Cluster 2 initially holds F-series and long-duration G-series heat pipes. Cluster 3 initially holds the G-series heat pipes that will be first removed for destructive test. Grouping all three kilowatt heat pipes on clusters 2 and 3 allows a uniform electrical potential to be applied to both clusters. As G-series heat pipes are removed, the configuration of clusters 2 and 3 will be rearranged to help balance the electrical load.

5.4 Chamber Gas Selection and Purity

For operation of refractory metal systems at increased temperature for a relatively long time, the concentration of oxygen in the ambient environment is critical to the life of the refractory system. For the proposed testing, the refractory metal components will be operated in a low-pressure environment of ultrahigh purity (UHP) Ar or He so that the thermal coupling between the heat pipe and calorimeter can be controlled. To achieve the desired gas purities, successive dilutions and pumpdown of the system are required. The pumpdown procedure will also include an initial bakeout of the system at ≈525 K to drive off water vapor (and other volatiles) from the gas lines, vacuum chamber, and test components.

A series of rough calculations was performed to assess the oxygen concentration in the heat pipe test chambers over successive dilutions with UHP fill gas, assuming an initial oxygen concentration of 209,500 ppm in air filling the test chambers (20.95% oxygen by volume). Calculations were performed assuming three cylindrical test chambers having approximate dimensions of 24 in diameter by 24 in length. The UHP He and Ar, purchased from Sexton Supply, have a guaranteed minimum purity of 99.999%. The UHP He has a maximum oxygen content of 3 ppm by volume, and UHP Ar has a maximum oxygen content of 1 ppm by volume. Figure 26 shows the concentration of oxygen in the test chambers in ppm (by volume) at a pressure of 70 torr (≈0.1 atm) after multiple dilutions of He or Ar.

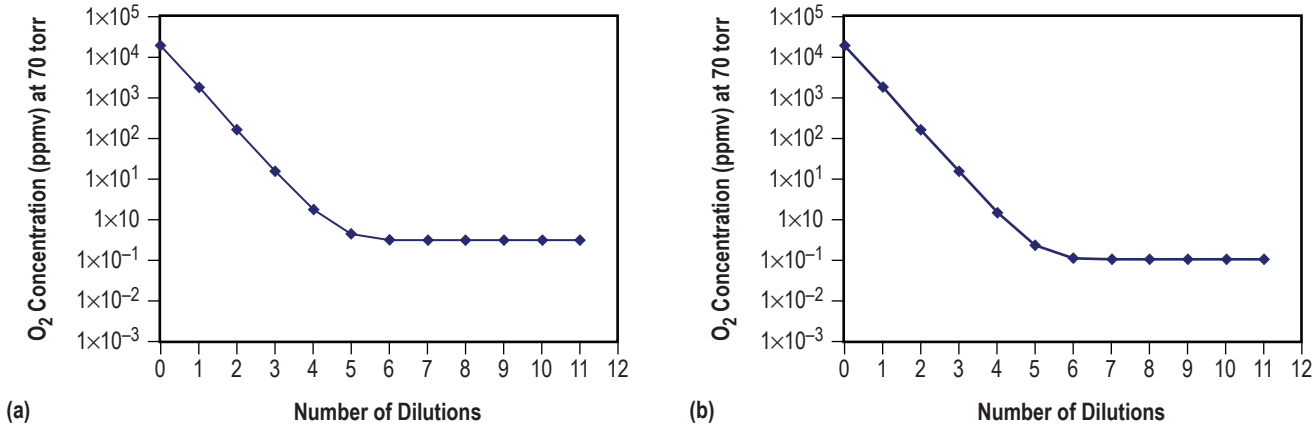

Figure 26. Oxygen concentration in the heat pipe test chambers after successive dilutions of (a) UHP He and (b) UHP Ar fill gas.

For this analysis, the chambers are pumped down from atmospheric pressure (760 torr) to 70 torr and then backfilled with the UHP gas to atmospheric pressure. Each subsequent dilution cycle reduces the oxygen concentration; pumping to a lower pressure in each cycle would further reduce the oxygen content over the same number of dilution cycles. After multiple dilutions (approximately six, based on fig. 26) the baseline oxygen concentration, established by the purity of the fill gas, is achieved; these values are 300 ppb for He and 100 ppb for Ar. Note that while these calculations ignore any additional contamination from impurities in the lines and test chamber, they do provide an ultimate baseline for the minimum achievable oxygen concentration for a given fill gas and operating pressure without additional gas purification. Initial bakeout of the system (under vacuum) will assist in driving out volatile impurities (primarily

water if the system is clean and degreased) from the test components and fill lines to reduce additional impurities in the system.

For comparison, an acceptable vacuum level for testing Mo-Re alloys is in the 10^{-6} torr range; at a pressure (1×10^{-6} torr) the oxygen concentration is 0.28 ppb in the vacuum test environment. The oxygen concentration provided by the UHP gases alone is insufficient to achieve the required level; therefore, additional purification is required. Two methods are employed to purify the test chamber gases: (1) An SAES ambient temperature MicroTorr gas purifier to clean the incoming gases and (2) an SAES MonoTorr point-of-use purifier incorporated in the test chamber recirculation system. Figure 27 illustrates a conceptual layout of the of the test chamber gas purification system.

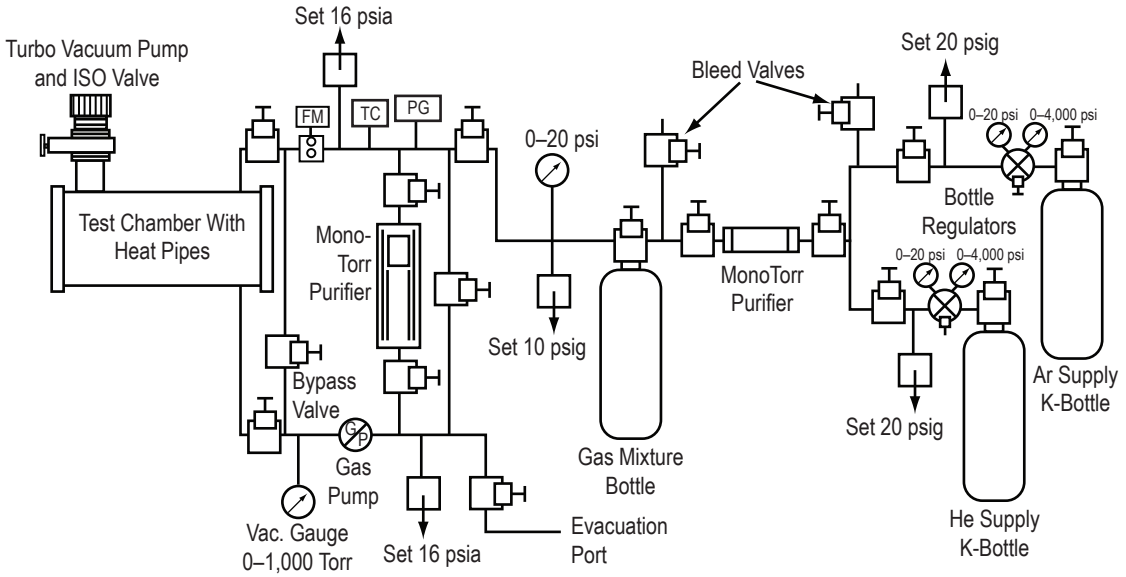

Figure 27. Initial concept for test chamber gas mixture system.

The MicroTorr unit has an advertised performance for purifying both He and Ar to a final oxygen concentration of 1 ppb. The gas mixture bottle can therefore be charged with an appropriate He/Ar mixture (purified to 1-ppb oxygen concentration using the inline MicroTorr unit) and, in turn, used to perform multiple dilution cycles on the test chamber. Using this new value of oxygen concentration in both He and Ar produces the trends shown in figure 28 over multiple dilution cycles. After nine dilution cycles, the final oxygen impurity concentration for both the He and Ar fill are 0.1 ppb at a 70-torr test chamber pressure. This condition meets the acceptable oxygen concentration for testing Mo-Re alloys, $\approx$0.28 ppb, that was discussed previously corresponding to the oxygen concentration in a 1×10^{-6} torr vacuum.

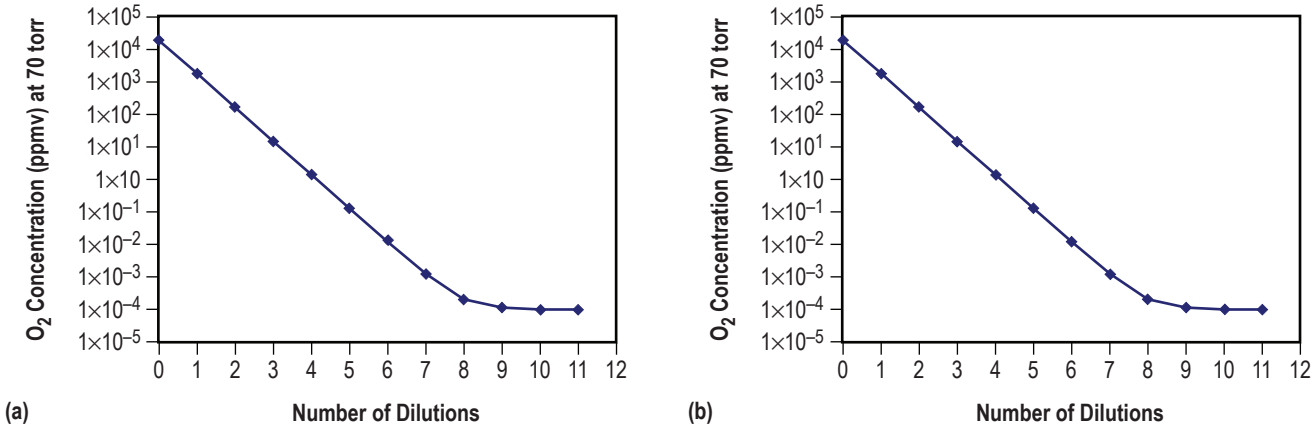

Figure 28. Final oxygen concentration in the heat pipe test chamber with (a) UHP He fill gas and (b) UHP Ar fill gas purified using an inline SAES MicroTorr ambient gas purifier.

To maintain the purity level of the test chamber environment during test operations, an SAES MonoTorr point-of-use purifier with a recirculation pump will also be incorporated in the system. Within the MonoTorr purifier, getter materials are used to irreversibly trap gaseous impurity molecules; these impurities are captured on the surface of the materials, and upon heating, diffuse into the bulk of the getter. When used with Ar or He, the MonoTorr purifier can be used to remove molecules of H_2O, O_2, H_2, CO, CO_2, N_2, and hydrocarbons. The performance of the purifier is dependent on the pumping speed at which it is operated. Table 12 provides a summary of the performance guarantee for the SAES MonoTorr Phase II 3000 for rare gases.

Table 12. SAES MonoTorr Phase II 3000 performance guarantee for rare gases.

	Pumping Rate	
Impurity	0–20 slpm	20–50 slpm
O_2	< 1 ppb	< 1 ppb
H_2O	< 1 ppb	< 1 ppb
CO	< 1 ppb	< 1 ppb
CO_2	< 1 ppb	< 1 ppb
N_2	< 1 ppb	< 10 ppb
H_2	< 1 ppb	< 10 ppb
CH_4	< 1 ppb	< 10 ppb

5.5 Heat Pipe Temperature Measurement

Temperature measurements are required to monitor overall operation and track performance of the heat pipe unit. The majority of the heat pipe unit is inaccessible due to the calorimeter and inductive heater assemblies. However, the primary location for a performance measurement is at the heat pipe evaporator exit, which is accessible through the small gap between the inductive heater and calorimeter.

Two potential techniques have been identified that are capable of taking this measurement and include type-C thermocouples and two-band optical pyrometers.

Thermocouples are an inexpensive method, but have a number of negative issues related to their usage. First, they are a contact measurement technique requiring direct attachment to the surface of the heat pipe. This can be troublesome since they frequently debond from the surface to which they are attached. In addition, to achieve a successful bond, especially in the case of refractory metals, an intermediate material such as nickel foil is typically required. The foil is bonded to the refractory metal surface and the thermocouple then bonded to the foil. This intermediate material is not the best option for long-term testing since nickel will diffuse into the heat pipe alloy, potentially resulting in undesirable and/or unknown effects. There is a possibility that the type-C thermocouples, which are available with a 26%Re content (the balance being tungsten), may have sufficient Re to allow them to be spot welded directly to the surface (testing would be required). In general, the use of spot welding is not an attractive idea since it can result in pitting of the heat pipe surface and potentially embed or trap impurities. Over the duration of the program, many spot welding cycles would be required to account for nondestructive evaluation (NDE) cycles, estimated at 6-mo intervals, and thermocouple repair. In addition, the thermocouple leads act as fins, locally cooling the location where the measurement was taken, and the long-term degradation of the thermocouple wires over time at high temperature introduces unknowns. If thermocouples were used, they would be paired at a minimum to provide backup.

The two-band optical pyrometer is a remote mounted, noncontact measuring technique that makes use of a lens to focus the field of view on the location where the temperature measurement is required. The two-color, infrared sensing uses a ratio technique between the radiosity at two wavelengths to determine temperature rather than the radiosity at a single wavelength. The result is a temperature measurement that is independent of emissivity, target size/shape, and dust/contamination on the windows in the optical path. The noncontact technique simplifies setup (no internal thermocouple wires) and eases operations involving loading and unloading of the heat pipe units. A typical two-band system, the M77S by Mikron, retails for $3,000–$4,000, depending on features, and has focusing capability allowing for a spot size of 0.16 in at a 14-in standoff.

The current recommendation is to make use of two-band optical pyrometers for all heat pipe measurements (total of 16 units required). This will significantly reduce the overall effort involved in setting up, attaching, and maintaining thermocouples inside the vacuum system. In addition, the two-band systems are completely external to the chamber, allowing for rapid replacement or troubleshooting should it be required. Thermocouples will still be used extensively on all other parts of the system such as the coolant flow, test chamber, etc. where they are easily accessible and operate in less severe conditions.

5.6 Water-Cooling System

Water-cooling has been baselined in the current calorimeter design and is also used to cool the test chamber walls and RF induction coils. The current conceptual layout for providing coolant water to a calorimeter cluster (a cluster is composed of five calorimeter units arranged in a pentagon) is illustrated in figure 29. There are two options to cool additional calorimeter clusters: (1) They can be attached to the system inlet and outlet manifolds if sufficient pumping/cooling power is available or (2) a duplicate of this system can be fabricated if necessary. The coolant system is fabricated from stainless steel and loaded

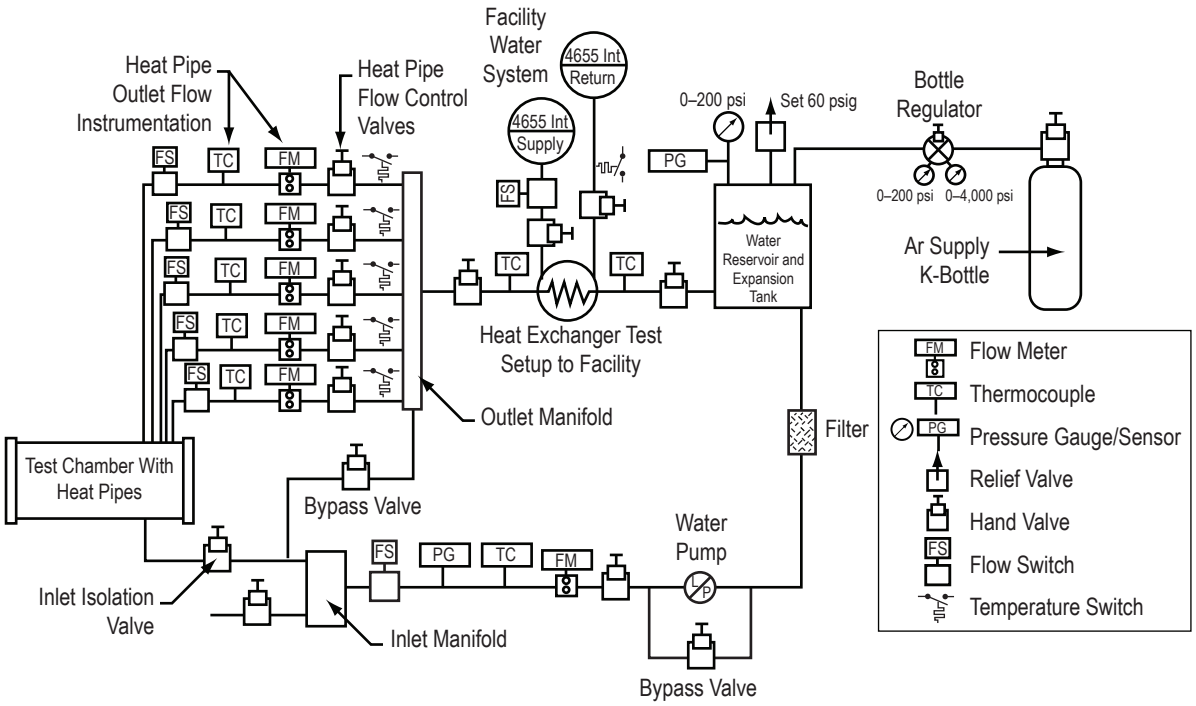

Figure 29. Initial concept for water-cooling system layout.

with deionized water (target of 10 MΩ-cm or better) and an inline filter to minimize conductivity and the potential for buildup of scale/rust etc. The water flow to each heat pipe calorimeter is regulated by a hand valve, located at the calorimeter exit. Temperature and flow rate measurements are also taken at this location so that calorimeter power can be determined. A facility water-coolant system is used to absorb the estimated 60,000 W of power from the heat pipe cooling loop through the use of a heat exchanger. The water pump selected (if a single pump is to supply all calorimeters) will be required to provide a flow rate of 12–15 gpm, operate at an inlet suction pressure of 65 psia, and provide a pressure rise of at least 20 psi to conservatively overcome plumbing losses. The facility and heat pipe cooling loops are equipped with flow and temperature switches to interrupt the RF generator power in the event of coolant circulation failure or an over-temperature condition. The system will be configured so it can be degassed (equipped with heating and evacuation capability) to reduce the potential for subcooled boiling. The final system configuration will need sufficient flow capability and capacity to remove the thermal capacity of the heat pipes (to a safe level) without system damage should an abrupt power-out condition be encountered.

To control the growth of organic material in the main flow circuit (potential to plug the filter and small flow paths), it is recommended that an inline, ultraviolet purifier be added. This setup should allow for low-maintenance operation while initial degassing of the water system and the use of inert cover gas would reduce free oxygen, limiting the potential for ozone production. An alternate technique would be the use of chemicals; however, concentrations need to be monitored and chemicals replenished on a regular basis. Depending on chemical selection, there is the risk of interaction with the copper calorimeter and potential breakdown of the chemicals at high temperature. In addition, to maintain the water quality (10–18 MΩ-cm water resistivity), it is possible to add a deionizing (polishing) loop to the main circuit with a throughput of 3%–5% of the main flow.

6. SUMMARY

A Mo-Re alloy refractory metal heat pipe design and test matrix have been proposed that attempt to systematically address the issues related to corrosion rates at operating temperatures anticipated for possible space nuclear operations. A series of test conditions have been proposed that vary temperature mass fluence and power to provide for acceleration of impurity transport and corrosion mechanisms. Power throughput covers a range from 1,000 to 5,000 W with planned operating times up to 3 yr and temperature ranges from 1,173 to 1,373 K. Performance testing of the initial heat pipes will be necessary to determine if the high-power/temperature conditions in the test matrix can be achieved. If boiling limits are exceeded, the test matrix will have to be adjusted to appropriately lower power/temperature conditions.

To absorb energy from the heat pipe condenser, a gas gap/laminar flow water calorimeter concept appears feasible. For all power levels, the gas gap width between the heat pipe surface and calorimeter can be sized at 0.020 in or larger, while still retaining performance margin by adjusting the gas mixture ratio of He to Ar in the test chamber. Likewise, geometric solutions exist for satisfying the calorimeter film flow coolant annulus thermal performance. It is noted that for the higher heat pipe power cases, 4,000 and 5,000 W, a higher calorimeter channel-wall temperature is required which reduces design margin. For all design cases examined, the smaller film flow annulus is desirable due to higher heat transfer coefficient; however, it carries a penalty of higher calorimeter pressure drop. Also, the smaller flow annulus width requires tight tolerances, taxing the fabrication and assembly process. For the large annulus gap examined, 0.020 in, a workable set of operating parameters was established with low-pressure loss for all but the high-power, 5,000-W case. This case exceeded laminar flow water limits, requiring a calorimeter temperature above the local water boiling point. The recommended coolant film gap width, based on the current assessment, is 0.015 in. It should be pointed out that there is a potential concern in using water as the calorimeter coolant fluid. A water-based system presents a risk for water leakage into the test chamber and the potential catastrophic interaction of water with refractory metals at high temperatures. To minimize this risk, the calorimeter and feed lines will be an all-welded design and He leak checked; however, there is always the potential for a leak.

In addition, initial analysis indicates that the oxygen level (ppb) within the test chamber can be reduced to a level consistent with that achieved under normal vacuum testing conditions (10^{-6} torr range) typically used for Mo-Re alloys. The use of commercial purifier systems will be implemented to further reduce the impurity level below that achieved by successive dilutions. The test chamber environment can be monitored with a residual gas analyzer. Also, the use of two-band, noncontact optical pyrometers to measure heat pipe evaporator exit temperature is highly recommended. These units significantly simplify setup/maintenance operations and provide better overall data. Additional work is underway to further develop hardware requirements and detailed layouts for all supporting systems, including the RF heating system and calorimeter/test chamber water-cooling systems.

APPENDIX A—HEAT PIPE LIFE TESTING—ALTERNATE APPROACH

A.1 Corrosion in High-Temperature Heat Pipes

An ideal heat pipe is thermodynamically closed with energy crossing the system (container) boundary at the evaporator and condenser. By definition, mass does not cross the boundary of a closed thermodynamic system. Impurities may diffuse across the container boundary of high-temperature heat pipes making the system, in part, thermodynamically open. The second law of thermodynamics predicts the conditions under and the extent to which a chemical reaction or physical process occurs. For a given set of conditions, such processes proceed spontaneously and unidirectionally toward an equilibrium state of minimum free energy. Reaction kinetics at high temperature can overcome many reaction energy barriers and hasten an alkali metal heat pipe's adjustment toward thermodynamic equilibrium.

Distillation of working fluid from the hot zone combined with diffusion and reactions among chemical species in the fluid and in the container accounts for impurity movement within a heat pipe. Solubility-induced corrosion may occur from interaction between the container and the relatively pure condensate in the cold zone. Heat pipe containers, selected to be insoluble in the pure working fluid to well under a part per million, usually are not susceptible to direct solubility corrosion.

Nonmetallic impurities in the cold zone structure can diffuse into the pure condensate. These impurities react with or are dissolved in the condensate that flows toward the evaporator. Such impurities accumulate in the evaporator and may precipitate, plugging the wick, or may form eutectic mixtures with the container. Ternary compounds may also form among the impurities, condensate, and container. Eutectics and ternary compounds with low melting-point temperatures can erode the container or contribute to dewetting.

A.2 Elementary Scaling Variables

Corrosion in alkali metal heat pipes is related to the initial concentration of nonmetallic impurities in the container and fluid plus any impurity movement into the system from external sources. Pure condensate forms a concentration gradient with respect to the container that tends to transfer impurities by condensate flow from the cold zone toward the hot zone. The total impurity content in the condenser and attached structures is then a key variable influencing corrosion. The initial mass of impurities in the condenser over the mass of impurities in the evaporator is a scaling variable affecting corrosion similarity between heat pipe structures. For heat pipe materials with uniform impurity concentration, the volume of condenser to evaporator structures may serve as a proxy for the impurity content ratio as follows:

$$\Xi \equiv (\text{impurity content in condenser}) \times (\text{impurity content in evaporator})^{-1} \approx V_c \left(V_e \right)^{-1} \quad . \tag{40}$$

Corrosion in high-temperature heat pipes can be inhibited with nonsoluble getters that trap impurities during operation. Such getters can be distributed to allow wetting by the condensate and can

be part of the heat pipe container or placed in packs. Assuming a well-distributed getter, the potential for corrosion should relate to the total impurity concentration compared with the total stoichiometric impurity capacity in the getter and container as,

$$\Sigma \equiv (\text{impurity capacity of heat pipe getter}) \times (\text{impurity content of heat pipe})^{-1} \quad . \tag{41}$$

Getter material in high-temperature heat pipes should be hyperstoichiometric compared with nonmetallic impurities from all sources. As a rule of thumb, the impurity capacity to impurity ratio should be at least 10:1 above stoichiometric proportions.

Most proposed mission lifetimes are greater than the time available to life test any reactor design. This constraint suggests the following natural time variable:

$$\tau \equiv (\text{duration of life test}) \times (\text{design life of heat pipe})^{-1} \quad . \tag{42}$$

Corrosion rates are influenced by temperature because of its exponential effect on reaction kinetics. Arrhenius-governed processes govern corrosion rates setting heat pipe lifetime for a set of reactions and temperatures. This suggests that test conditions can be normalized using an expression like,

$$\alpha(T) = \exp\left\{\left(\Delta H(k)^{-1}\right)\left[T_0^{-1} - T^{-1}\right]\right\} \ , \tag{43}$$

where ΔH is activation energy, k is Boltzmann's constant, T_0 is the design temperature, and T is the heat pipe test temperature. Note the numerical results presented here use generic activation energies that are not necessarily representative of the material systems considered. It can be argued that since testing at high temperature accelerates Arrhenius-governed kinetics, this same acceleration applies to heat pipe life. Such simplistic views must be approached with caution. The nature of chemical reactions and their kinetics can change dramatically with absolute temperature. Conditions that apply at one temperature do not necessarily hold for others. Without deeper understanding of the underlying reaction mechanisms, conclusions drawn from such tests can be misleading.

As working fluid flows into the evaporator, it vaporizes, concentrating the impurities and possibly making the corrosion rate dependent on mass fluence. The radial heat flux applied to the evaporator is given by $\dot{q}_{rad} = \dot{q}\ (\pi\ d\ L_e)^{-1}$; mass flux through the evaporator is a function of the radial heat flux, $G = \dot{q}_{rad}\ (h_{fg})^{-1}$. The mass fluence through the evaporator is then given by $M'' = G\ \tau$, yielding

$$M'' = \dot{q}\left(\pi\, d\, L_e\right)^{-1}\left(h_{fg}\right)^{-1} \tau \quad . \tag{44}$$

Mass fluence can easily be increased by applying power along a shortened heat pipe evaporator length. Variation of the mass fluence can be used to accelerate heat pipe life or to affordably test subscale versions of a flight unit.

A.3 Possible Life Test Configuration

A series of accelerated life heat pipes can be designed to permit compression of life-limiting mechanisms from the mission duration to a period consistent with the schedule of a flight program.

Condenser calorimetry, using forced convection of a cooling fluid, is required to achieve the necessary power density and provide realistic boundary conditions for a flight system. A life test heat pipe can be enclosed in a metallic chamber. Mass transfer can be minimized between the heat pipe and its surround-ings by several artifices. A thin-walled tube welded to the cold heat pipe condenser cover mechanically attaches and electrically grounds the heat pipe to an Mo holding fixture. This single point of contact creates a low-temperature boundary that minimizes solid-state diffusion from external impurity sources. Power is applied to the heat pipe evaporator through a noncontact induction heating coil. The chamber is filled with a noble gas mixture that slowly circulates through a hot titanium getter. The gas conducts energy across a gap between the heat pipe condenser and a gas- or water-cooled calorimeter. Coupling between the condenser and the calorimeter is controlled by composition of the gas mixture. The total pressure of the gas mixture is kept just high enough to avoid ionization between the induction coil and the heat pipe. Low chamber gas pressure tends to reduce heat pipe exposure to residual impurity concentrations in the gas mixture. Heat pipe surface temperature is measured with a noncontact, two-band pyrometer.

A.4 Life Test Methods

There are several ways to establish heat pipe material system life without a full-term test. Unfortunately, current budgetary limitations and material availability allow comparatively few tests to study a few key variables. Under current constraints the relevance of subscale testing must be seriously considered. The best available processing procedures must be used for all pipes unless the test scope is greatly expanded. Contamination getters should provide margins typical of flight heat pipe designs, at least 10:1. A heat pipe life test matrix can be developed for a few key material combinations, operating temperatures, and evaporator mass fluences. Boundary conditions should be imposed on the heat pipe to avoid random introduction of external impurities. One remotely possible outcome of a realistic, yet necessarily limited, life test series might be a null result that conclusively confirms the absence of corrosion over the conditions considered. After such an unexpected result, it is a good idea to build a few heat pipes and operate them to deliberately induce corrosion or failure. Life tests that compress operating time may operate near boiling limit margins. Achievable compression will not be known for sure until the first couple of pipes are performance tested.

A.5 Baseline Heat Pipe Life Test

Table 13 shows one possible approach to life testing—a few heat pipes with short evaporators and long condensers. A long condenser serves as a proxy for a large-condenser impurity load. A similar impurity load can be achieved with thickened or impurity-doped condenser walls. A short evaporator increases mass fluence, concentrating impurities, tends to enhance impurity-induced corrosion. The 19:1 condenser-to-evaporator length ratio is not geometrically similar to the 2:1 ratio of the reference design.

The size of the baseline life test series reflects the limited materials now available for heat pipes with comparatively long condensers. The baseline heat pipes in table 13 could be tested over a 3-yr period in the configuration outlined in figure 30. Unfortunately, four heat pipes are insufficient to conduct a meaningful G68–80 series life test. One possible test method varies mass fluence and temperature above the design condition. Both of these variables might change during off-nominal reactor operation, and characterization of their functional relationship is important. To exceed the design mass fluence over the 3-yr period, radial heat flux is concentrated up to 10× the radial heat flux of the reference design. The short

Table 13. Baseline life tests.

Heat Pipe	Wall/Wick Material/ Fluid	L_c/L_e	D_i (cm)	T (K)	$\alpha(T)$	$\dot{q}$ (W)	$\dot{Q}_{rad}$ (W/cm^2)	G (kg/cm^2–s)	t (hr)	M'' (kg/cm^2)
Design	Mo-Re/Na	2	1.41	1,250	1.00	5,752	22	0.059	105,120	2,220
B(1)	Mo-Re/Na	19	1.41	1,273	1.30	5,000	226	0.599	26,280	5,669
B(2)	Mo-Re/Na	19	1.41	1,273	3.74	3,000	136	0.368	26,280	3,483
B(3)	Mo-Re/Na	19	1.41	1,373	1.30	3,000	136	0.36	26,280	3,401
B(4)	Mo-Re/Na	19	1.41	1,173	2.25	4,000	181	0.48	26,280	4,589

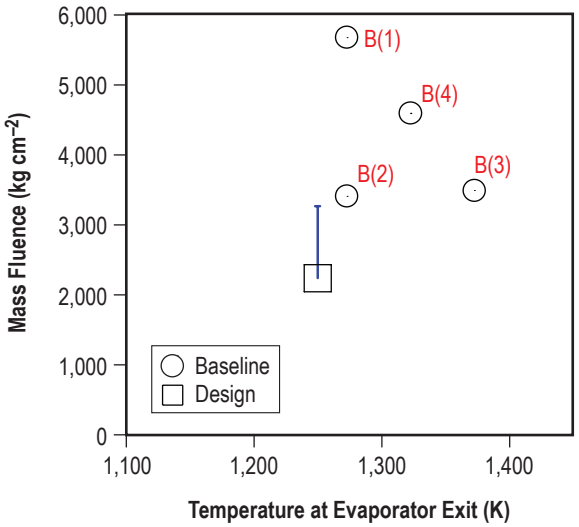

Figure 30. Baseline life test matrix assuming a maximum 1-μm nucleation site radius.

evaporator and high attendant evaporator radial heat fluxes of these life test heat pipes force operation closer to the boiling limit than the reference design. A limited-scope performance test will be required to demonstrate whether these high-radial heat fluxes are achievable with existing fabrication and processing procedures. Nondestructive testing by x-ray and ultrasound techniques can be conducted on each heat pipe at various intervals. At the test conclusion (after 3 yr), appropriate destructive test measurements can include changes in fluid composition, species distribution, and grain boundary conditions, as well as noncondensable gas production measured by residual gas analysis.

A.6 Alternative Heat Pipe Life Test: Option A

The baseline is by no means the only approach possible to life testing given the current constraints. Another approach that attempts to conserve available material, ease fabrication, provide more relevant data, and permit the use of more numerous, yet compact, test fixtures is described here. Instead of building four heat pipes with long condenser sections of uniform cross section, a series of ≈16 short heat pipes with thick-walled condensers could be constructed. These short heat pipes would have similar condenser-to-evaporator area ratios as the reference design. Condenser impurity loading can be imposed by condenser wall thickness.

The boiling limit for the baseline design is invariant with condenser length, so the short heat pipes should perform identically to the longer baseline versions.

This approach potentially offers practical and theoretical benefits. Long Mo wicks are Zr brazed to end plugs near 2,000 K by induction heating of a vacuum-enclosed furnace susceptor. Such an operation is well within the current technology base, but is time consuming to perform. A simpler alternative is to braze end plugs to shorter wicks inside a Centorr furnace. Refractory metal tubes and rods (for gun drilling) for short heat pipes are easier to procure and process. Precious materials are conserved for future use. Figures 31 and 32 show wire-mesh screen requirements for the baseline and option A approaches.

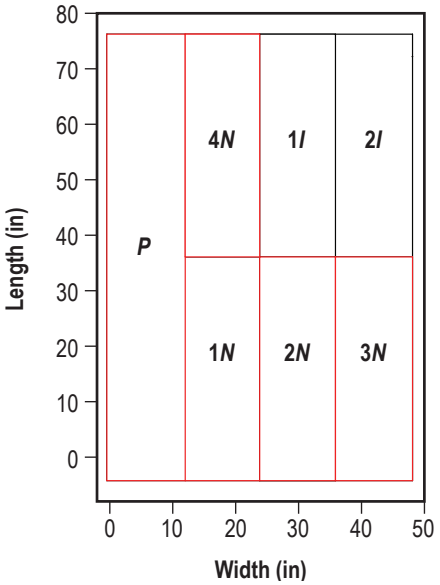

Figure 31. Baseline life test wire cloth use. Symbols *P*, *N*, and *I* represent performance, baseline life, and irradiation tests, respectively.

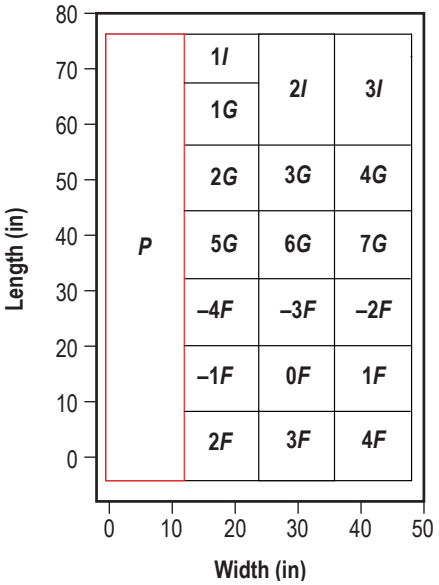

Figure 32. Option A life test wire cloth use. Symbols *P*, *F*, *G*, and *I* represent performance, Fisher, G68–80, and irradiation tests, respectively.

Properly designed short heat pipes tested at relevant temperatures and mass fluence can be made geometrically similar (L_c/L_e) to the reference design heat pipes. Short heat pipes form the basis for virtually all long-term heat pipe corrosion testing to date.[7] A series of short heat pipes permits extrapolation of corrosion effects of a reference design from separate tests conducted over different durations. Relevant information becomes available within months, not years. With this approach, destructive examination of the first life test heat pipe can begin within 6 mo of test initiation. In addition, testing more pipes allows better identification of random manufacturing and processing defects.

Corrosion or reaction metrics can be taken for each test specimen and measurable results can be plotted versus time. NDE of wall and wick integrity by three-dimensional, x-ray computed tomography could be conducted on the entire series at 6-mo intervals. A plot of the corrosion rate versus time normally exhibits a slope that decreases with time; this will be experimentally verified. The long-term corrosion

rate is extrapolated from the slope near the longest test time. This method is outlined in ASTM G68–80.[4] Conditions of an extrapolated test series can closely match those of a proposed reference. Extrapolation tests conducted at prototypic temperatures avoid possible ambiguity in interpreting elevated temperature results.

Since the extrapolation is an accepted and defendable test practice, consideration should be given to following the ASTM G68–80 guidelines for initial screening of life test heat pipes for any material system seriously considered.[4] If time and budget constraints limit the number of life heat pipe tests, extrapolation should be favored over other test methods.

Tables 14 and 15 show a possible test series consisting of ≈16 short heat pipes. One or more experiments from an extrapolation test series could be used to cross-correlate fluence conditions with a Fisher multifactor star design test series conducted at various temperatures and fluences.[3] Such life tests can establish and isolate corrosion trends as a function of temperature and mass fluence. Figures 33 and 34 plot the heat flux, fluence, and temperature relations for the combined test series.

Table 14. Option A life tests Fisher series.

Heat Pipe	Wall/Wick Material/ Fluid	L_c/L_e	D_i (cm)	T (K)	$\alpha(T)$	$\dot{q}$ (W)	$\dot{Q}_{rad}$ (W/cm^2)	G (kg/cm^2–s)	t (hr)	M'' (kg/cm^2)
Design	Mo-Re/Na	2	1.41	1,250	1.00	5,752	22	0.059	105,120	2,233
F(–4)	Mo-Re/Na	3	1.41	1,273	1.30	5,000	226	0.599	26,280	5,669
F(–3)	Mo-Re/Na	3	1.41	1,273	1.30	1,000	45	0.120	26,280	1,134
F(–2)	Mo-Re/Na	3	1.41	1,373	3.74	3,000	136	0.368	26,280	3,483
F(–1)	Mo-Re/Na	3	1.41	1,173	0.38	3,000	136	0.351	26,280	3,321
F(0)	Mo-Re/Na	3	1.41	1,273	1.30	3,000	136	0.360	26,280	3,401
F(1)	Mo-Re/Na	3	1.41	1,223	0.72	2,000	90	0.237	26,280	2,241
F(2)	Mo-Re/Na	3	1.41	1,223	0.72	4,000	181	0.474	26,280	4,481
F(3)	Mo-Re/Na	3	1.41	1,323	2.25	2,000	90	0.243	26,280	2,295
F(4)	Mo-Re/Na	3	1.41	1,323	2.25	4,000	181	0.485	26,280	4,589

Table 15. Option A life tests G68–80 series.

Heat Pipe	Wall/Wick Material/ Fluid	L_c/L_e	D_i (cm)	T (K)	$\alpha(T)$	$\dot{q}$ (W)	$\dot{Q}_{rad}$ (W/cm^2)	G (kg/cm^2–s)	t (hr)	M'' (kg/cm^2)
Design	Mo-Re/Na	2	1.41	1,250	1.00	5,752	22	0.059	105,120	2,233
G–1	Mo-Re/Na	3	1.41	1,273	1.30	3,000	136	0.360	4,380	567
G–2	Mo-Re/Na	3	1.41	1,273	1.30	3,000	136	0.360	8,760	1,134
G–3	Mo-Re/Na	3	1.41	1,273	1.30	3,000	136	0.360	13,140	1,701
G–4	Mo-Re/Na	3	1.41	1,273	1.30	3,000	136	0.360	17,520	2,267
G–5	Mo-Re/Na	3	1.41	1,273	1.30	3,000	136	0.360	21,900	2,834
G–6	Mo-Re/Na	3	1.41	1,273	1.30	3,000	136	0.360	26,280	3,401
G–7	Mo-Re/Na	3	1.41	1,273	1.30	3,000	136	0.360	30,660	3,968

These test series attempt to systematically understand heat pipe corrosion behavior at several temperatures and mass fluences. Conditions for the Fisher test (table 14) represent a two factor (2^2+2 ×2+1) central composite configuration, with temperature and radial heat flux to the evaporator as the two controlled factors. Assuming corrosion is measurable and adequate and forensics are conducted, a multifactor response surface can be developed from this heat pipe corrosion test. In this case, results from the partial two-level factorial test series can identify first-order effects and interactions between the two factors and estimate second-order curvature effects in the data.[3]

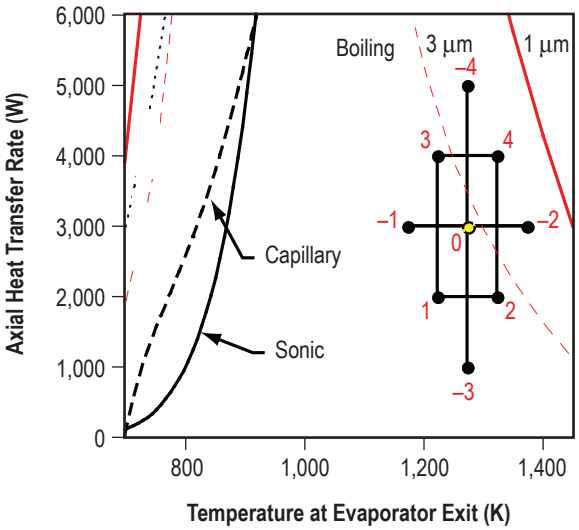

Figure 33. Option A life test design compared to boiling limits at two-nucleation site radii.

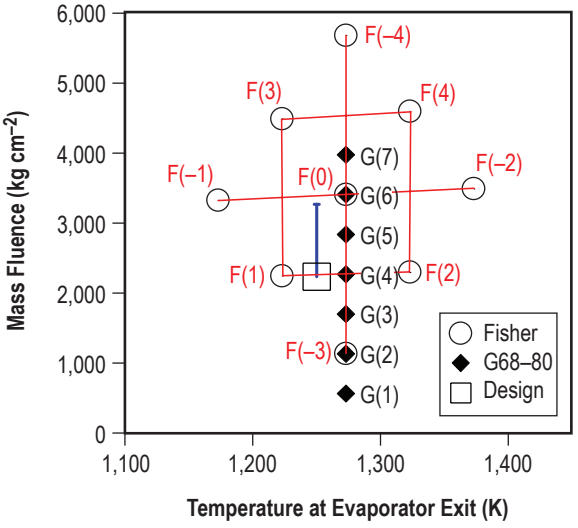

Figure 34. Option A life test matrix assuming a maximum 1-µm nucleation site radius.

APPENDIX B—HEAT PIPE WICK PROCUREMENT SPECIFICATION

B.1 MSFC IFMP Procurement Specification for Heat Pipe Wick Assembly Fabrication

Description—Manufacture complete heat pipe wick assemblies from refractory metal material.

Quantity—18 units.

Material—Government-supplied Mo-5%Re mesh and 0.5-in-diameter Mo-44.5%Re rod stock.

Delivery—ARO 18–22 wk.

Potential Suppliers:

- Advanced Methods and Materials
  1190 Mountain View-Alviso Rd.
  Suite P
  Sunnyvale, CA 94089
  POC: Peter Ring (408–745–7772)

- Refrac Systems
  7201 W. Oakland St.
  Chandler, AZ 85226–2434
  POC: Norm Hubele (480–940–0068)

Source—Competitive (not planning on using a sole source).

B.2 Wick Assembly Fabrication Specifications

After final acceptance of completed wick assemblies, they will be shipped to an MSFC-specified contractor facility. Previous experience fabricating similar hardware components using refractory metal (Mo-Re alloy) mesh material is a significant technical benefit for vendors. The vendor will state relevant experience, procedures, etc. in their response with references of past work and the overall success of these past projects. Heat pipe wick assembly will be fabricated with specifications listed in section B.2.1.

B.2.1 General Specifications

(1) The wick will be fabricated from Mo-5%Re wire cloth with a 400×400 mesh and nominal wire diameter of 0.001 in provided by NASA or its representative.

(2) The wire cloth will be chemically cleaned before processing to remove trace impurities such as iron and carbon. The chemical cleaning steps will be discussed with and approved by MSFC. A sample procedure is provided in section B.3.

(3) During cleaning, the wire cloth material will also be vacuum- or hydrogen-fired (hydrogen dewpoint less then –77 °C), the nature of which will be discussed with and approved by MSFC. During heat treatments, the material will be kept within the cumulative time-temperature envelope, shown in section B.4, to prevent recrystallization of the Mo-5%Re material. (This includes multiple heat-treat steps at different temperatures.) The total number of heat treatments and temperature/time of exposures must be discussed with and approved by MSFC. A sample fabrication process flow is provided in section B.5.

(4) The finished wicks will be composed of seven layers of mesh material that has been drawn or swaged with appropriate procedures discussed with and approved by MSFC to the final dimensions as follows: 0.481-in outside diameter and 0.453-in inside diameter (dimensional tolerance specified in fig. 35, vendor will discuss capabilities with MSFC). The fabricated wick length will be sufficiently long enough to allow material samples to be taken at various fabrication steps (as necessary) for purity measurements and cut to provide a number of final wick products. Estimated wick length is 12.5 in; final exact length will be discussed and approved by MSFC.

(5) Wick straightness will be 0.01 in/ft maximum with wick outside diameter variation not to exceed +0.000/–0.005 in. Ovality (diameters at any cross section) will not violate the tolerance set by the wick outside diameter.

(6) The wick maximum pore radius will be <35 μm once final drawing/swaging has been completed. Bubble-point tests with pure ethyl alcohol will be performed on each wick tube to verify pore radius after fabrication of the wick. Error limits for radius measurement will be within 10% of measured value. Any wick that does not meet the pore size requirement will be marked as defective and set aside.

(7) The condenser end of the wick will remain open.

(8) Fabricate evaporator end plugs from Mo-44.5%Re alloy material supplied by MSFC and custom fit to each wick tube that passes bubble-point test criteria. The vendor will provide design options for the wick evaporator plug that are suitable for crimp attachment of the wick (engineering drawing in fig. 35 serves as a baseline). The proposed design/attachment technique will be supplied to MSFC for discussion and approval.

(9) The maximum pore radius of the final wick assembly (wick with attached evaporator plug) will be <35 μm. Bubble-point tests with pure ethyl alcohol will be performed on each final wick assembly to verify pore size. Any wick assembly that does not meet the pore size requirement will be marked as defective and set aside. The wick tube will be cleaned by hydrogen firing with a hydrogen dewpoint of less than –77 °C) as discussed and approved by MSFC (any heating process will conform to predetermined time-temperature requirements so as not to result in recrystallization of the Mo-5%Re mesh; see item (3).

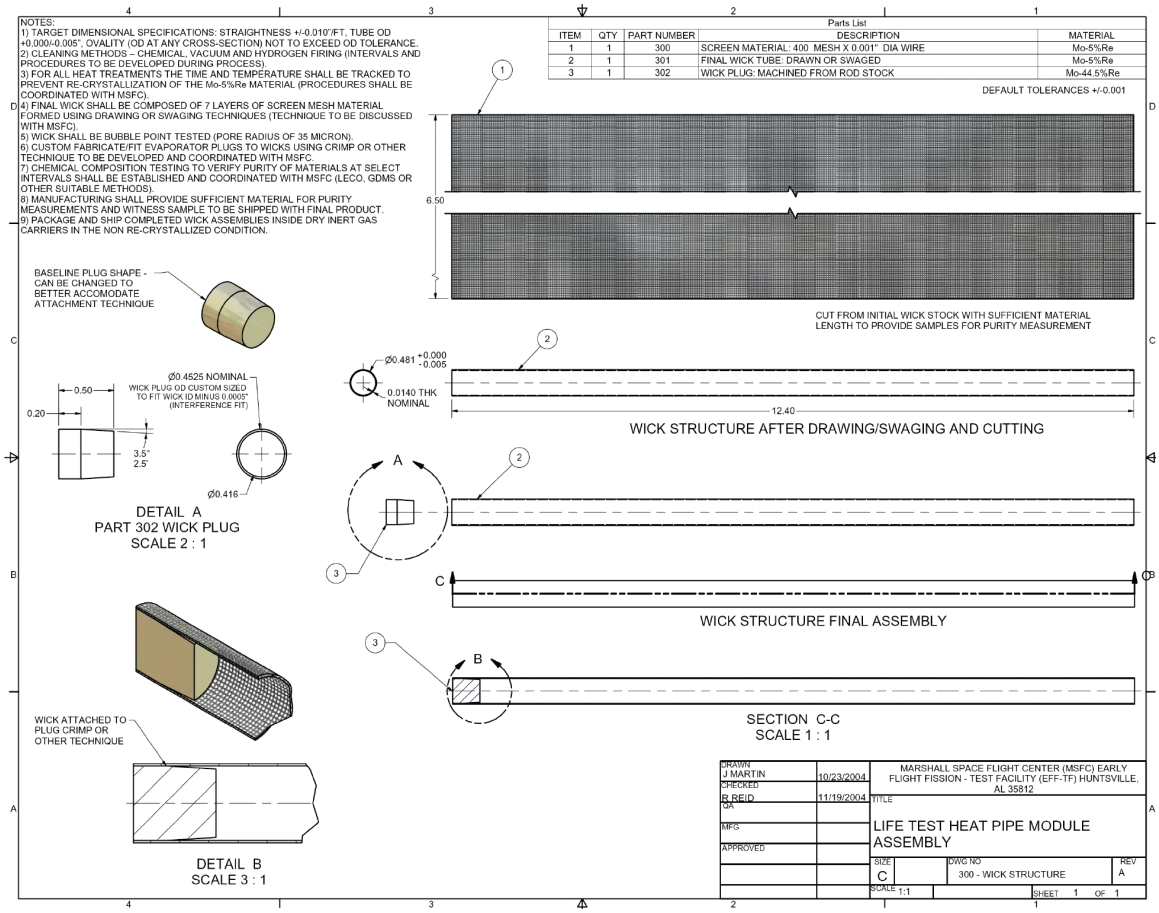

Figure 35. Wick assembly drawing.

(10) Material chemical composition tests (measured in weight parts per million) to determine purity will be performed on the wick material at major manufacturing steps to assess introduction of impurities and quality of the final product (using a LECO elemental analyzer, GDMS, or other suitable method). Initially, the as-received material will be randomly sampled. Additional sampling intervals during wick development (first several units) include required steps (b) and (e) and the recommended but not required steps (a), (c), and (d) as follows:

(a) Random sampling of mesh material after chemical cleaning.

(b) Random sampling of mesh material after vacuum/hydrogen cleaning.

(c) Sample wick material after mandrel dissolution.

(d) Sample wick assembly after plug attachment.

(e) Sample final wick assembly after bubble-point testing and hydrogen-fire cleaning using any excess wick material on the wick assembly or any excess wick tube material from the lot that has accompanied the process as a witness sample. Hydrogen gas used in firing will have a dewpoint less than –77 °C.

Required sample intervals for wick production are as follows:

(a) Sample final complete wick assembly after bubble-point testing and hydrogen-fire cleaning using any excess wick material on the wick assembly or any excess wick tube material from the lot that has accompanied the process as a witness sample. Hydrogen gas used in firing will have a dewpoint less than –77 °C.

The maximum acceptable and target concentrations of each impurity are listed in table 16. Error limits for purity measurements will be within 10% of measured value. The chemical composition will be documented for all testing and provided to MSFC.

Table 16. Impurity chemical composition (acceptable) final wick assembly.

Element	Maximum Acceptable (wppm)	Target (wppm)
O	220	<25
C	85	<20
N	100	<5
H	50	<3
Ca	7	<7
Fe	130	<50
Ni	160	<50
W	300	<100
Si	30	<10
Mg	10	<10
Mn	4	<4
Co	30	<30
Sn	20	<20
B	20	<10

(11) Figure 35 provides an engineering drawing for the wick/wick assembly.

(12) Wick assemblies will be cut to the specified final length prior to packaging and shipment. The residual wick material (2 in or more drawn from each processed assembly) will be packaged with appropriate identification so that it can be matched to the final wicks produced from that drawing process. The residual wick material will be used to document the purity of each wick assembly at an MSFC-designated contractor facility.

(13) Final wick assemblies will be delivered to an MSFC-designated contractor facility. Wick assemblies (with cutoff residual material) will be transported inside inert gas carriers in the uncrystallized condition. Witness tests on the residual material will be conducted at the MSFC-designated contractor facility to verify wick assembly purity (LECO elemental analyzer or other suitable method) and on the wick assemblies to verify maximum pore size (bubble point). For final review/acceptance, the vendor will generate and supply to MSFC “how they did it” documentation for the assembly operation (no proprietary processing) with the results of purity testing, dimensional tolerance checks, bubble-point testing, cleaning, and final assembled weight for each completed heat pipe.

B.3 General Cleaning Procedure for Mo and Mo-Re Parts

(1) Wash the piece in PF solvent, an R113 substitute, until all signs of grease have been removed.

(2) Soak piece for 1–2 min in one part by volume HCl and one part by volume deionized water (target of 10 MΩ-cm or better) to remove residual iron surface impurities.

(3) Soak piece for 5 min in caustic cleaning solution consisting of 11 parts by volume deionized water (target of 10 MΩ-cm or better), 1 part by volume NaOH, and 1 part by volume H_2O_2. Remove piece from caustic bath. Replenish or replace solution as required.

(4) Wash part in hot deionized water (target of 10 MΩ-cm or better) for at least 5 min.

(5) Repeat steps (3) and (4) three times.

(6) Rinse the piece in ethanol inside an ultrasonic cleaner for 5 min.

(7) Vacuum fire or hydrogen fire part as appropriate using not-to-exceed time-temperature relation given in section B.4. Hydrogen gas used in firing will have a dewpoint less than –77 °C.

B.4 Time-Temperature Relation for Mo-5%Re Material

To prevent recrystallization of the Mo-5%Re wick materials, the cumulative time at temperature must be assessed for all expected heat treatments, as shown in table 17. For multiple heat-treat steps at different temperatures, the following relation will apply:

$$\sum\left[\tau_i / \tau_m\left(T_i\right)\right] < 1 \ , \tag{45}$$

where τ_i is the time at temperature, T_i for a given step, and τ_m is the maximum time at temperature for the given step.

Table 17. Mo-5%Re cumulative time at temperature.

Temperature (K)	Maximum Time at Temperature (min)
1,000	2,049.0
1,010	1,448.9
1,020	1,031.6
1,030	739.3
1,040	533.2
1,050	387.0
1,060	282.6
1,070	207.6
1,080	153.3
1,090	113.9
1,100	85.1
1,110	63.9
1,120	48.2
1,130	36.5
1,140	27.9
1,150	21.3
1,160	16.4
1,170	12.7
1,180	9.8
1,190	7.7
1,200	6.0
1,210	4.7
1,220	3.7
1,230	2.9
1,240	2.3
1,250	1.9
1,260	1.5
1,270	1.2
1,280	1.0
1,290	0.8
1,300	0.6

B.5 Sample Process Flow for Heat Pipe Wick Fabrication Simplified Process Flow

(1) Inspect and lay out supplied mesh (received condition).

- Required random material chemical/purity sampling.

(2) Chemically clean supplied mesh.

(3) Vacuum-/hydrogen-fire supplied mesh.

- Required random material chemical/purity sampling of supplied mesh material (during the development process of first several assemblies).

(4) Fabricate mandrels and sheaths.

(5) Clean mandrels and sheaths.

(6) Mount mesh material on mandrel.

(7) Draw.

(8) Clean any lubricants used in process.

(9) Remove mandrel and sheath.

(10) Bubble-point formed wick tube.

(11) Attach evaporator plug to wick tube.

(12) Bubble-point wick tube.

(13) Hydrogen-fire wick assembly.

- Required material chemical/purity sampling of extra wick material carried through the process.

(14) Pack unit for shipment to MSFC.

APPENDIX C—HEAT PIPE MATERIAL PROCUREMENT SPECIFICATION

C.1 IFMP Procurement Specification for Mo-Based Refractory Material

Description—Procure refractory material—Tube and rod stock.

Material—Refractory Mo-44.5%Re or Mo-47.5%Re material.

Quantity—Listed in specification section.

Delivery—ARO 16–20 wk.

Potential Suppliers:

- Rhenium Alloys, Inc.
  1190 Mountain View-Alviso Rd.
  1329 Taylor Street
  Elyria, OH 44036–0245
  POC: Todd Leonhardt (440–365–7388 ext. 243)

- Rembar Compay, Inc.
  P.O. Box 67
  67 Main Street
  Dobbs Ferry, NY 10522
  POC: Walter Pastor (914–693–2620)

- Schwarzkopf Technologies Corp.
  115 Constitution Blvd.
  Franklin, MA 02038
  POC: Sales (800–782–6659)

- H.C. Starck
  460 Jay St.
  Coldwater, MI 49036
  POC: Sales (201–438–9000)

Source—Competitive (not planning on using a sole source).

C.2 Material Specification

Mo-Re alloy tube and rod stock will be produced with a baseline Re composition of either 44.5% or 47.5% (weight percentage—the final composition to be specified by MSFC). The material for the rod and tube products can be formed by powder metallurgy or arc cast, provided that the final drawn/swaged and machined tube and rod stock is fully dense. Previous experience manufacturing similar material shapes from various Mo-Re alloys is a significant technical benefit for the vendor. The vendor will state relevant experience, capability, and manufacturing specifications/guidelines in their response.

Material processing specifications will include the following:

- Straightness and ovality—ASTM A269, A213, or equivalent.
- Mo alloy (rod, bar, wire)—ASTM B387.
- Estimate the average grain size of metals—ASTM E112.
- Density measurement/microstructure technique/specification—determine ductility of final product, procedure/specification to be provided by the vendor.
- Porosity measurement technique/specification—determine ductility of final product, procedure/specification to be provided by the vendor.
- Bending test technique/specification—determine ductility of final product, procedure/specification to be provided by the vendor.

C.2.1 Dimensional

Material stock will conform to the following requirements (vendor will state what they are capable of providing):

- Permissible variations in outside diameter ± 0.005 in.
- Permissible variation in wall thickness for tubing is ±10%.
- Permissible ovality variations in tubing diameter at any cross section cannot exceed the variation in outside diameter given above.
- Permissible straightness is 0.010-in/ft length for 5/8-in-diameter tubes and 0.05 in/ft for 1/4-in-diameter tubes.
- Surface roughness on all tube and rod stock will be 64–125 μin.
- The use of centerless grinding results in a permissible diameter reduction of the outside diameter to ± 0.003 in; however, permissible variation in wall thickness must be maintained in the case of tubing.

C.2.2 Metallurgical

The Mo-Re alloy material for both tubing and rod stock will be processed to conform to the following requirements:

- All material stock will have no interconnecting porosity that would serve as a leak path to He.
- All material stock will be uniform and free of defects/imperfections such as draw marks, cracks, splits, voids, dimples, etc. on both the inner and outer surfaces impacting the use and performance of the parts.
- All material stock will be free of surface and embedded contamination such as residues and films that might be introduced during the fabrication processes, handling, furnace treatments, and chemical cleaning/rinsing.
- All material stock will be furnished in the annealed temper condition with a hardness range to be provided by the vendor to MSFC for approval.
- All material stock can show no more than 1% microstructure as deformation twins of platelet morphology. For the Mo-47.5%Re alloy, it can contain up to a 5% nodular sigma phase (hard and brittle intermetallic compound). For the special alloy Mo-44.5%Re, no sigma phase is present.
- The vendor will provide details regarding the smallest average grain size they are capable of providing in all products (a maximum average grain size of 0.0015 in or smaller is desirable). The vendor will identify a method to be used to quantify the grain size and discuss with MSFC.
- Ductility tests will be performed to verify ductility of product (from material batch). For tubing, this could possibly consist of cutting out a piece of the wall and then bending to a specification. The vendor will determine method and then discuss with MSFC.
- For all Mo-Re alloys, the percentage of Re will be ±0.3% by weight or better.

C.2.3 Material Density Sampling

Random sampling will be performed for each material batch from which the tubing and rod stock is produced. In addition, density sampling will be performed on all final drawn/swaged tube and rod stock to determine effect of processing—documenting the final product density with a target of fully dense. The vendor will provide technique/specification and discuss with/get approval from MSFC.

C.2.4 Chemical Composition

Random material purity sampling will be performed for initial material batch from which the tube and rod stock is produced. In addition, purity tests on all final drawn/swaged and cleaned tube and rod stock (of drawn length) will be performed, documenting the final purity of the product. The test method will conform to LECO elemental analyzer and GDMS or other acceptable methods (will be discussed with and approved by MSFC) to examine both bulk and surface compositions. The maximum acceptable and

target concentrations of each impurity for powder metallurgy material is listed in table 18. Error limits for purity measurements will be within 10% of measured value. The balance of material will be Mo and Re with the weight percentage of Re at ±0.3% of the prescribed composition (44.5% or 47.5%).

Table 18. Impurity chemical composition (acceptable) final heat Mo-Re alloy material (PM).

Element	Maximum (wppm)	Target (wppm)
O	20	<10
C	20	<10
N	30	<3
H	25	<1
Ca	7	<5
Fe	75	<20
Ni	50	<20
W	300	<100
Si	30	<10
Mg	10	<10
Mn	4	<4
Co	30	<30
Sn	20	<20
B	20	<10

For arc cast Mo-Re alloy material, the concentration of oxygen will be maintained at 20 ppm while that of carbon can range from 40 to 80 ppm.

C.2.5 Cleaning

To ensure the purest material stock possible, cleaning will be performed as necessary during processing. The material can be chemically, vacuum/hydrogen fired (hydrogen dewpoint less than –77 °C), or other to accomplish this task. Specific selection and documented procedures will be provided by the vendor and discussed with MSFC for approval (a general sample chemical cleaning specification is provided in section C.4).

C.2.6 Leak Checking

Leak checking will be performed to verify leak tightness of all heat pipe components. Tubing and welded assemblies will be checked with an He mass spectrometer leak detector with a sensitivity capable of detecting leaks rates of 1×10^{-10} std-cc/s of He or lower. All of the tubing (100%) will be leak tested and any defective units identified. Corrective action to repair units with leakage will be discussed and approved by MSFC.

C.2.7 Final Acceptance and Packaging

All tube and rod stock will be verified to conform to required size, quantity, purity, density, leak tightness, and microstructure. Process controls will be in place that document these items and enable tracing of material lots. This documentation will be provided to MSFC for acceptance. All materials

will be packaged in containers that are accepted by common carriers for safe transport and provide the following: (1) Sufficient protection to protect against damage during shipment, (2) cleanliness of the product and prevention of oxidation, and (3) safe transport at the lowest cost rate. All items will be shipped to either MSFC or a designated contractor facility.

C.3 Material Size and Quantity Specifications

The quantity for all items has been increased above the required estimate by 5% to account for production waste and machining as follows with the total price estimated on best available data:

- Item 1
  - Quantity = 246 in—Final product in 13.25-in lengths or multiples.
  - OD = 0.625-in tube.
  - Wall = 0.05 in.

- Item 2
  - Quantity = 38 in—Final product lengths in multiples of 2 in.
  - OD = 0.625-in tube.
  - Wall = 0.03 in.

- Item 3
  - Quantity = 86 in—Final product lengths in multiples of 1.5 in.
  - OD = 0.5-in tube.
  - Wall = 0.03 in.

- Item 4
  - Quantity = 114 in—Final product lengths in multiples of 6 in.
  - OD = 0.25-in tube.
  - Wall = 0.03 in.

- Item 5
  - Quantity = 48 in—Final product lengths in multiples of ≈12 in.
  - OD = 0.625 in rod.

- Item 6
  - Quantity = 20 in—Final product lengths in multiples of ≈12 in.
  - OD = 0.5-in rod.

- Item 7
  - Quantity = 20 in—Final product length in multiples of ≈12 in.
  - OD = 0.05-in rod.

- Item 8
  - Quantity = 20 in^2—Minimum size to cut out 1-in^2 items.
  - THK = 0.03-in sheet.

C.4 General Cleaning Procedure for Mo and Mo-Re Parts

(1) Wash the piece in PF solvent, an R113 substitute, until all signs of grease have been removed.

(2) Soak piece for 1–2 min in one part by volume HCl and one part by volume deionized water (target of 10 MΩ-cm or better) to remove residual iron surface impurities.

(3) Soak piece for 5 min in caustic cleaning solution consisting of 11 parts by volume deionized water (target of 10 MΩ-cm or better), 1 part by volume NaOH, and 1 part by volume H_2O_2. Remove piece from caustic bath. Replenish or replace solution as required.

(4) Wash part in hot, deionized water (target of 10 MΩ-cm or better) for at least 5 min.

(5) Repeat steps (3) and (4) three times.

(6) Rinse piece for 5 min in ethanol inside an ultrasonic cleaner.

APPENDIX D—HEAT PIPE FABRICATION/ASSEMBLY PROCUREMENT SPECIFICATION

D.1 IFMP Procurement Specification for Fabrication of Mo-Alloy Heat Pipe Units

Description—Procure assembled refractory metal Mo alloy-based heat pipe units.

Material—Refractory material and wick assemblies supplied by MSFC (unless otherwise specified in the specifications).

Quantity—18 units.

Delivery—ARO 16–20 wk.

Potential Suppliers:

- Advanced Methods and Materials
  1190 Mountain View-Alviso Rd.
  Suite P
  Sunnyvale, CA 94089
  POC: Peter Ring (408–745–7772)

- Refrac Systems
  7201 W. Oakland St.
  Chandler, AZ 85226–2434
  POC: Norm Hubele (480–940–0068)

- Lockheed-Martin
  Denver, CO
  POC: Suraj Rawal (303–971–9378)

Source—Competitive (not planning on using a sole source).

D.2 Heat Pipe Layout Specification

Heat pipe units will be fabricated from Mo-Re alloy with a baseline Re composition of either 44.5% or 47.5%. The engineering drawings, provided in figures 36 and 37, detail the hardware layout. The Mo-Re heat pipe material and completed wick assemblies will be supplied by MSFC or its representative. The heat pipes will also be equipped with a getter pack located in the evaporator plug. The contractor will purchase the Zr materials required for getter construction as part of this contract. The final output is a fully assembled and cleaned heat pipe unit that is ready for loading with an alkali metal working fluid.

It is a significant technical benefit if the vendor has previous experience manufacturing similar material shapes from various Mo-Re alloys. The vendor will state relevant experience, capability, and manufacturing specifications/guidelines in their response.

D.2.1 Material and assembly specifications include the following:

- Straightness and ovality—ASTM A269 (or equivalent).
- Mo alloy (rod, bar, wire)—ASTM B387 (or equivalent).
- Other applicable machining techniques/specifications:
  - – Determine ductility of final product, procedure/specification to be provided by the vendor.
- Sample EB welds (or other applicable process).
  - – Performed to verify room temperature ductility of final closeout welds; vendor will supply methods to test and verify.

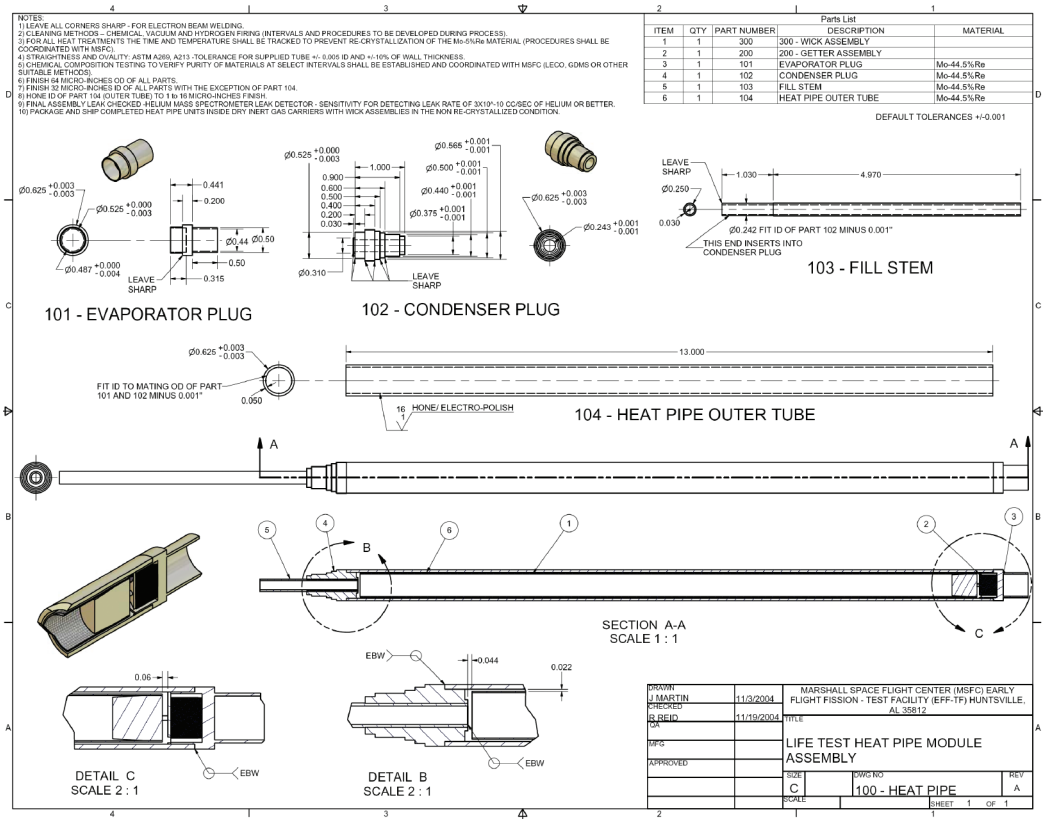

Figure 36. Heat pipe unit layout.

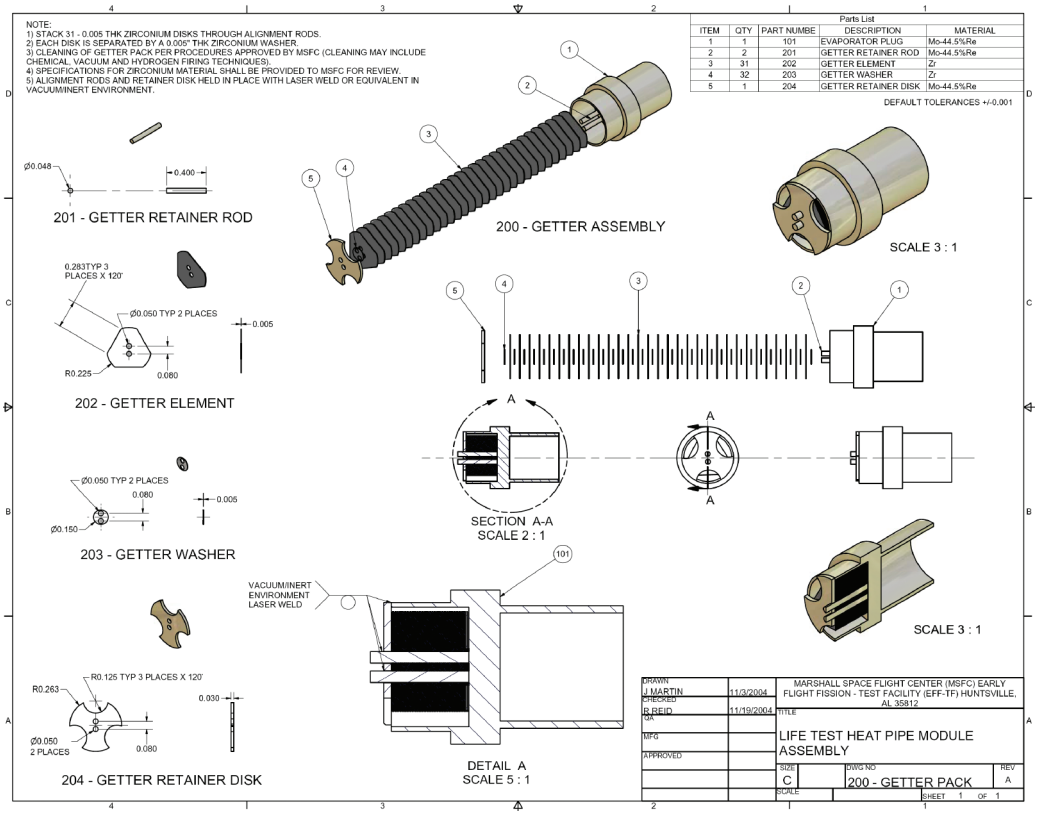

Figure 37. Heat pipe getter pack.

D.2.2 Dimensional

The material stock should conform to the following target requirements (as provided by MSFC material vendor):

- Permissible variations in outside diameter ±0.005 in.
- Permissible variation in wall thickness for tubing is ±10%.
- Permissible ovality variations in tubing diameter at any cross section cannot exceed the variation in outside diameter given above.
- Permissible straightness is 0.01 in/ft length for 5/8-in-diameter tubes and 0.05 in/ft for 1/4-in-diameter tubes. The use of centerless grinding provides for a permissible variation in the outside diameter to ±0.003 in; however, the permissible variation in wall thickness must be maintained in the case of tubing. Deviations will be documented and discussed with MSFC for determination of course of action by the heat pipe fabrication vendor (machining, straightening, material rejection, etc.).

D.2.3 Surface Roughness

All tube and rod stock provided by MSFC will have a 64–125 μin surface finish in the as-received condition. The contractor during fabrication will machine the outer surface of all heat pipe components (tubeand rod) to a surface finish of 64 μin or better. The inner surface of all heat pipe components (tube and rod) will be machined to a surface finish of 32 μin or better. The exception is the inner surface of the heat pipe outer tube (dwg No. 100–HEAT PIPE, item 104) that will be honed to a surface finish of 1–16 μin.

D.2.4 Wick Assembly Verification

The wick assemblies will be received in ready-to-install condition from either MSFC or a specified contractor. Each assembly will include a residual wick piece 2 in or longer to be used in purity tests. These assemblies will be provided by MSFC in a clean condition and contained in inert gas carriers with the Mo-5%Re wick material in an uncrystallized condition. Upon receipt, the contractor will visually inspect the wick assemblies to identify potential shipping damage. During inspection, the wicks will be handled in a clean, inert environment to minimize potential contamination. After inspection, the wick will be stored in the inert gas carriers in a safe location. Two specific tests on the as-received, completed wick assemblies will be conducted by the contractor as follows:

(1) Bubble-point testing will be performed using pure ethyl alcohol with a maximum acceptable pore radius of 35 μm. Any wick assembly that does not meet the pore size requirement will be identified and set aside. This process will be documented and results provided to MSFC.

(2) Material chemical analysis will be performed on a section of residual wick material and provided with each lot of wick assemblies. Residual material that serves as a witness sample should be marked using a LECO elemental analyzer, GDMS, or other suitable method to identify which assemblies it belongs with, the composition documented, and the results provided to MSFC. The maximum acceptable and target concentrations of each impurity for the MSFC-supplied wick assemblies are listed in table 19. The as-received wick assembly chemical analysis will be available to the vendor for comparison.

Table 19. Impurity chemical composition (acceptable) wick assembly.

Element	Maximum Acceptable (wppm)	Target (wppm)
O	220	<25
C	85	<20
N	100	<5
H	50	<3
Ca	7	<7
Fe	130	<50
Ni	160	<50
W	300	<100
Si	30	<10
Mg	10	<10
Mn	4	<4
Co	30	<30
Sn	20	<20
B	20	<10

D.2.5 Chemical Composition

Material purity sampling will be performed (all but getter pack/wick) during the assembly development phase for the first several heat pipe units processed. Material purity tests (measured in weight parts per million) will be performed on components at major assembly steps to determine the introduction of impurities and the quality of the final product. The test method will be LECO elemental analyzer, GDMS, or other acceptable method to examine bulk and surface impurities (will be discussed with and approved by MSFC). The maximum acceptable and target concentrations of each impurity for the MSFC-supplied materials is listed in table 20. The as-received material chemical analysis will be available to the heat pipe assembly contractor and serve as a baseline to monitor the fabrication process (objective is to have no to minimal pickup of impurities during processing). Sampling intervals during development of the process (first several heat pipe units) includes the following potential steps:

- Random sampling of supplied stock (based on lots) recommended.

- Required—Surface sampling of assembled heat pipe components prior to final assembly (just prior to welding).

- It is recommended that a sample material item subjected to similar machining, cleaning, and other processing serve as a witness piece and be carried through the initial production sequence and monitored to get an idea of any contamination pickup.

- Sampling interval for heat pipe production:

  – Surface sampling of complete assembled heat pipes (random locations) after final cleaning and just prior to packaging for shipment.

The fabrication process will be devised so as to introduce no additional impurities above the as-received condition. Error limits for purity measurements will be within 10% of the measured value.

Table 20. Impurity chemical composition (acceptable) final heat Mo-Re alloy material (PM).

Element	Maximum (wppm)	Target (wppm)
O	20	< 10
C	20	< 10
N	30	< 3
H	25	< 1
Ca	7	< 5
Fe	75	< 20
Ni	50	< 20
W	300	< 100
Si	30	< 10
Mg	10	< 10
Mn	4	< 4
Co	30	< 30
Sn	20	< 20
B	20	< 10

D.2.6 Cleaning

Each of the heat pipe components and completed assemblies will be chemically cleaned and/or vacuum-hydrogen fired as specified in procedures (to be discussed with and approved by MSFC). A sample general Mo-Re chemical cleaning specification is provided in section D.3. Each individual part will be cleaned by vacuum-hydrogen firing (does not include the wick/getter pack) once final machining is completed and prior to EB welding. The final heat pipe configuration with installed wick assembly will be cleaned by hydrogen firing (to be discussed with and approved by MSFC). During any heat treatments that involve the wick assembly, the unit will be kept within the cumulative time-temperature envelope, shown in section D.4, to prevent recrystallization of the Mo-5%Re material. (This includes multiple heat-treat steps at different temperatures and past history.) The total number of heat treatments and temperature/time of exposures must be discussed with and approved by MSFC. After final cleaning of the complete heat pipe units, they will be charged (internally) with 1-atm, dry, oil-free Ar (99.999% pure) and the fill stem sealed using a Swagelok compression-type fitting. Specific chemical cleaning procedures for the Zr getter pack with to-be-approved process that will be discussed with and approved by MSFC. Hydrogen gas used in firing to have a dewpoint less than –77 °C.

D.2.7 Leak Checking

Leak checking will be performed to verify leak tightness of all heat pipe components. Tubing and welded assemblies will be checked with an He mass spectrometer leak detector with a sensitivity capable of detecting leaks rates of 1×10^{-10} std-cc/s of He or lower. All components (100% of the heat pipe units) will be leak tested and any defective units identified. Corrective action to repair units identified to leak will be discussed with and approved by MSFC. A minimum of three leak-check intervals (to be used on all heat pipes) are identified:

(1) After EB welding the heat pipe outer tube (dwg. No. 100–HEAT PIPE, item 104) to the evaporator plug (dwg. No. 100–HEAT PIPE, item 101), the wick assembly has not been installed.

(2) After EB welding the fill stem tube (dwg. No. 100–HEAT PIPE, item 103) to the condenser plug (dwg. No. 100–HEAT PIPE, item 102).

(3) After closeout the complete heat pipe assembly—The final EB weld of the heat pipe outer tube (dwg. No. 100–HEAT PIPE, item 104) to the condenser plug (dwg. No. 100–HEAT PIPE, item 102).

D.2.8 Final Acceptance and Packaging

Documentation will be generated for all specific process steps/operations including how they did it (no proprietary processing), results of purity, dimensional tolerances checks, leak testing, cleaning, and final assembled weight; documentation for each completed heat pipe will be provided to MSFC for final review/acceptance. The complete heat pipe units, after acceptance, will be packaged inside inert gas protective transport carriers (type of transport will be discussed with MSFC); the Mo-5%Re wick assemblies will remain in the uncrystallized condition (cumulative time/temperature heat treatments that have involved the wick structure have not exceeded limits to be discussed and approved by MSFC). Additionally, section D.5 lists a sample process flow for the fabrication and assembly process.

D.3 General Cleaning Procedure for Mo and Mo-Re Parts

(1) Wash piece in PF solvent, an R113 substitute, until all signs of grease have been removed.

(2) Soak piece for 1–2 min in one part by volume HCl and one part by volume deionized water (target of 10 MΩ-cm or better) to remove residual iron surface impurities.

(3) Soak piece for 5 min in caustic cleaning solution consisting of 11 parts by volume deionized water (target of 10 MΩ-cm or better), 1 part by volume NaOH, and 1 part by volume H_2O_2. Remove piece from caustic bath. Replenish or replace solution as required.

(4) Wash part in hot, deionized water (target of 10 MΩ-cm or better) for at least 5 min.

(5) Repeat steps (3) and (4) three times.

(6) Rinse piece for 5 min in ethanol inside an ultrasonic cleaner.

(7) Vacuum fire or hydrogen fire part as appropriate using not-to-exceed time-temperature relation given in section D.4). Hydrogen dewpoint will be less than –77 °C.

D.4 Time-Temperature Relation for Mo-5%Re Material

To prevent recrystallization of the Mo-5%Re wick materials, the cumulative time at temperature must be assessed for all expected heat treatments, as shown in table 21. For multiple heat-treat steps at different temperatures, the following relation will apply:

$$\sum\left[\tau_i / \tau_m\left(T_i\right)\right] < 1 \ , \tag{46}$$

where τ_i is the time at temperature, T_i for a given step, and τ_m is the maximum time at temperature for the given step.

Table 21. Mo-5%Re cumulative time at temperature.

Temperature (K)	Maximum Time at Temperature (min)
1,000	2,049.0
1,010	1,448.9
1,020	1,031.6
1,030	739.3
1,040	533.2
1,050	387.0
1,060	282.6
1,070	207.6
1,080	153.3
1,090	113.9
1,100	85.1
1,110	63.9
1,120	48.2
1,130	36.5
1,140	27.9
1,150	21.3
1,160	16.4
1,170	12.7
1,180	9.8
1,190	7.7
1,200	6.0
1,210	4.7
1,220	3.7
1,230	2.9
1,240	2.3
1,250	1.9
1,260	1.5
1,270	1.2
1,280	1.0
1,290	0.8
1,300	0.6

D.5 Sample Process Flow for Heat Pipe Fabrication/Assembly

D.5.1 Simplified Process Flow

(1) Inspect and lay out supplied materials (received condition).

(2) Machine parts.

(3) Chemically clean and or vacuum-hydrogen fire materials.

- Required—Random material chemical/purity sampling of supplied material or sample witness pieces carried through the operations (during development process of first several assemblies).

(4) Fabricate getter pack and assemble in evaporator plug.

(5) Weld heat pipe assembly, except for condenser/fill stem plug to heat pipe body.

(6) Insert wick structure.

(7) Final weld of condenser/fill stem plug to heat pipe body.

(8) Clean unit with hydrogen firing:

- Required—Material chemical/purity sampling of surface or sample material pieces carried through the assembly operation.

(9) Pack unit for shipment to MSFC.

D.5.2 Cost Estimation

- Item 1: Evaporator plug/condenser plug/fill stem—Machine, clean, and EB-weld fill stem to condenser plug – Quantity = 18 of each.

- Item 2: Getter assemblies—With spot welds into the evaporator plugs – Quantity = 18 of each.

- Item 3: Heat pipe tube–Honing, machining, clean, EB weld to evaporator plug and leak check – Quantity = 18 of each.

- Item 4: Heat pipe tube final assembly—Wick, cleaning, leak check, and final cleaning/sampling – Quantity = 18 of each.

- Item 5: Fill stem closeout tube—Machine, assemble, leak check, and clean – Quantity = 18 of each.

- Item 6: Final checkout/packaging and shipping – Quantity = 18 of each.

APPENDIX E—MATERIAL PROPERTIES USED IN ANALYSIS

E.1 Helium/Argon Mixture—Thermal Conductivity Property

The ideal gas approximation is used for the equation of state and specific heat of the He-Ar gas mixture in the gap between the heat pipe and the calorimeter. Thermal conductivities for He-Ar mixtures in the gap are found in data from Touloukian as follows:[25]

$$k_{\mathrm{He}} = 0.0025672 T^{0.716} \quad , \tag{47}$$

$$k_{\mathrm{Ar}} = \left[1.39 \times 10^{-4} T^{0.852} - 1.5 \times 10^{-8} (T - 300)(T - 300)\right]\left[1 + 2 \times 10^{-8} P\right] \quad , \tag{48}$$

and

$$k_{\mathrm{He-Ar}} = f_{\mathrm{Ar}} k_{\mathrm{Ar}} + f_{\mathrm{He}} k_{\mathrm{He}} - \left(k_{\mathrm{Ar}} + k_{\mathrm{He}}\right) f_{\mathrm{Ar}} f_{\mathrm{He}}^{1.5} \quad . \tag{49}$$

Properties for pure He are given in table 22 and figures 38–40, 316 stainless steel in table 23 and figures 41–45, Mo-44%Re in table 24 and figures 46–48, and water in table 25 and figures 49–53.[26–28]

Table 22. Pure He properties at 76 torr.

Temperature (K)	Density (kg/m^3)	Kinematic Viscosity (ν) (m^2/s)	Thermal Conductivity (k) (W/m-K)	Specific Heat (C_p) (J/kg-K)
300	0.016260	1.224×10^{-3}	0.155	5,193
400	0.012190	1.993×10^{-3}	0.189	5,193
500	0.009756	2.911×10^{-3}	0.221	5,193
700	0.006968	5.152×10^{-3}	0.280	5,193
1,000	0.004878	9.471×10^{-3}	0.360	5,193
1,300	0.003752	1.482×10^{-2}	0.434	5,193
1,500	0.003252	1.891×10^{-2}	0.480	5,193

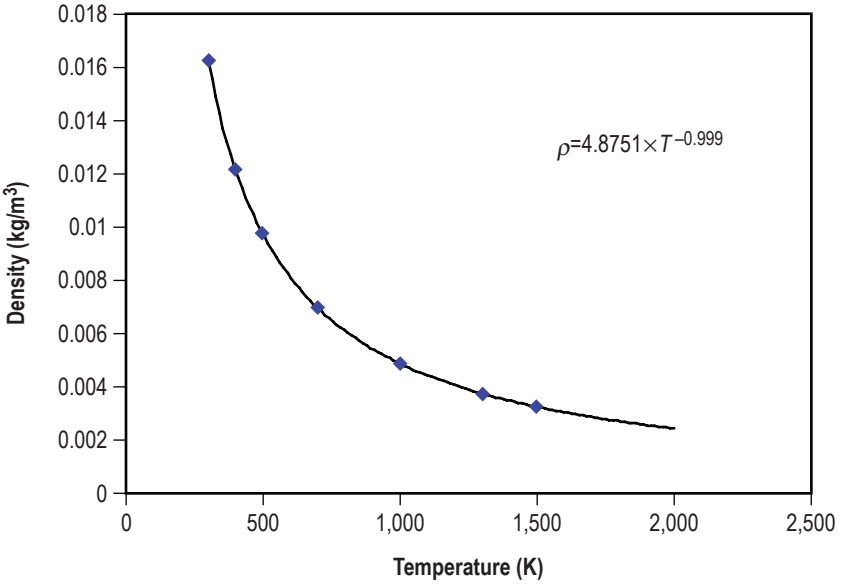

Figure 38. Helium density at 76 torr (1.5 psia).

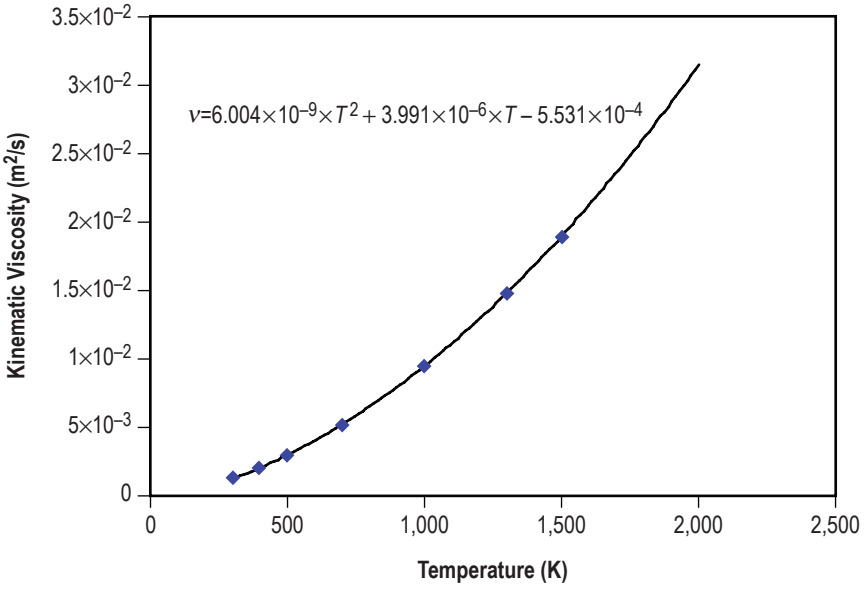

Figure 39. Helium kinematic viscosity at 76 torr (1.5 psia).

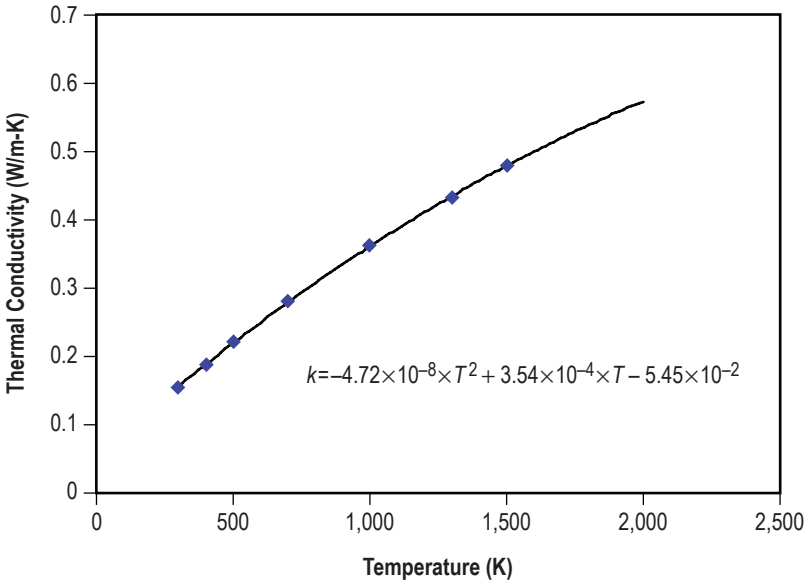

Figure 40. Helium thermal conductivity at 76 torr (1.5 psia).

Table 23. 316 stainless steel properties.

Temperature (K)	Density (kg/m^3)	Emissivity*	Thermal Conductivity (W/m-K)	Specific Heat (J/kg-K)	Coefficient Thermal Expansion (1/K)
273	7972.70	0.33	12.99	456.39	1.49×10^{-5}
300	7960.74	0.34	13.46	467.69	1.52×10^{-5}
400	7916.46	0.37	15.14	502.87	1.60×10^{-5}
500	7872.18	0.41	16.77	529.17	1.67×10^{-5}
600	7827.89	0.44	18.35	548.71	1.74×10^{-5}
700	7783.61	0.47	19.88	563.59	1.79×10^{-5}
800	7739.32	0.50	21.34	575.91	1.83×10^{-5}
900	7695.04	0.54	22.76	587.78	1.87×10^{-5}
1,000	7650.75	0.57	24.11	601.31	1.90×10^{-5}
1,100	7606.47	0.60	25.40	618.61	1.93×10^{-5}
1,200	7562.19	0.63	26.64	641.77	1.95×10^{-5}
1,300	7517.90	0.67	27.81	672.91	1.97×10^{-5}

* Number 8 finish and degraded 33%.

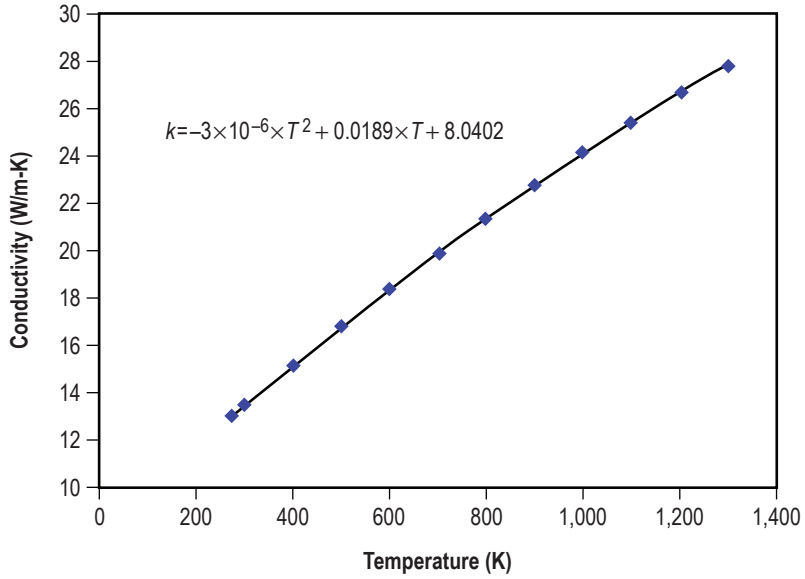

Figure 41. 316 stainless steel thermal conductivity.

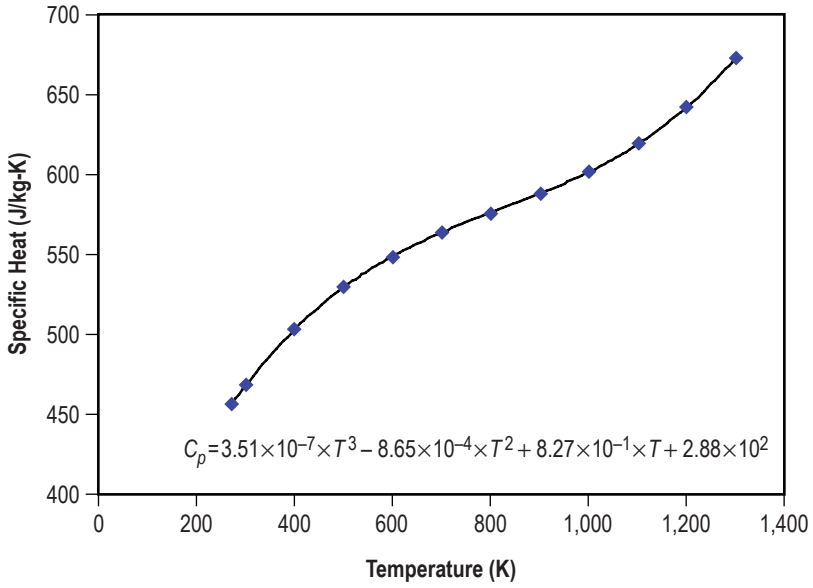

Figure 42. 316 stainless steel specific heat.

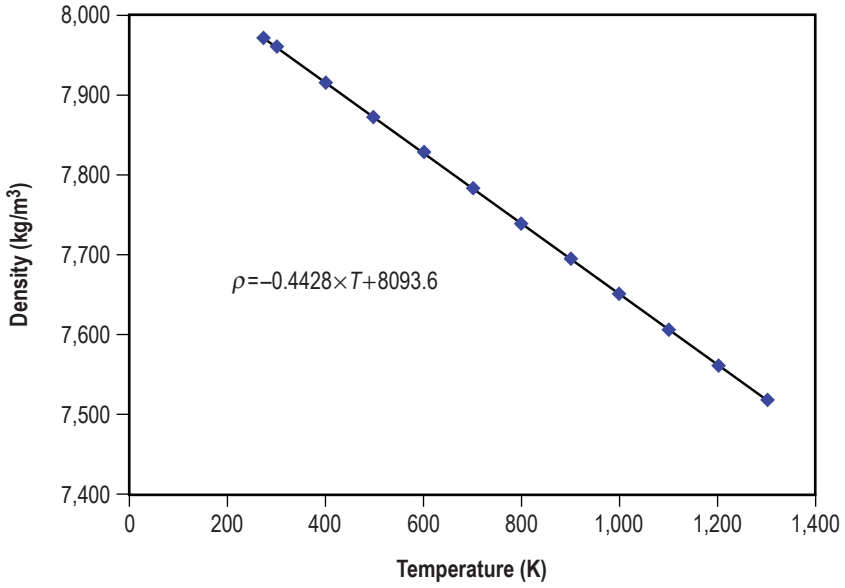

Figure 43. 316 stainless steel density.

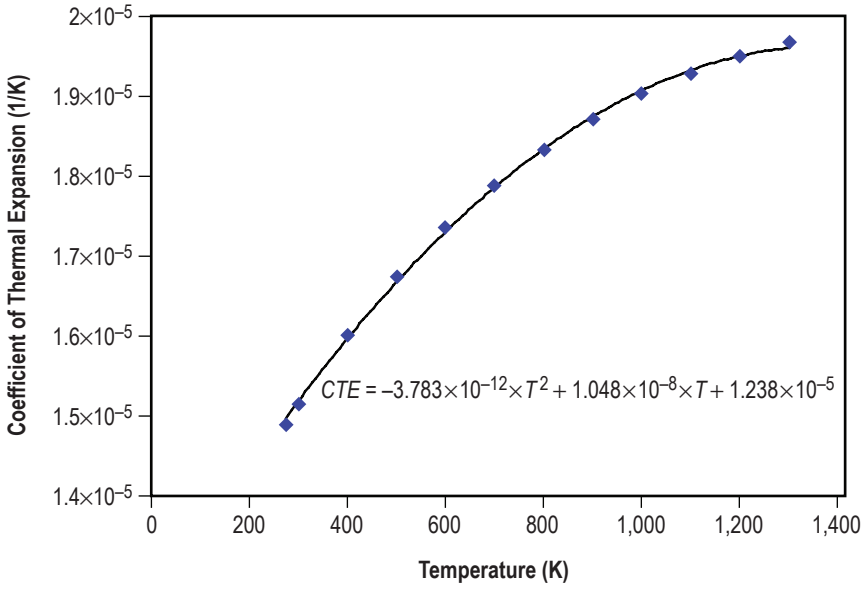

Figure 44. 316 stainless steel *CTE*.

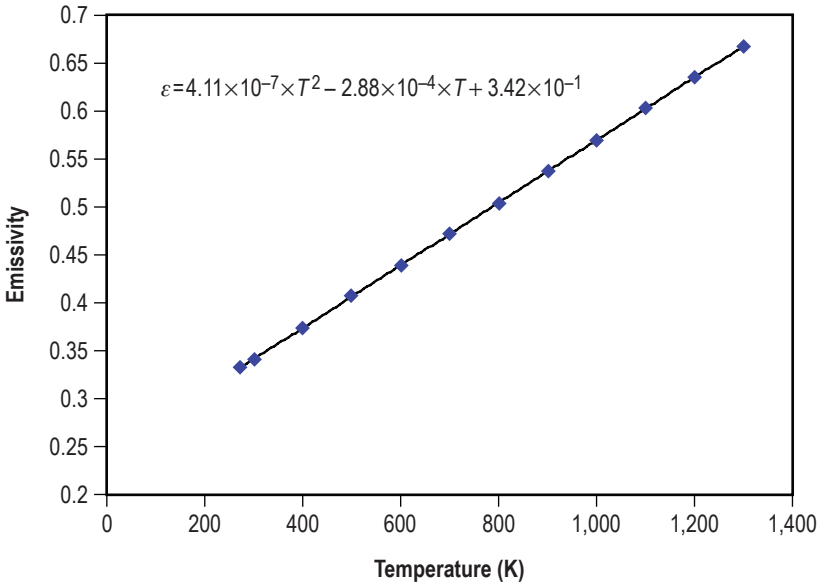

Figure 45. 316 stainless steel emissivity.

Table 24. Mo-44%Re properties.

Density (273 K) = 13.5 g/cm^3 Specific Heat (283 K) = 200 J/kg-K			
Temperature (K)	Emissivity*	Thermal Conductivity (W/m-K)	Coefficient Thermal Expansion (1/K)
273	0.051	41.04	5.84×10^{-6}
300	0.055	41.96	5.85×10^{-6}
400	0.067	45.21	5.9×10^{-6}
500	0.079	48.20	6×10^{-6}
600	0.091	50.94	6.13×10^{-6}
700	0.102	53.42	6.3×10^{-6}
800	0.113	55.65	6.51×10^{-6}
900	0.124	57.62	6.76×10^{-6}
1,000	0.134	59.33	7.04×10^{-6}
1,100	0.144	60.79	7.36×10^{-6}
1,200	0.153	61.99	7.73×10^{-6}
1,300	0.162	62.94	8.12×10^{-6}
1,400	0.171	63.63	8.56×10^{-6}
1,500	0.180	64.07	9.03×10^{-6}
1,600	0.188	64.25	9.55×10^{-6}
1,700	0.196	64.18	1.01×10^{-5}
1,800	0.203	63.85	1.07×10^{-5}
1,900	0.210	63.27	1.13×10^{-5}
2,000	0.217	62.43	1.2×10^{-5}
2,100	0.223	61.34	1.27×10^{-5}
2,200	0.229	59.99	1.34×10^{-5}

* Grit-blasted surface.

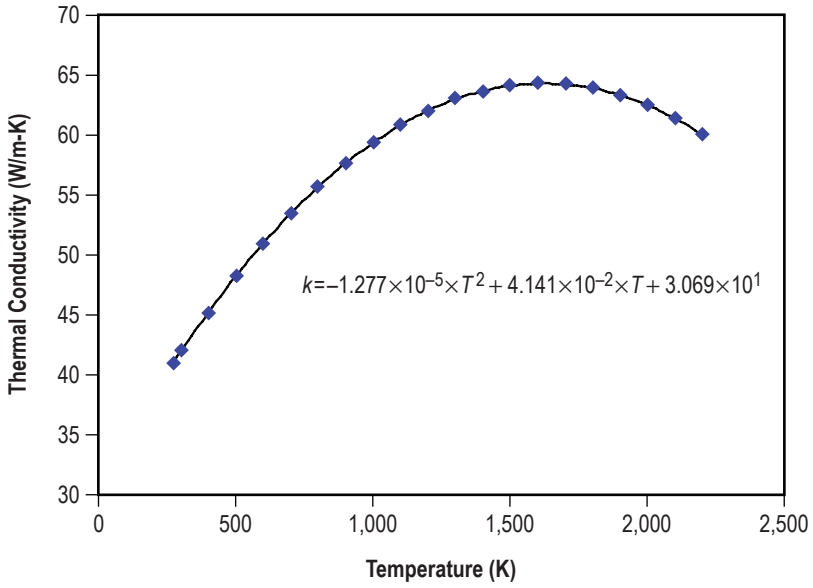

Figure 46. Mo-44%Re thermal conductivity.

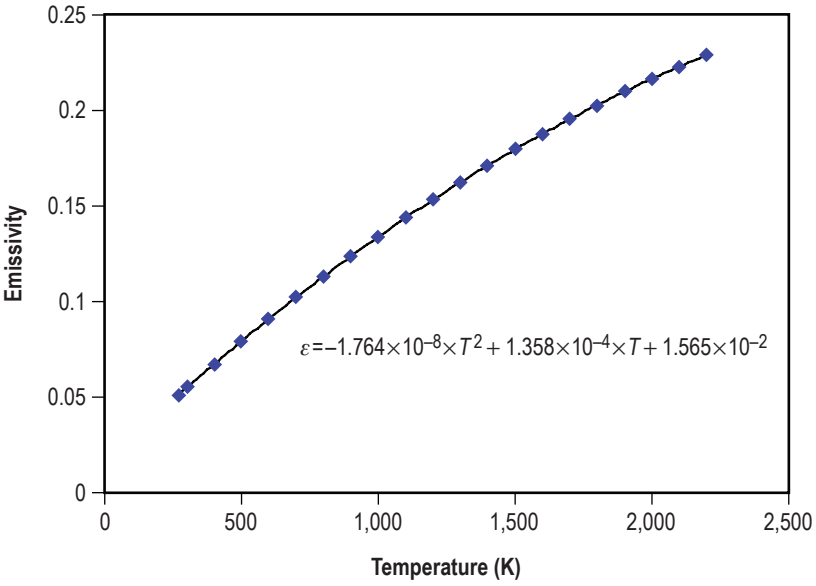

Figure 47. Mo-44%Re emissivity.

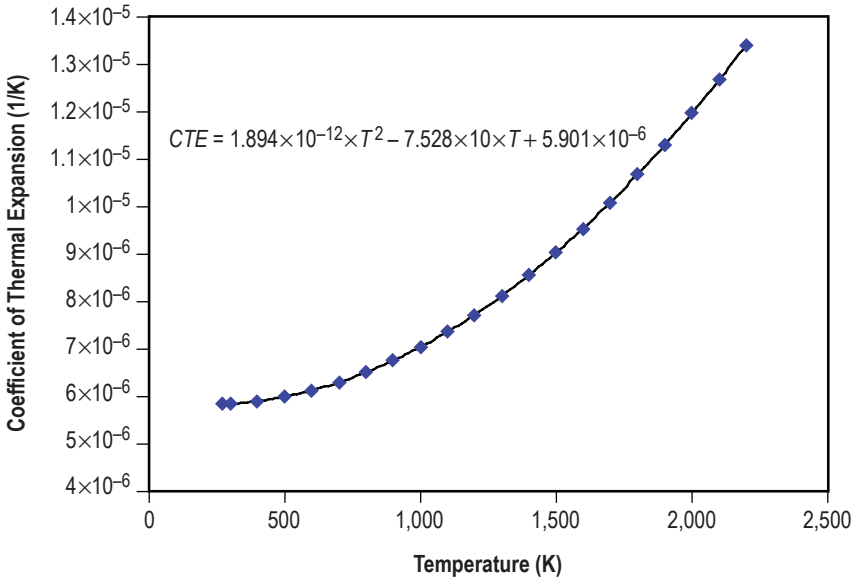

Figure 48. Mo-44%Re *CTE*.

Table 25. Water properties at 0.448 MPa (65 psia).[28]

Temperature (K)	Density (kg/m^3)	Absolute Viscosity (kg/m-s)	Thermal Conductivity (W/m-K)	Specific Heat (J/kg-K)
280	1,000.10	1.433×10^{-3}	0.574	4,199.5
290	998.96	1.084×10^{-3}	0.593	4,185.5
300	996.71	8.538×10^{-4}	0.610	4,179.7
310	993.54	6.936×10^{-4}	0.626	4,178.4
320	989.58	5.771×10^{-4}	0.640	4,179.7
330	984.94	4.896×10^{-4}	0.651	4,182.9
340	979.69	4.221×10^{-4}	0.661	4,187.5
350	973.88	3.689×10^{-4}	0.668	4,193.7
360	967.56	3.262×10^{-4}	0.674	4,201.6
370	960.75	2.915×10^{-4}	0.678	4,211.4
380	953.48	2.628×10^{-4}	0.681	4,223.3
390	945.76	2.388×10^{-4}	0.683	4,237.8
400	937.59	2.187×10^{-4}	0.684	4,255.0
410	928.98	2.015×10^{-4}	0.684	4,275.2
420	919.93	1.867×10^{-4}	0.683	4,298.9

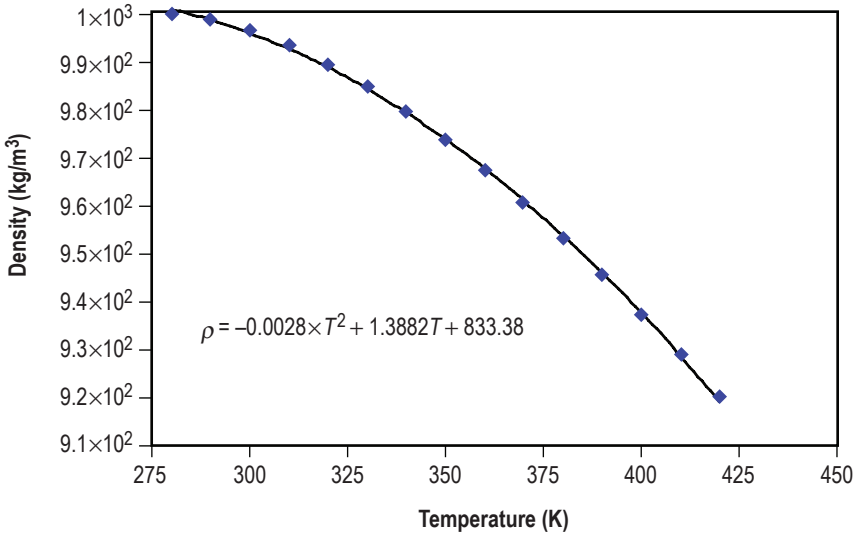

Figure 49. Water density at 0.448 MPa (65 psia).

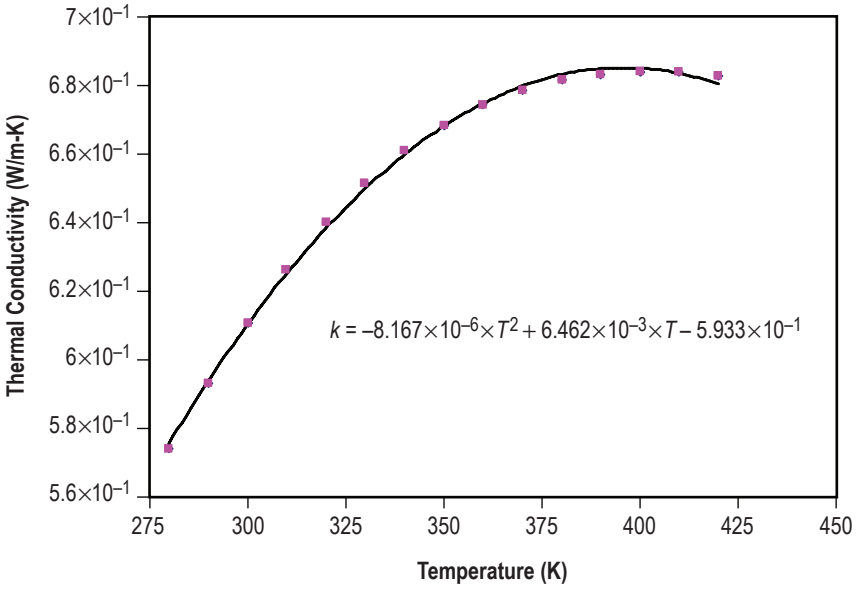

Figure 50. Water thermal conductivity at 0.448 MPa (65 psia).

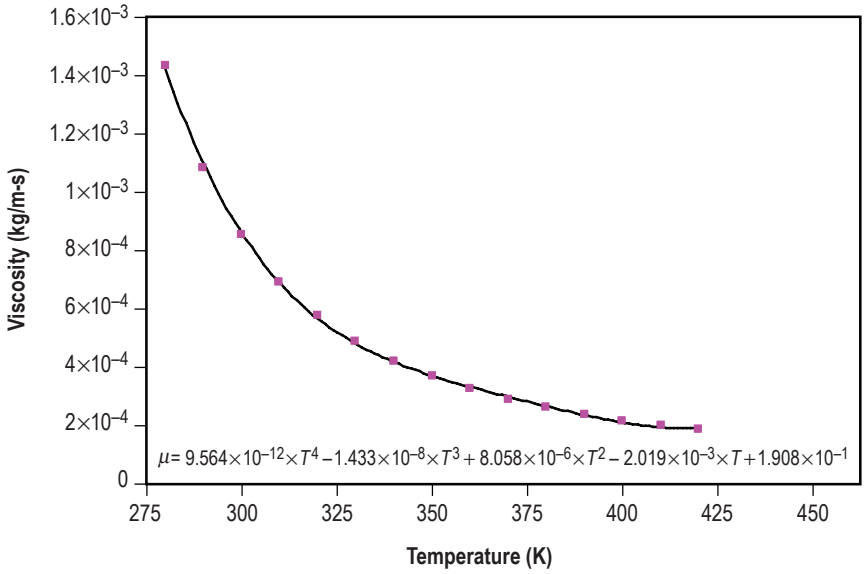

Figure 51. Water absolute viscosity at 0.448 MPa (65 psia).

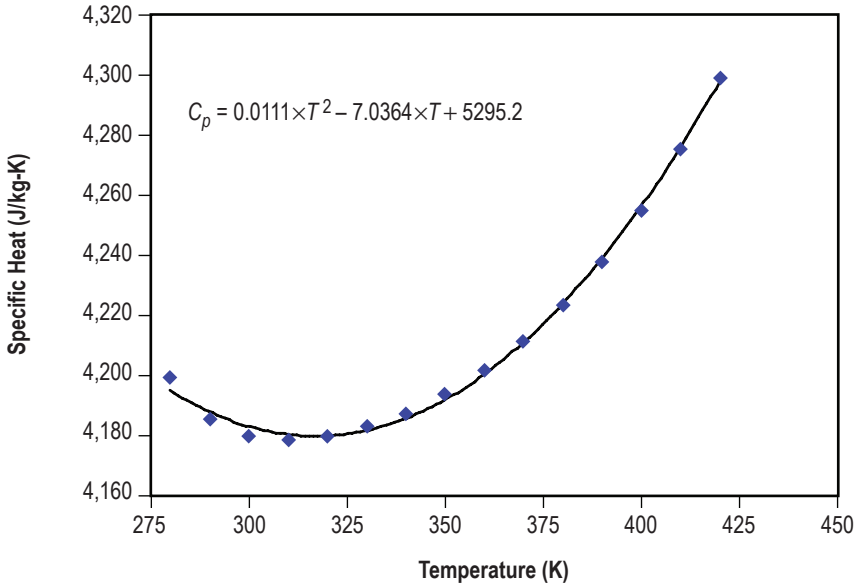

Figure 52. Water specific heat at 0.448 MPa (65 psia).

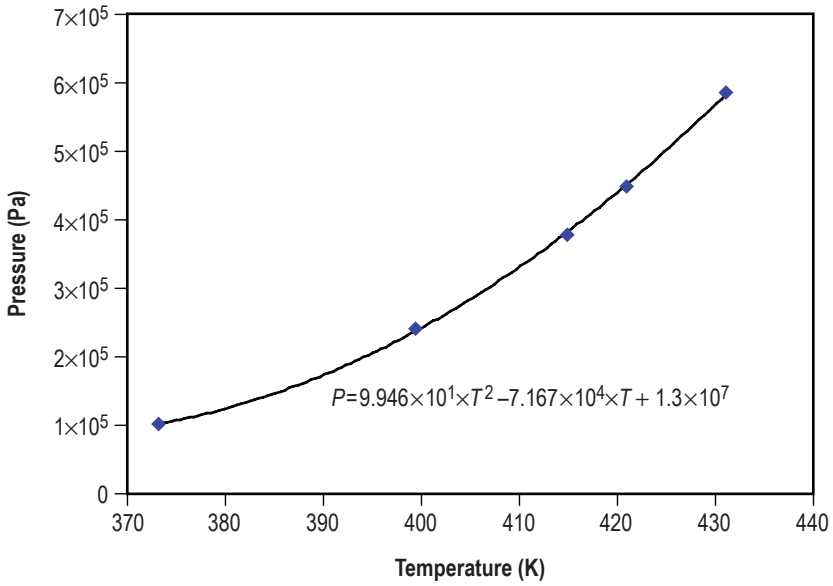

Figure 53. Water boiling point.

APPENDIX F—POWER EXTRACTION PERFORMANCE WORKSHEET

Tables 26–28 provide a quick geometry and performance assessment for water calorimeter heat pipe life time testing with a cooling film annulus of 0.010, 0.015, and 0.020 in.

Table 26. Calorimeter geometry and performance for a cooling film annulus = 0.010 in.

For NRPCT Work Item #2
Water Calorimeter Quick Assessment for Heat pipe life time testing
Assumes: helium/argon gas flooded test chamber at low pressure to improve coupling to calorimeter

- Direct Input Value
- Value Carried From Other Input Location
- parameters of interest

Heat pipe Inputs					
Heat ppe length	0.3048		12	nch	ratio Cond/Evap
Evaporator length	0.06985	m	2.75	nch	
Adiabatic length	0	m	0	nch	
Condenser length	0.23495	m	9.25	nch	
Diameter	0.015875	m	0.625	n OD	
Calorimeter Inputs					
length of cabrmeter	0.3302	m	13	nch	
Cabrmeter Area	0.01171167	m^2	18.153125	nch^2	covering heat ppe
Cabrmeter Area	0.004747974	m^3	7.359375	nch^3	covering support
NormalInlet Temperature	299.8166667	K	80	deg F	
NormalFlowrate	0.027491492	kg/sec	0.435	gabns/mn	
nlet water pressure	446599	Pa	65	psi	
Target Surface Temp (ID)	351	K	172.13	F	on the IDsurface exposed to hot heat pipe (boihg = 420 K at 65psia)
ChannelWalthickness	0.0014732	m	0.058	nch	nner tube exposed to hot heat pipe
ShelWalthickness	0.0014732	m	0.058	nch	middle tube creating the frn flowpath
Cover Walthickness	0.0014732	m	0.058	nch	outer tube seahg the return path
frn flowGap	0.000254	m	0.01	nch	water flowgap on nner annulus (outlet flow) next to heat ppe - this absorbs the heat
Return FlowGap	0.003175	m	0.125	nch	water flowgap on outer annulus (nlet flow)

Variables	Units	Test Condition → G series	F(-4)	F(-3)	F(-2)	F(-1)	F(1)	F(2)	F(3)	F(4)	F(0)
Power (W)	W	3000	5000	1000	3000	3000	2000	4000	2000	4000	3000
Heat Ppe Surface Temperature	K	1273	1273	1273	1373	1173	1223	1223	1323	1323	1273
Average Gas Gap Temperature	K	811.5	829	800.5	861.5	761.5	779	794	829	844	811.5
Cabrmeter ChannelID Temperature	K	350	385	328	350	350	335	365	335	365	350
Cabrmeter ChannelWalOD Temperature	K	349.05	383.42	327.74	349.07	349.04	334.39	363.71	334.40	363.72	349.05
Cabrmeter ChannelWalDeta Temp	K	0.95	1.58	0.26	0.93	0.96	0.61	1.29	0.60	1.28	0.95
Dimensions (meters)											
Heat Ppe OD at Room Temperature	m	0.01588	0.01588	0.01588	0.01588	0.01588	0.01588	0.01588	0.01588	0.01588	0.01588
Heat Ppe OD at Temperature	m	0.01597	0.01597	0.01597	0.01598	0.01595	0.01596	0.01596	0.01597	0.01597	0.01597
Condenser Length	m	0.23495	0.23495	0.23495	0.23495	0.23495	0.23495	0.23495	0.23495	0.23495	0.23495
Gas Gap Width - HP OD to Cabrmeter ID	m	0.00065	0.00063	0.00265	0.00078	0.00053	0.00084	0.00043	0.00117	0.00051	0.00065
Cabrmeter ChannelWallD	m	0.01726	0.01723	0.02126	0.01754	0.01702	0.01785	0.01681	0.01831	0.01699	0.01726
Cabrmeter ChannelWalOD	m	0.02021	0.02018	0.02420	0.02049	0.01997	0.02079	0.01976	0.02125	0.01994	0.02021
Cabrmeter ChannelWalThickness	m	0.00147	0.00147	0.00147	0.00147	0.00147	0.00147	0.00147	0.00147	0.00147	0.00147
Cabrmeter ShelWallD	m	0.02072	0.02069	0.02471	0.02100	0.02048	0.02130	0.02026	0.02176	0.02045	0.02072
Cabrmeter ShelWalOD	m	0.02366	0.02363	0.02766	0.02395	0.02342	0.02425	0.02321	0.02471	0.02339	0.02366
Cabrmeter ShelWalThickness	m	0.00147	0.00147	0.00147	0.00147	0.00147	0.00147	0.00147	0.00147	0.00147	0.00147
Cabrmeter Cover WallD	m	0.03001	0.02998	0.03401	0.03030	0.02977	0.03060	0.02956	0.03106	0.02974	0.03001
Cabrmeter Cover WalOD	m	0.03296	0.03293	0.03695	0.03324	0.03272	0.03354	0.03251	0.03400	0.03269	0.03296
Cabrmeter Cover WalThickness	m	0.00147	0.00147	0.00147	0.00147	0.00147	0.00147	0.00147	0.00147	0.00147	0.00147
Frn FlowGap Thickness	m	0.00025	0.00025	0.00025	0.00025	0.00025	0.00025	0.00025	0.00025	0.00025	0.00025
Return FlowGap Thickness	m	0.00318	0.00318	0.00318	0.00318	0.00318	0.00318	0.00318	0.00318	0.00318	0.00318
Frn Hydraulc Diameter (Douter-Dnner)	m	0.000508	0.000508	0.000508	0.000508	0.000508	0.000508	0.000508	0.000508	0.000508	0.000508
Dimensions (inches)											
Heat Ppe OD at Room Temperature	n	0.6250	0.6250	0.6250	0.6250	0.6250	0.6250	0.6250	0.6250	0.6250	0.6250
Heat Ppe OD at Temperature	n	0.6286	0.6286	0.6286	0.6290	0.6281	0.6283	0.6283	0.6288	0.6288	0.6286
Condenser Length	n	9.2500	9.2500	9.2500	9.2500	9.2500	9.2500	9.2500	9.2500	9.2500	9.2500
Gas Gap Width - HP OD to Cabrmeter ID	n	0.0255	0.0249	0.1041	0.0309	0.0210	0.0371	0.0167	0.0460	0.0201	0.0255
Cabrmeter ChannelWallD	n	0.6796	0.6784	0.8368	0.6907	0.6701	0.7026	0.6618	0.7207	0.6690	0.6796
Cabrmeter ChannelWalOD	n	0.7956	0.7944	0.9528	0.8067	0.7861	0.8186	0.7778	0.8367	0.7850	0.7956
Cabrmeter ChannelWalThickness	n	0.0580	0.0580	0.0580	0.0580	0.0580	0.0580	0.0580	0.0580	0.0580	0.0580
Cabrmeter ShelWallD	n	0.8156	0.8144	0.9728	0.8267	0.8061	0.8386	0.7978	0.8567	0.8050	0.8156
Cabrmeter ShelWalOD	n	0.9316	0.9304	1.0888	0.9427	0.9221	0.9546	0.9138	0.9727	0.9210	0.9316
Cabrmeter ShelWalThickness	n	0.0580	0.0580	0.0580	0.0580	0.0580	0.0580	0.0580	0.0580	0.0580	0.0580
Cabrmeter Cover WallD	n	1.1816	1.1804	1.3388	1.1927	1.1721	1.2046	1.1638	1.2227	1.1710	1.1816
Cabrmeter Cover WalOD	n	1.2976	1.2964	1.4548	1.3087	1.2881	1.3206	1.2798	1.3387	1.2870	1.2976
Cabrmeter Cover WalThickness	n	0.0580	0.0580	0.0580	0.0580	0.0580	0.0580	0.0580	0.0580	0.0580	0.0580
Frn FlowGap Thickness	n	0.0100	0.0100	0.0100	0.0100	0.0100	0.0100	0.0100	0.0100	0.0100	0.0100
Return FlowGap Thickness	n	0.1250	0.1250	0.1250	0.1250	0.1250	0.1250	0.1250	0.1250	0.1250	0.1250
Frn Hydraulc Diameter (Douter-Dnner)	n	0.0200	0.0200	0.0200	0.0200	0.0200	0.0200	0.0200	0.0200	0.0200	0.0200
Material Emissivity											
Emissivty Mo-44.5Re @ Temp		0.16	0.16	0.16	0.17	0.15	0.16	0.16	0.16	0.16	0.16
Emissivty Copper C122		0.44	0.44	0.44	0.44	0.44	0.44	0.44	0.44	0.44	0.44
Effective Emissivty		0.13	0.14	0.13	0.14	0.13	0.13	0.13	0.14	0.14	0.13
Heat Transfer Gas Gap											
Radiation Heat Transfer Gap	W	235.31	234.79	235.67	333.99	160.81	195.56	195.11	281.58	281.10	235.31
Conduction Heat Transfer Gap	W	2764.69	4765.21	764.33	2666.01	2839.19	1804.44	3804.89	1718.42	3718.90	2764.69
Gas Gap Composition	Helium-Argon	32% Ar	6% Ar	32% Ar	32% Ar	32% Ar	32% Ar	32% Ar	32% Ar	32% Ar	32% Ar
Helium Thermal conductivity @ Avg Temp	W/m-K	0.31	0.32	0.31	0.32	0.30	0.30	0.31	0.32	0.32	0.31
Gas Gap Compensation factor		0.51	0.88	0.51	0.51	0.51	0.51	0.51	0.51	0.51	0.51
Effective Gas Gap Thermal Conductivty	W/m-K	0.1585	0.2777	0.1569	0.1655	0.1513	0.1538	0.1560	0.1609	0.1630	0.1585
Cabrmeter Material		copper C122	copper C122	copper C122	copper C122	copper C122	copper C122	copper C122	copper C122	copper C122	copper C122
Cabrmeter ChannelWalThermalConductivty	W/m-K	339.0	339.0	339.0	339.0	339.0	339.0	339.0	339.0	339.0	339.0
Calorimeter Cooling Fluid		Water	Water	Water	Water	Water	Water	Water	Water	Water	Water
Avg Temp Used for Fluid Properties	K	314.7	326.6	313.1	315.0	314.4	311.4	317.7	311.7	318.1	314.7
Water FlowRate	kg/sec	0.024	0.022	0.009	0.024	0.025	0.021	0.027	0.020	0.026	0.024
Water FlowRate	gal/min	0.382	0.354	0.142	0.374	0.390	0.328	0.423	0.319	0.415	0.382
Inlet Water Pressure	Pa	446599	446599	446599	446599	446599	446599	446599	446599	446599	446599
Inlet Water Pressure	psi	65.00	65.00	65.00	65.00	65.00	65.00	65.00	65.00	65.00	65.00
Water Inlet Temperature	K	299.82	299.82	299.82	299.82	299.82	299.82	299.82	299.82	299.82	299.82
Log mean Water Frn Flowtemp Walto Fluid	K	33.15	54.08	9.26	32.67	33.57	21.63	44.92	21.15	44.48	33.15
Average Water Frn FlowTemperature	K	314.66	326.58	313.11	315.01	314.36	311.35	317.72	311.68	318.05	314.66
Water frn flowtemp deta (nlet to outlet)	K	29.69	53.52	26.58	30.38	29.09	23.07	35.82	23.72	36.47	29.69
Water Outlet Temperature	K	329.51	353.34	326.40	330.20	328.90	322.89	335.63	323.54	336.29	329.51
Water specfic heat Cp	J/kg-K	4180.15	4181.12	4180.25	4180.13	4180.16	4180.44	4180.10	4180.40	4180.10	4180.15
Water thermal conductivty k	W/m-K	0.63	0.65	0.63	0.63	0.63	0.63	0.64	0.63	0.64	0.63
water density rho	kg/m3	992.96	988.11	993.53	992.83	993.07	994.17	991.79	994.05	991.66	992.96
Water Absolute Viscosty mu	kg/m-s	0.000641	0.000518	0.000661	0.000637	0.000645	0.000685	0.000604	0.000680	0.000601	0.000641
Log Mean Temperature Difference Walto Fluid	K	33.15	54.08	9.26	32.67	33.57	21.63	44.92	21.15	44.48	33.15
Heat Transfer To Cooling Fluid											
ChannelFlowTube surface		smooth	smooth	smooth	smooth	smooth	smooth	smooth	smooth	smooth	smooth
ShelFlowTube surface		smooth	smooth	smooth	smooth	smooth	smooth	smooth	smooth	smooth	smooth
Type of flow(Re<2300 = Lamnar)		Lamnar	Lamnar	Lamnar	Lamnar	Lamnar	Lamnar	Lamnar	Lamnar	Lamnar	Lamnar
Frn FlowArea	m^2	1.63E-05	1.63E-05	1.95E-05	1.65E-05	1.61E-05	1.68E-05	1.60E-05	1.72E-05	1.61E-05	1.63E-05
Frn FlowVelocty	m/sec	1.49	1.39	0.46	1.44	1.54	1.24	1.69	1.18	1.64	1.49
Reynolds Number		1173.92	1345.37	354.59	1139.23	1205.44	916.26	1407.13	878.00	1377.93	1173.92
Nusset Number		4.88	4.88	4.88	4.88	4.88	4.88	4.88	4.88	4.88	4.88
Convective heat Transfer Coeff h	W/m^2-K	6070.63	6210.99	6045.76	6074.60	6067.12	6026.85	6109.50	6030.49	6113.20	6070.63
Check on power balance -convection side	*W*	*3000.00*	*5000.00*	*1000.00*	*3000.00*	*3000.00*	*2000.00*	*4000.00*	*2000.00*	*4000.00*	*3000.00*
Check power balance - water flow side	*W*	*3000.00*	*5000.00*	*1000.00*	*3000.00*	*3000.00*	*2000.00*	*4000.00*	*2000.00*	*4000.00*	*3000.00*
Pressure Drop in Film Channel											
viscosty ratio (mu-buk to mu-wal)		1.70	2.12	1.31	1.69	1.71	1.50	1.91	1.49	1.90	1.70
annular passage dia ratio dinner/douter		0.975	0.975	0.979	0.976	0.975	0.976	0.975	0.977	0.975	0.975
annular passage adjustment factor		1.49998	1.49998	1.49999	1.49999	1.49998	1.49999	1.49998	1.49999	1.49998	1.49998
factor for f/Re expression		84.0	79.6	89.8	84.2	83.9	86.7	81.6	86.8	81.7	84.0
friction factor f smooth channel		0.072	0.059	0.253	0.074	0.070	0.095	0.058	0.099	0.059	0.072
Cabrmeter Length	m	0.330	0.330	0.330	0.330	0.330	0.330	0.330	0.330	0.330	0.330
Data pressure in Frn Channel	Pa	51381.0	36578.7	17631.2	49283.4	53308.6	47202.5	53269.0	44716.0	51616.1	51380.9
Data pressure in Frn Channel	psi	7.5	5.3	2.6	7.2	7.8	6.9	7.8	6.5	7.5	7.5
Data Pressure/Inlet Pressure		0.115	0.082	0.039	0.110	0.119	0.106	0.119	0.100	0.116	0.115

Table 27. Calorimeter geometry and performance for a cooling film annulus = 0.015 in.

For NRPCT Work Item #2
Water Calorimeter Quick Assessment for Heat pipe life time testing
Assumes: helium/argon gas flooded test chamber at low pressure to improve coupling to calorimeter

- Dect Input Value
- Value Carried From Other Input Location
- parameters of interest

Heat pipe Inputs					
Heat ppe length	0.3048		12	nch	ratio Cond/Evap
Evaporator length	0.06985	m	2.75	nch	
Adiabatic length	0	m	0	nch	
Condenser length	0.23495	m	9.25	nch	
Diameter	0.015875	m	0.625	n OD	
Calorimeter Inputs					
length of calorimeter	0.3302	m	13	nch	
Calorimeter Area	0.01171167	m^2	18.153125	nch^2	covering heat pipe
Calorimeter Area	0.004747974	m^3	7.359375	nch^3	covering support
Nominal Inlet Temperature	299.8166667	K	80	deg F	
Nominal Flowrate	0.027491492	kg/sec	0.435	gpm/min	
inlet water pressure	446599	Pa	65	psi	
Target Surface Temp (ID)	351	K	172.13	F	on the ID surface exposed to hot heat pipe (boihg = 420 K at 65psia)
Channel Wall thickness	0.0014732	m	0.058	nch	inner tube exposed to hot heat pipe
Shell Wall thickness	0.0014732	m	0.058	nch	middle tube creating the ffm flowpath
Cover Wall thickness	0.0014732	m	0.058	nch	outer tube sealing the return path
ffm flow Gap	0.000381	m	0.015	nch	water flow gap on inner annulus (outlet flow) next to heat ppe - this absorbs the heat
Return Flow Gap	0.003175	m	0.125	nch	water flow gap on outer annulus (inlet flow)

Variables	Units	Test Condition --> G series	F(-4)	F(-3)	F(-2)	F(-1)	F(1)	F(2)	F(3)	F(4)	F(0)
Power (W)	W	3000	5000	1000	3000	3000	2000	4000	2000	4000	3000
Heat Pipe Surface Temperature	K	1273	1273	1273	1373	1173	1223	1223	1323	1323	1273
Average Gas Gap Temperature	K	816.5	834.5	805.5	866.5	766.5	781.5	801.5	831.5	851.5	816.5
Calorimeter Channel ID Temperature	K	360	396	338	360	360	340	380	340	380	360
Calorimeter Channel Wall OD Temperature	K	359.05	394.42	337.74	359.07	359.04	339.39	378.71	339.40	378.72	359.05
Calorimeter Channel Wall Delta Temp	K	0.95	1.58	0.26	0.93	0.96	0.61	1.29	0.60	1.28	0.95
Dimensions (meters)											
Heat Pipe OD at Room Temperature	m	0.01588	0.01588	0.01588	0.01588	0.01588	0.01588	0.01588	0.01588	0.01588	0.01588
Heat Pipe OD at Temperature	m	0.01597	0.01597	0.01597	0.01598	0.01595	0.01596	0.01596	0.01597	0.01597	0.01597
Condenser Length	m	0.23495	0.23495	0.23495	0.23495	0.23495	0.23495	0.23495	0.23495	0.23495	0.23495
Gas Gap Width - HP OD to Calorimeter ID	m	0.00064	0.00063	0.00083	0.00078	0.00053	0.00094	0.00042	0.00116	0.00051	0.00064
Calorimeter Channel Wall ID	m	0.01725	0.01722	0.02122	0.01754	0.01701	0.01784	0.01680	0.01830	0.01698	0.01725
Calorimeter Channel Wall OD	m	0.02020	0.02017	0.02416	0.02048	0.01996	0.02079	0.01975	0.02125	0.01993	0.02020
Calorimeter Channel Wall Thickness	m	0.00147	0.00147	0.00147	0.00147	0.00147	0.00147	0.00147	0.00147	0.00147	0.00147
Calorimeter Shell Wall ID	m	0.02096	0.02093	0.02493	0.02124	0.02072	0.02155	0.02051	0.02201	0.02069	0.02096
Calorimeter Shell Wall OD	m	0.02391	0.02388	0.02787	0.02419	0.02367	0.02449	0.02346	0.02495	0.02364	0.02391
Calorimeter Shell Wall Thickness	m	0.00147	0.00147	0.00147	0.00147	0.00147	0.00147	0.00147	0.00147	0.00147	0.00147
Calorimeter Cover Wall ID	m	0.03026	0.03023	0.03422	0.03054	0.03002	0.03084	0.02981	0.03130	0.02999	0.03026
Calorimeter Cover Wall OD	m	0.03320	0.03317	0.03717	0.03349	0.03296	0.03379	0.03275	0.03425	0.03293	0.03320
Calorimeter Cover Wall Thickness	m	0.00147	0.00147	0.00147	0.00147	0.00147	0.00147	0.00147	0.00147	0.00147	0.00147
Ffm Flow Gap Thickness	m	0.00038	0.00038	0.00038	0.00038	0.00038	0.00038	0.00038	0.00038	0.00038	0.00038
Return Flow Gap Thickness	m	0.00318	0.00318	0.00318	0.00318	0.00318	0.00318	0.00318	0.00318	0.00318	0.00318
Ffm Hydraulic Diameter (Outer-Inner)	m	0.000762	0.000762	0.000762	0.000762	0.000762	0.000762	0.000762	0.000762	0.000762	0.000762
Dimensions (inches)											
Heat Pipe OD at Room Temperature	n	0.6250	0.6250	0.6250	0.6250	0.6250	0.6250	0.6250	0.6250	0.6250	0.6250
Heat Pipe OD at Temperature	n	0.6286	0.6286	0.6286	0.6290	0.6281	0.6283	0.6283	0.6288	0.6288	0.6286
Condenser Length	n	9.2500	9.2500	9.2500	9.2500	9.2500	9.2500	9.2500	9.2500	9.2500	9.2500
Gas Gap Width - HP OD to Calorimeter ID	n	0.0253	0.0247	0.1034	0.0307	0.0208	0.0370	0.0165	0.0458	0.0199	0.0253
Calorimeter Channel Wall ID	n	0.6792	0.6780	0.8353	0.6904	0.6698	0.7023	0.6614	0.7204	0.6686	0.6792
Calorimeter Channel Wall OD	n	0.7952	0.7940	0.9513	0.8064	0.7858	0.8183	0.7774	0.8364	0.7846	0.7952
Calorimeter Channel Wall Thickness	n	0.0580	0.0580	0.0580	0.0580	0.0580	0.0580	0.0580	0.0580	0.0580	0.0580
Calorimeter Shell Wall ID	n	0.8252	0.8240	0.9813	0.8364	0.8158	0.8483	0.8074	0.8664	0.8146	0.8252
Calorimeter Shell Wall OD	n	0.9412	0.9400	1.0973	0.9524	0.9318	0.9643	0.9234	0.9824	0.9306	0.9412
Calorimeter Shell Wall Thickness	n	0.0580	0.0580	0.0580	0.0580	0.0580	0.0580	0.0580	0.0580	0.0580	0.0580
Calorimeter Cover Wall ID	n	1.1912	1.1900	1.3473	1.2024	1.1818	1.2143	1.1734	1.2324	1.1806	1.1912
Calorimeter Cover Wall OD	n	1.3072	1.3060	1.4633	1.3184	1.2978	1.3303	1.2894	1.3484	1.2966	1.3072
Calorimeter Cover Wall Thickness	n	0.0580	0.0580	0.0580	0.0580	0.0580	0.0580	0.0580	0.0580	0.0580	0.0580
Ffm Flow Gap Thickness	n	0.0150	0.0150	0.0150	0.0150	0.0150	0.0150	0.0150	0.0150	0.0150	0.0150
Return Flow Gap Thickness	n	0.1250	0.1250	0.1250	0.1250	0.1250	0.1250	0.1250	0.1250	0.1250	0.1250
Ffm Hydraulic Diameter (Outer-Inner)	n	0.0300	0.0300	0.0300	0.0300	0.0300	0.0300	0.0300	0.0300	0.0300	0.0300
Material Emissivity											
Emissivity Mo-44.5Re @ Temp		0.16	0.16	0.16	0.17	0.15	0.16	0.16	0.16	0.16	0.16
Emissivity Copper C122		0.44	0.44	0.44	0.44	0.44	0.44	0.44	0.44	0.44	0.44
Effective Emissivity		0.13	0.14	0.13	0.14	0.13	0.13	0.13	0.14	0.14	0.13
Heat Transfer Gas Gap											
Radiation Heat Transfer Gap	W	235.16	234.64	235.50	333.84	160.66	195.48	194.88	281.49	280.89	235.16
Conduction Heat Transfer Gap	W	2764.84	4765.36	764.50	2666.16	2839.34	1804.52	3805.12	1718.51	3719.11	2764.84
Gas Gap Composition	Helium-Argon	32% Ar	6% Ar	32% Ar	32% Ar	32% Ar	32% Ar	32% Ar	32% Ar	32% Ar	32% Ar
Helium Thermal conductivity @ Avg. Temp	W/m-K	0.31	0.32	0.31	0.33	0.30	0.30	0.31	0.32	0.32	0.31
Gas Gap Compensation factor		0.51	0.88	0.51	0.51	0.51	0.51	0.51	0.51	0.51	0.51
Effective Gas Gap Thermal Conductivity	W/m-K	0.1592	0.2790	0.1576	0.1662	0.1520	0.1542	0.1570	0.1613	0.1641	0.1592
Calorimeter Material		copper C122	copper C122	copper C122	copper C122	copper C122	copper C122	copper C122	copper C122	copper C122	copper C122
Calorimeter Channel Wall Thermal Conductivity	W/m-K	339.0	339.0	339.0	339.0	339.0	339.0	339.0	339.0	339.0	339.0
Calorimeter Cooling Fluid		Water	Water	Water	Water	Water	Water	Water	Water	Water	Water
Avg Temp Used for Fluid Properties	K	309.2	312.1	317.4	309.9	308.6	306.8	311.2	307.4	311.8	309.2
Water Flow Rate	kg/sec	0.038	0.049	0.007	0.036	0.041	0.034	0.042	0.031	0.040	0.038
Water Flow Rate	gal/min	0.605	0.769	0.107	0.565	0.645	0.543	0.665	0.497	0.630	0.605
Inlet Water Pressure	Pa	446599	446599	446599	446599	446599	446599	446599	446599	446599	446599
Inlet Water Pressure	psi	65.00	65.00	65.00	65.00	65.00	65.00	65.00	65.00	65.00	65.00
Water Inlet Temperature	K	299.82	299.82	299.82	299.82	299.82	299.82	299.82	299.82	299.82	299.82
Log mean Water Ffm Flow temp Wall to Fluid	K	50.22	83.28	13.77	49.45	50.88	32.72	68.17	31.97	67.46	50.22
Average Water Ffm Flow Temperature	K	309.20	312.12	317.43	309.87	308.62	306.79	311.20	307.43	311.83	309.20
Water ffm flow temp delta (inlet to outlet)	K	18.78	24.61	35.23	20.11	17.60	13.94	22.76	15.22	24.02	18.78
Water Outlet Temperature	K	318.59	324.43	335.04	319.93	317.42	313.76	322.58	315.04	323.83	318.59
Water specific heat Cp	J/kg-K	4180.76	4180.35	4180.09	4180.65	4180.86	4181.24	4180.46	4181.10	4180.38	4180.76
Water thermal conductivity k	W/m-K	0.62	0.63	0.64	0.62	0.62	0.62	0.63	0.62	0.63	0.62
water density rho	kg/m3	994.92	993.89	991.90	994.69	995.12	995.73	994.22	995.52	994.00	994.92
Water Absolute Viscosity mu	kg/m-s	0.000716	0.000674	0.000608	0.000706	0.000725	0.000754	0.000687	0.000744	0.000678	0.000716
Log Mean Temperature Difference Wall to Fluid	K	50.21	83.27	13.77	49.45	50.88	32.72	68.17	31.97	67.46	50.21
Heat Transfer To Cooling Fluid											
Channel Flow Tube surface		smooth	smooth	smooth	smooth	smooth	smooth	smooth	smooth	smooth	smooth
Shell Flow Tube surface		smooth	smooth	smooth	smooth	smooth	smooth	smooth	smooth	smooth	smooth
Type of flow (Re<2300 = Laminar)		Laminar	Laminar	Laminar	Laminar	Laminar	Laminar	Laminar	Laminar	Laminar	Laminar
Ffm Flow Area	m^2	2.49E-05	2.48E-05	2.94E-05	2.50E-05	2.43E-05	2.53E-05	2.41E-05	2.59E-05	2.43E-05	2.49E-05
Ffm Flow Velocity	m/sec	1.56	1.99	0.23	1.44	1.68	1.36	1.76	1.22	1.65	1.56
Reynolds Number		1651.62	2294.20	289.99	1542.72	1760.48	1389.09	1936.03	1244.12	1842.06	1651.62
Nusset Number		4.90	4.90	4.89	4.90	4.90	4.90	4.90	4.89	4.90	4.90
Convective heat Transfer Coeff h	W/m^2-K	4009.09	4035.15	4075.22	4014.70	4004.10	3986.03	4027.64	3991.38	4032.91	4009.09
Check on power balance -convection side	*W*	*3000.00*	*5000.00*	*1000.00*	*3000.00*	*3000.00*	*2000.00*	*4000.00*	*2000.00*	*4000.00*	*3000.00*
Check power balance - water flow side	*W*	*3000.00*	*5000.00*	*1000.00*	*3000.00*	*3000.00*	*2000.00*	*4000.00*	*2000.00*	*4000.00*	*3000.00*
Pressure Drop in Film Channel											
viscosity ratio (mu-bulk to mu-wall)		2.14	3.22	1.39	2.11	2.17	1.77	2.62	1.75	2.59	2.14
annular passage diameter ratio dinner/douter		0.964	0.964	0.969	0.964	0.963	0.965	0.963	0.965	0.963	0.964
annular passage adjustment factor		1.49997	1.49997	1.49998	1.49997	1.49996	1.49997	1.49996	1.49997	1.49996	1.49997
factor for f/Re expression		79.4	71.7	88.4	79.7	79.1	83.2	75.4	83.5	75.7	79.4
friction factor f smooth channel		0.048	0.032	0.305	0.052	0.045	0.061	0.039	0.067	0.041	0.048
Calorimeter Length	m	0.330	0.330	0.330	0.330	0.330	0.330	0.330	0.330	0.330	0.330
Data pressure in Ffm Channel	Pa	25219.2	27328.4	3562.0	22992.4	27466.3	24280.1	25871.7	21539.4	24074.4	25219.2
Data pressure in Ffm Channel	psi	3.7	4.0	0.5	3.3	4.0	3.5	3.8	3.1	3.5	3.7
Data Pressure/Inlet Pressure		0.056	0.061	0.008	0.051	0.062	0.054	0.058	0.048	0.054	0.056

Table 28. Calorimeter geometry and performance for a cooling film annulus = 0.020 in.

For NRPCT Work Item #2
Water Calorimeter Quick Assessment for Heat pipe life time testing
Assumes: helium/argon gas flooded test chamber at low pressure to improve coupling to calorimeter

- Direct Input Value
- Value Carried From Other Input Location
- parameters of interest

Heat pipe Inputs

Heat ppe length	0.3048		12	nch	ratio Cond/Evap
Evaporator length	0.06985	m	2.75	nch	
Adiabatic length	0	m	0	nch	
Condenser length	0.23495	m	9.25	nch	
Diameter	0.015875	m	0.625	n OD	

Calorimeter Inputs

length of calorimeter	0.3302	m	13	nch	
Calorimeter Area	0.01171167	m^2	18.153125	nch^2	covering heat pipe
Calorimeter Area	0.004747974	m^3	7.359375	nch^3	covering support
Nominal Inlet Temperature	299.8166667	K	80	deg F	
Nominal Flowrate	0.027491492	kg/sec	0.435	gal/min	
inlet water pressure	446599	Pa	65	psi	
Target Surface Temp (ID)	351	K	172.13	F	on the ID surface exposed to hot heat pipe (boiling = 420 K at 65psia)
Channel Wall thickness	0.0014732	m	0.058	nch	inner tube exposed to hot heat pipe
Shell Wall thickness	0.0014732	m	0.058	nch	middle tube creating the film flow path
Cover Wall thickness	0.0014732	m	0.058	nch	outer tube sealing the return path
film flow Gap	0.000508	m	0.02	nch	water flow gap on inner annulus (outlet flow) next to heat ppe - this absorbs the heat
Return Flow Gap	0.003175	m	0.125	nch	water flow gap on outer annulus (inlet flow)

Variables	Units	Test Condition --> G series	F(-4)	F(-3)	F(-2)	F(-1)	F(1)	F(2)	F(3)	F(4)	F(0)
Power (W)	W	3000	5000	1000	3000	3000	2000	4000	2000	4000	3000
Heat Pipe Surface Temperature	K	1273	1273	1273	1373	1173	1223	1223	1323	1323	1273
Average Gas Gap Temperature	K	824	846.5	805	874	774	786.5	812	836.5	861.5	824
Calorimeter Channel ID Temperature	K	375	420	337	375	375	350	401	350	400	375
Calorimeter Channel Wall OD Temperature	K	374.05	418.42	336.74	374.07	374.04	349.39	399.71	349.40	398.72	374.05
Calorimeter Channel Wall Delta Temp	K	0.95	1.58	0.26	0.93	0.96	0.61	1.29	0.60	1.28	0.95
Dimensions (meters)											
Heat Pipe OD at Room Temperature	m	0.01588	0.01588	0.01588	0.01588	0.01588	0.01588	0.01588	0.01588	0.01588	0.01588
Heat Pipe OD at Temperature	m	0.01597	0.01597	0.01597	0.01598	0.01595	0.01596	0.01596	0.01597	0.01597	0.01597
Condenser Length	m	0.23495	0.23495	0.23495	0.23495	0.23495	0.23495	0.23495	0.23495	0.23495	0.23495
Gas Gap Width - HP OD to Calorimeter ID	m	0.00064	0.00062	0.00263	0.00077	0.00052	0.00093	0.00041	0.00116	0.00050	0.00064
Calorimeter Channel Wall ID	m	0.01724	0.01720	0.02122	0.01752	0.01700	0.01783	0.01679	0.01828	0.01697	0.01724
Calorimeter Channel Wall OD	m	0.02019	0.02015	0.02417	0.02047	0.01995	0.02077	0.01973	0.02123	0.01991	0.02019
Calorimeter Channel Wall Thickness	m	0.00147	0.00147	0.00147	0.00147	0.00147	0.00147	0.00147	0.00147	0.00147	0.00147
Calorimeter Shell Wall ID	m	0.02120	0.02116	0.02518	0.02148	0.02096	0.02179	0.02075	0.02225	0.02093	0.02120
Calorimeter Shell Wall OD	m	0.02415	0.02411	0.02813	0.02443	0.02391	0.02473	0.02370	0.02519	0.02388	0.02415
Calorimeter Shell Wall Thickness	m	0.00147	0.00147	0.00147	0.00147	0.00147	0.00147	0.00147	0.00147	0.00147	0.00147
Calorimeter Cover Wall ID	m	0.03050	0.03046	0.03448	0.03078	0.03026	0.03108	0.03005	0.03154	0.03023	0.03050
Calorimeter Cover Wall OD	m	0.03344	0.03340	0.03743	0.03373	0.03321	0.03403	0.03299	0.03449	0.03317	0.03344
Calorimeter Cover Wall Thickness	m	0.00147	0.00147	0.00147	0.00147	0.00147	0.00147	0.00147	0.00147	0.00147	0.00147
Film Flow Gap Thickness	m	0.00051	0.00051	0.00051	0.00051	0.00051	0.00051	0.00051	0.00051	0.00051	0.00051
Return Flow Gap Thickness	m	0.00318	0.00318	0.00318	0.00318	0.00318	0.00318	0.00318	0.00318	0.00318	0.00318
Film Hydraulic Diameter (Douter-Dinner)	m	0.001016	0.001016	0.001016	0.001016	0.001016	0.001016	0.001016	0.001016	0.001016	0.001016
Dimensions (inches)											
Heat Pipe OD at Room Temperature	n	0.6250	0.6250	0.6250	0.6250	0.6250	0.6250	0.6250	0.6250	0.6250	0.6250
Heat Pipe OD at Temperature	n	0.6286	0.6286	0.6286	0.6290	0.6281	0.6283	0.6283	0.6288	0.6288	0.6286
Condenser Length	n	9.2500	9.2500	9.2500	9.2500	9.2500	9.2500	9.2500	9.2500	9.2500	9.2500
Gas Gap Width - HP OD to Calorimeter ID	n	0.0251	0.0243	0.1035	0.0304	0.0206	0.0367	0.0163	0.0455	0.0196	0.0251
Calorimeter Channel Wall ID	n	0.6787	0.6771	0.8355	0.6898	0.6693	0.7018	0.6609	0.7199	0.6680	0.6787
Calorimeter Channel Wall OD	n	0.7947	0.7931	0.9515	0.8058	0.7853	0.8178	0.7769	0.8359	0.7840	0.7947
Calorimeter Channel Wall Thickness	n	0.0580	0.0580	0.0580	0.0580	0.0580	0.0580	0.0580	0.0580	0.0580	0.0580
Calorimeter Shell Wall ID	n	0.8347	0.8331	0.9915	0.8458	0.8253	0.8578	0.8169	0.8759	0.8240	0.8347
Calorimeter Shell Wall OD	n	0.9507	0.9491	1.1075	0.9618	0.9413	0.9738	0.9329	0.9919	0.9400	0.9507
Calorimeter Shell Wall Thickness	n	0.0580	0.0580	0.0580	0.0580	0.0580	0.0580	0.0580	0.0580	0.0580	0.0580
Calorimeter Cover Wall ID	n	1.2007	1.1991	1.3575	1.2118	1.1913	1.2238	1.1829	1.2419	1.1900	1.2007
Calorimeter Cover Wall OD	n	1.3167	1.3151	1.4735	1.3278	1.3073	1.3398	1.2989	1.3579	1.3060	1.3167
Calorimeter Cover Wall Thickness	n	0.0580	0.0580	0.0580	0.0580	0.0580	0.0580	0.0580	0.0580	0.0580	0.0580
Film Flow Gap Thickness	n	0.0200	0.0200	0.0200	0.0200	0.0200	0.0200	0.0200	0.0200	0.0200	0.0200
Return Flow Gap Thickness	n	0.1250	0.1250	0.1250	0.1250	0.1250	0.1250	0.1250	0.1250	0.1250	0.1250
Film Hydraulic Diameter (Douter-Dinner)	n	0.0400	0.0400	0.0400	0.0400	0.0400	0.0400	0.0400	0.0400	0.0400	0.0400
Material Emissivity											
Emissivity Mo-44.5Re @ Temp		0.16	0.16	0.16	0.17	0.15	0.16	0.16	0.16	0.16	0.16
Emissivity Copper C122		0.44	0.44	0.44	0.44	0.44	0.44	0.44	0.44	0.44	0.44
Effective Emissivity		0.13	0.14	0.13	0.14	0.13	0.13	0.13	0.14	0.14	0.13
Heat Transfer Gas Gap											
Radiation Heat Transfer Gap	W	234.94	234.30	235.52	333.62	160.44	195.33	194.57	281.33	280.63	234.94
Conduction Heat Transfer Gap	W	2765.06	4765.70	764.48	2666.38	2839.56	1804.67	3805.43	1718.67	3719.37	2765.06
Gas Gap Composition	He/Ar - Argon	32% Ar	6% Ar	32% Ar	32% Ar	32% Ar	32% Ar	32% Ar	32% Ar	32% Ar	32% Ar
He/Ar Thermal conductivity @ Avg. Temp	W/m-K	0.31	0.32	0.31	0.33	0.30	0.30	0.31	0.32	0.32	0.31
Gas Gap Compensation factor		0.51	0.88	0.51	0.51	0.51	0.51	0.51	0.51	0.51	0.51
Effective Gas Gap Thermal Conductivity	W/m-K	0.1602	0.2819	0.1575	0.1672	0.1531	0.1549	0.1585	0.1620	0.1655	0.1602
Calorimeter Material		copper C122	copper C122	copper C122	copper C122	copper C122	copper C122	copper C122	copper C122	copper C122	copper C122
Calorimeter Channel Wall Thermal Conductivity	W/m-K	339.0	339.0	339.0	339.0	339.0	339.0	339.0	339.0	339.0	339.0
Calorimeter Cooling Fluid		Water	Water	Water	Water	Water	Water	Water	Water	Water	Water
Avg Temp Used for Fluid Properties	K	307.6	307.9	314.7	308.6	306.8	306.1	309.6	307.0	309.4	307.6
Water Flow Rate	kg/sec	0.046	0.074	0.006	0.041	0.052	0.038	0.049	0.033	0.050	0.046
Water Flow Rate	gal/min	0.727	1.175	0.127	0.646	0.817	0.604	0.774	0.527	0.791	0.727
Inlet Water Pressure	Pa	446599	446599	446599	446599	446599	446599	446599	446599	446599	446599
Inlet Water Pressure	psi	65.00	65.00	65.00	65.00	65.00	65.00	65.00	65.00	65.00	65.00
Water Inlet Temperature	K	299.82	299.82	299.82	299.82	299.82	299.82	299.82	299.82	299.82	299.82
Log mean Water Film Flow temp Wall to Fluid	K	67.08	111.95	18.42	66.01	68.01	43.62	91.05	42.60	90.28	67.08
Average Water Film Flow Temperature	K	307.62	307.87	314.72	308.60	306.76	306.08	309.60	307.00	309.39	307.62
Water film flow temp delta (inlet to outlet)	K	15.62	16.10	29.81	17.57	13.89	12.53	19.57	14.37	19.14	15.62
Water Outlet Temperature	K	315.43	315.92	329.63	317.39	313.71	312.35	319.38	314.19	318.96	315.43
Water specific heat Cp	J/kg-K	4181.06	4181.01	4180.14	4180.86	4181.24	4181.40	4180.69	4181.19	4180.72	4181.06
Water thermal conductivity k	W/m-K	0.62	0.62	0.63	0.62	0.62	0.62	0.62	0.62	0.62	0.62
water density rho	kg/m3	995.45	995.37	992.94	995.12	995.74	995.96	994.78	995.66	994.85	995.45
Water Absolute Viscosity mu	kg/m-s	0.000741	0.000737	0.000640	0.000725	0.000755	0.000766	0.000710	0.000751	0.000713	0.000741
Log Mean Temperature Difference Wall to Fluid	K	67.07	111.94	18.42	66.01	68.00	43.62	91.05	42.59	90.27	67.07
Heat Transfer To Cooling Fluid											
Channel Flow Tube surface		smooth	smooth	smooth	smooth	smooth	smooth	smooth	smooth	smooth	smooth
Shell Flow Tube surface		smooth	smooth	smooth	smooth	smooth	smooth	smooth	smooth	smooth	smooth
Type of flow (Re<2300 = Laminar)		Laminar	Laminar	Laminar	Laminar	Laminar	Laminar	Laminar	Laminar	Laminar	Laminar
Film Flow Area	m^2	3.30E-05	3.29E-05	3.94E-05	3.35E-05	3.26E-05	3.39E-05	3.23E-05	3.47E-05	3.29E-05	3.30E-05
Film Flow Velocity	m/sec	1.40	2.26	0.21	1.23	1.59	1.13	1.52	0.96	1.54	1.40
Reynolds Number		1909.46	3108.23	323.56	1709.81	2131.62	1491.88	2166.48	1299.16	2185.17	1909.46
Nusset Number		4.91	4.91	4.90	4.91	4.91	4.91	4.91	4.91	4.91	4.91
Convective heat Transfer Coeff h	W/m^2-K	3003.32	3005.07	3045.72	3009.65	2997.65	2991.69	3017.55	2997.54	3015.83	3003.32
Check on power balance - convection side	*W*	*3000.00*	*5000.00*	*1000.00*	*3000.00*	*3000.00*	*2000.00*	*4000.00*	*2000.00*	*4000.00*	*3000.00*
Check power balance - water/flow side	*W*	*3000.00*	*5000.00*	*1000.00*	*3000.00*	*3000.00*	*2000.00*	*4000.00*	*2000.00*	*4000.00*	*3000.00*
Pressure Drop in Film Channel											
viscosity ratio (mu-bulk to mu-wall)		2.65	4.26	1.44	2.60	2.70	2.04	3.63	2.00	3.60	2.65
annular passage dia ratio dinner/douter		0.952	0.952	0.960	0.953	0.952	0.953	0.951	0.954	0.951	0.952
annular passage adjustment factor		1.49994	1.49994	1.49996	1.49994	1.49994	1.49994	1.49994	1.49995	1.49994	1.49994
factor for f/Re expression		75.2	66.8	87.6	75.6	74.9	80.4	69.6	80.8	69.7	75.2
friction factor f smooth channel		0.039	0.021	0.271	0.044	0.035	0.054	0.032	0.062	0.032	0.039
Calorimeter Length	m	0.330	0.330	0.330	0.330	0.330	0.330	0.330	0.330	0.330	0.330
Delta pressure in Film Channel	Pa	12462.7	17825.7	1840.6	10763.6	14369.6	11113.0	12030.1	9347.2	12268.1	12462.7
Delta pressure in Film Channel	psi	1.8	2.6	0.3	1.6	2.1	1.6	1.8	1.4	1.8	1.8
Delta Pressure/Inlet Pressure		0.028	0.040	0.004	0.024	0.032	0.025	0.027	0.021	0.027	0.028

APPENDIX G—HEAT PIPE/CALORIMETER ENVIRONMENTAL LOSSES

Tables 29 and 30 provide a quick assessment of environmental losses from the heat pipe and calorimeter unit using environments of pure He and He-32%Ar.

Table 29. Heat pipe/calorimeter thermal loss spreadsheet for pure He environment.

For NRPCT Work Item #2
Environmental Losses From Heat Pipe and Calorimeter Unit (Quick Assessment)
Estimates for Condenser Support, Calorimeter Cover, and Evaporator
Assumes: helium gas flooded test chamber at low pressure (75 torr)

Calorimeter Length	13.00	in	0.3302	m
Calorimeter Outer Diameter	1.375	in	0.034925	m
Calorimeter Inner tube ID	0.675	in	0.017145	m
Condenser Support Length	4.5	in	0.1143	m
Condenser Support OD	0.5	in	0.0127	m
Condenser Support Wall Thickness	0.03	in	0.000762	m
Condenser Support Gas Gap Width	0.0875	in	0.0022225	m
Evaporator Length Under RF coils	3		0.0762	m
Evaporator Length Exposed	1	in	0.0254	m
Evaporator Length Total	4	in	0.1016	m
Heat Pipe Diameter	0.625	in	0.015875	m
Distance Between RF Coil and Heat Pipe	0.25	in	0.00635	m
Inner Diameter of RF Coil	1.125	in	0.028575	m
RF Inductive Coil Temperature			350	K
Ambient Environment Temp			300	K
Heat Pipe Support Temperature			400	K
Condenser Support Surface Area			0.004558055	m2
Condenser Support Cross Section Area			2.85638E-05	m2
Calorimeter Surface Area			0.036211218	m2
Evaporator Surface Area Under RF Coils			0.00379838	m2
Evaporator Surface Area Exposed			0.001266127	m2

Test Condition —>		Gseries	F(-4)	F(-3)	F(-2)	F(-1)	F(1)	F(2)	F(3)	F(4)	F(0)
Variables	**Units**										
Heat Pipe Power Level	W	3000	5000	1000	3000	3000	2000	4000	2000	4000	3000
Heat Pipe Temperature	K	1273	1273	1273	1373	1173	1223	1223	1323	1323	1273
Heat Pipe Cal. Surface Temp	K	360	398	338	360	360	340	380	380	340	360
Coolant Outlet Temp	K	332.1	329.8	328.0	333.5	331.0	315.3	338.4	316.7	339.5	332.1
Gas Composition Factor (1=pure He)		1.00	1.00	1.00	1.00	1.00	1.00	1.00	1.00	1.00	1.00
Condenser Support Losses											
Condenser Support Avg Temp	K	836.5	836.5	836.5	886.5	786.5	811.5	811.5	861.5	861.5	836.5
Avg Gas Temperature	K	598.3	617.3	587.3	623.3	573.3	575.8	595.8	620.8	600.8	598.3
Avg Mo-44Re Thermal Cond k	W/m-K	55.3	55.3	55.3	56.6	54.0	54.6	54.6	55.9	55.9	55.3
Avg gas Thermal Cond k	W/m-K	0.249	0.255	0.246	0.257	0.242	0.243	0.249	0.256	0.250	0.249
Emissivity Mo-44Re		0.12	0.12	0.12	0.12	0.11	0.11	0.11	0.12	0.12	0.12
Solid Conduction Loss	W	12.1	12.1	12.1	13.8	10.4	11.2	11.2	12.9	12.9	12.1
Radiation Loss	W	14.3	14.0	14.4	19.0	10.5	12.4	12.2	16.4	16.6	14.3
Gas Conduction Loss	W	284.2	267.5	293.4	323.4	246.8	273.7	256.6	294.9	312.0	284.2
Calorimeter Surface Losses											
Avg Calorimeter Surface Temp	K	332	330	328	333	331	315	338	317	340	332
Avg Environment Temp	K	316	315	314	317	315	308	319	308	320	316
Gas Thermal Conductivity (k)	W/m-K	0.16	0.16	0.16	0.16	0.16	0.16	0.16	0.16	0.16	0.16
Thermal Expansion Coeff(β)	1/K	0.00316	0.00318	0.00318	0.00316	0.00317	0.00325	0.00313	0.00324	0.00313	0.00316
Specific Heat (cp)		5193	5193	5193	5193	5193	5193	5193	5193	5193	5193
Kinematic Viscosity (ν)	m2/sec	0.00131	0.00130	0.00129	0.00131	0.00130	0.00124	0.00133	0.00125	0.00134	0.00131
Density (ρ)	kg/m3	0.015	0.015	0.016	0.015	0.015	0.016	0.015	0.016	0.015	0.015
Thermal Diffusivity (α)	m2/sec	0.0020	0.0020	0.0020	0.0020	0.0020	0.0019	0.0020	0.0019	0.0021	0.0020
Prandtl Number		0.65	0.65	0.65	0.65	0.65	0.64	0.65	0.64	0.65	0.65
Rayleigh Number		16.10	15.19	14.44	16.61	15.65	8.66	18.39	9.35	18.80	16.10
Nusselt Number		1.23	1.22	1.21	1.23	1.22	1.12	1.25	1.13	1.26	1.23
Convective Heat Transfer Coeff h	W/m2-K	5.68	5.61	5.56	5.71	5.65	5.09	5.83	5.15	5.86	5.68
Natural Convection	W	6.37	5.85	5.43	6.68	6.11	2.72	7.81	3.00	8.09	6.37
Evaporator Surface Losses											
Avg Environment Temp	K	811.5	811.5	811.5	861.5	761.5	786.5	786.5	836.5	836.5	811.5
Emissivity Mo-44Re		0.16	0.16	0.16	0.17	0.15	0.16	0.16	0.16	0.16	0.16
Gas Thermal Conductivity (k)	W/m-K	0.311	0.311	0.311	0.324	0.297	0.304	0.304	0.318	0.318	0.311
Thermal Expansion Coeff(β)	1/K	0.00123	0.00123	0.00123	0.00116	0.00131	0.00127	0.00127	0.00120	0.00120	0.00123
Specific Heat (cp)		5193	5193	5193	5193	5193	5193	5193	5193	5193	5193
Kinematic Viscosity (ν)	m2/sec	0.0066	0.0066	0.0066	0.0073	0.0060	0.0063	0.0063	0.0070	0.0070	0.0066
Density (ρ)	kg/m3	0.0060	0.0060	0.0060	0.0057	0.0064	0.0062	0.0062	0.0058	0.0058	0.0060
Thermal Diffusivity (α)	m2/sec	0.0100	0.0100	0.0100	0.0110	0.0089	0.0094	0.0094	0.0105	0.0105	0.010
Prandtl Number		0.67	0.67	0.67	0.67	0.67	0.67	0.67	0.67	0.67	0.67
Rayleigh Number		0.71	0.71	0.71	0.60	0.85	0.78	0.78	0.66	0.66	0.71
Nusselt Number		0.81	0.81	0.81	0.80	0.83	0.82	0.82	0.81	0.81	0.81
Convective Heat Transfer Coeff h	W/m2-K	15.93	15.93	15.93	16.33	15.51	15.72	15.72	16.13	16.13	15.93
Radiation Loss	W	120.24	120.24	120.24	171.91	81.56	99.44	99.44	144.28	144.28	120.24
Gas Conduction Loss	W	233.46	233.46	233.46	270.21	198.80	215.87	215.87	251.58	251.58	233.46
Natural Convection Loss	W	74.46	74.46	74.46	84.60	64.65	69.51	69.51	79.49	79.49	74.46
Total Heat Loss	W	745	728	753	890	619	685	673	803	825	745

Table 30. Heat pipe/calorimeter thermal loss spreadsheet for He-32%Ar environment.

For NRPCT Work Item #2
Environmental Losses From Heat Pipe and Calorimeter Unit (Quick Assessment)
Estimates for Condenser Support, Calorimeter Cover, and Evaporator
Assumes: helium gas flooded test chamber at low pressure (75 torr)

Calorimeter Length	13.00	in	0.3302	m
Calorimeter Outer Diameter	1.375	in	0.034925	m
Calorimeter Inner tube ID	0.675	in	0.017145	m
Condenser Support Length	4.5	in	0.1143	m
Condenser Support OD	0.5	in	0.0127	m
Condenser Support Wall Thickness	0.03	in	0.000762	m
Condenser Support Gas Gap Width	0.0875	in	0.0022225	m
Evaporator Length Under RF coils	3		0.0762	m
Evaporator Length Exposed	1	in	0.0254	m
Evaporator Length Total	4	in	0.1016	m
Heat Pipe Diameter	0.625	in	0.015875	m
Distance Between RF Coil and Heat Pipe	0.25	in	0.00635	m
Inner Diameter of RF Coil	1.125	in	0.028575	m
RF Inductive Coil Temperature			350	K
Ambient Environment Temp			300	K
Heat Pipe Support Temperature			400	K
Condenser Support Surface Area			0.004558055	m2
Condenser Support Cross Section Area			2.85638E-05	m2
Calorimeter Surface Area			0.036211218	m2
Evaporator Surface Area Under RF Coils			0.00379838	m2
Evaporator Surface Area Exposed			0.001286127	m2

Test Condition —>		Gseries	F(-4)	F(-3)	F(-2)	F(-1)	F(1)	F(2)	F(3)	F(4)	F(0)
Variables	**Units**										
Heat Pipe Power Level	W	3000	5000	1000	3000	3000	2000	4000	2000	4000	3000
Heat Pipe Temperature	K	1273	1273	1273	1373	1173	1223	1223	1323	1323	1273
Heat Pipe Cal. Surface Temp	K	360	398	338	360	360	340	380	380	340	360
Coolant Outlet Temp	K	332.1	329.8	328.0	333.5	331.0	315.3	338.4	316.7	339.5	332.1
Gas Composition Factor (1= pure He)		0.51	0.51	0.51	0.51	0.51	0.51	0.51	0.51	0.51	0.51
Condenser Support Losses											
Condenser Support Avg Temp	K	836.5	836.5	836.5	886.5	786.5	811.5	811.5	861.5	861.5	836.5
Avg Gas Temperature	K	598.3	617.3	587.3	623.3	573.3	575.8	595.8	620.8	600.8	598.3
Avg Mo-44Re Thermal Condk	W/m-K	55.3	55.3	55.3	56.6	54.0	54.6	54.6	55.9	55.9	55.3
Avg gas Thermal Condk	W/m-K	0.127	0.130	0.126	0.131	0.123	0.124	0.127	0.131	0.128	0.127
Emissivity Mo-44Re		0.12	0.12	0.12	0.12	0.11	0.11	0.11	0.12	0.12	0.12
Solid Conduction Loss	W	12.1	12.1	12.1	13.8	10.4	11.2	11.2	12.9	12.9	12.1
Radiation Loss	W	14.3	14.0	14.4	19.0	10.5	12.4	12.2	16.4	16.6	14.3
Gas Conduction Loss	W	145.0	136.4	149.7	164.9	125.9	139.6	130.9	150.4	159.1	145.0
Calorimeter Surface Losses											
Avg Calorimeter Surface Temp	K	332	330	328	333	331	315	338	317	340	332
Avg Environment Temp	K	316	315	314	317	315	308	319	308	320	316
Gas Thermal Conductivity (k)	W/m-K	0.08	0.08	0.08	0.08	0.08	0.08	0.08	0.08	0.08	0.08
Thermal Expansion Coeff(β)	1/K	0.00316	0.00318	0.00318	0.00316	0.00317	0.00325	0.00313	0.00324	0.00313	0.00316
Specific Heat(cp)		5193	5193	5193	5193	5193	5193	5193	5193	5193	5193
Kinematic Viscosity (ν)	m2/sec	0.00131	0.00130	0.00129	0.00131	0.00130	0.00124	0.00133	0.00125	0.00134	0.00131
Density (ρ)	kg/m3	0.015	0.015	0.016	0.015	0.015	0.016	0.015	0.016	0.015	0.015
Thermal Diffusivity (α)	m2/sec	0.0010	0.0010	0.0010	0.0010	0.0010	0.0010	0.0010	0.0010	0.0010	0.0010
Prandtl Number		1.27	1.27	1.27	1.27	1.27	1.26	1.27	1.26	1.28	1.27
Rayleigh Number		31.57	29.79	28.31	32.58	30.68	16.97	36.05	18.34	36.86	31.57
Nusselt Number		1.43	1.42	1.40	1.44	1.42	1.29	1.46	1.31	1.47	1.43
Convective Heat Transfer Coeff h	W/m2-K	3.38	3.34	3.30	3.40	3.36	3.00	3.48	3.04	3.49	3.38
Natural Convection	W	3.79	3.47	3.23	3.98	3.63	1.60	4.65	1.77	4.82	3.79
Evaporator Surface Losses											
Avg Environment Temp	K	811.5	811.5	811.5	861.5	761.5	786.5	786.5	836.5	836.5	811.5
Emissivity Mo-44Re		0.16	0.16	0.16	0.17	0.15	0.16	0.16	0.16	0.16	0.16
Gas Thermal Conductivity (k)	W/m-K	0.158	0.158	0.158	0.165	0.151	0.155	0.155	0.162	0.162	0.158
Thermal Expansion Coeff(β)	1/K	0.00123	0.00123	0.00123	0.00116	0.00131	0.00127	0.00127	0.00120	0.00120	0.00123
Specific Heat(cp)		5193	5193	5193	5193	5193	5193	5193	5193	5193	5193
Kinematic Viscosity (ν)	m2/sec	0.0066	0.0066	0.0066	0.0073	0.0060	0.0063	0.0063	0.0070	0.0070	0.0066
Density (ρ)	kg/m3	0.0060	0.0060	0.0060	0.0057	0.0064	0.0062	0.0062	0.0058	0.0058	0.0060
Thermal Diffusivity (α)	m2/sec	0.0051	0.0051	0.0051	0.0056	0.0045	0.0048	0.0048	0.0053	0.0053	0.005
Prandtl Number		1.31	1.31	1.31	1.30	1.31	1.31	1.31	1.31	1.31	1.31
Rayleigh Number		1.40	1.40	1.40	1.18	1.66	1.52	1.52	1.28	1.28	1.40
Nusselt Number		0.91	0.91	0.91	0.89	0.93	0.92	0.92	0.90	0.90	0.91
Convective Heat Transfer Coeff h	W/m2-K	9.10	9.10	9.10	9.31	8.88	8.99	8.99	9.20	9.20	9.10
Radiation Loss	W	120.24	120.24	120.24	171.91	81.56	99.44	99.44	144.28	144.28	120.24
Gas Conduction Loss	W	119.07	119.07	119.07	137.81	101.39	110.09	110.09	128.31	128.31	119.07
Natural Convection Loss	W	42.53	42.53	42.53	48.22	37.01	39.74	39.74	45.36	45.36	42.53
Total Heat Loss	W	457	448	461	560	370	414	408	499	511	457

APPENDIX H—THE GENERALIZED FLUID SYSTEM SIMULATION PROGRAM

GFSSP has gone through extensive V&V since the first version was released in 1996. The following three methods have been used for V&V: (1) Comparison with classical analytical and numerical solution, (2) comparison with other code, and (3) comparison with test data.[29–34] GFSSP (version 3) was a joint winner of the 2001 NASA Software of the Year Award and has been patented. Concepts NREC Inc. has been licensed for GFSSP commercialization. Further information is available online, <http://mi.msfc.nasa.gov/GFSSP/index.shtml>.

GFSSP was developed and used during the design of the Simplex turbopump at MSFC. Predictions matched well to test data. However, the code was more extensively used during the design of the Fastrac turbopump at MSFC in which both steady state and transient calculations were performed. The Fastrac engine is a 60,000-lbf thrust liquid oxygen and rocket propellant 1 engine developed by MSFC. When the Fastrac turbopump was being designed, GFSSP was used to predict the steady-state internal flows and net axial thrust. This turbopump has since been tested at MSFC. Data from this testing program have been used to validate the transient capabilities of GFSSP.

Modeling a component test of the Fastrac turbopump provided the opportunity to compare the GFSSP-predicted flow field with measured pressures and temperatures. The boundary conditions for this transient model were derived from measured pressure and temperature data taken from a Fastrac turbopump component test conducted at MSFC. Results from the steady-state GFSSP model are shown in figure 54. Additionally, a representative plot comparing results from the GFSSP transient model to test data is shown in figure 55. In both the steady state and transient cases, good agreement (within 10%) was observed between the model predictions and test data at all model nodes shown.

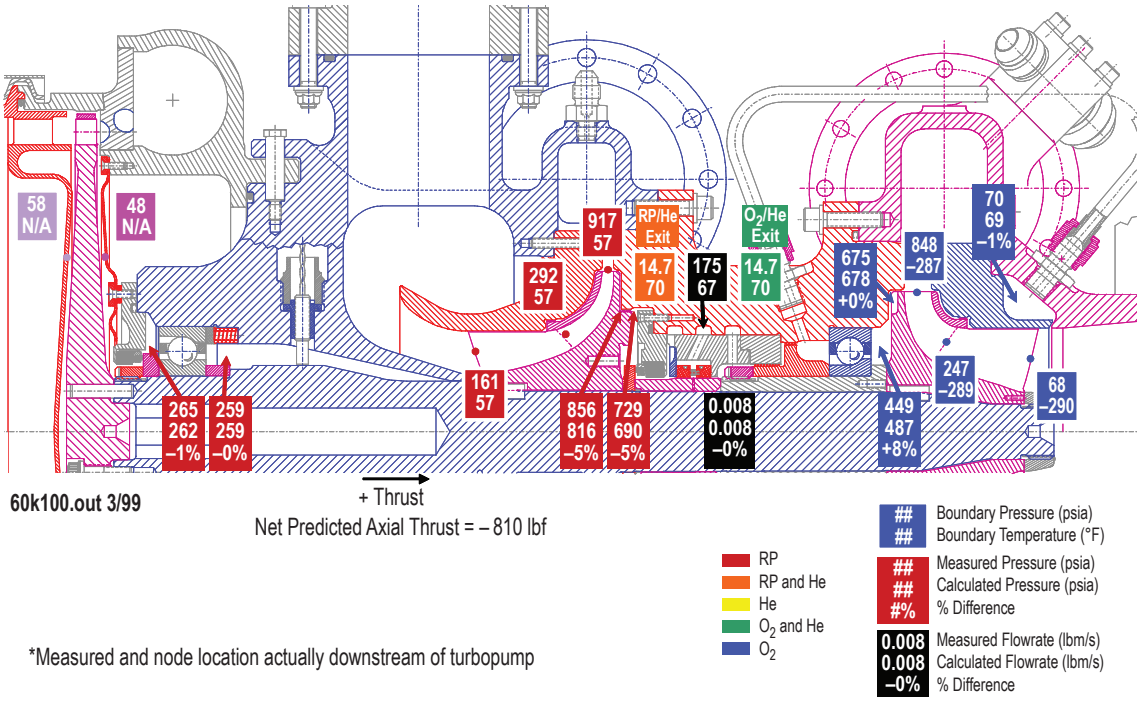

Figure 54. Steady-state results from the Fastrac turbopump GFSSP model.

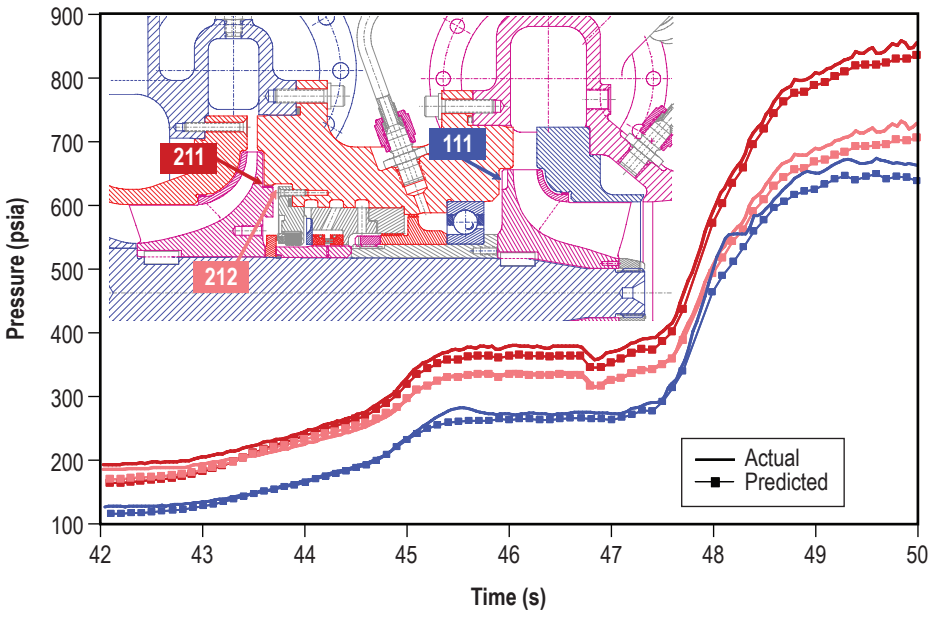

Figure 55. Representative transient pressure results from the Fastrac turbopump GFSSP model.

REFERENCES

1. Feber, R.C.; and Merrigan, M.A.: "Thermochemical Modeling of Mass Transport in High-Temperature Heat Pipes," *Proc. VI Int. Heat Pipe Conf*., Grenoble, France, 1987.

2. Sena, J.T.; and Merrigan, M.A.: "Niobium 1% Zirconium Potassium and Titanium Potassium Life-Test Heat Pipe Design and Testing," M.S. El-Genk and M.D. Hoover (eds.), *Proc. Seventh Symposium on Space Nuclear Power Systems*, CONF–900109, Albuquerque, NM, January 7–11, 1990.

3. Deming, S.N.; and Morgan, S.L.: *Experimental Design: A Chemometric Approach,* Elsevier, New York, NY, January 1987.

4. "Standard Practice for Liquid Sodium Corrosion Testing of Metals and Alloys," *ASTM G68–80*, ASTM International, West Conshohocken, PA, 1980.

5. Van Dyke, M.K.: "Early Flight Fission Test Facilities (EFF–TF) to Support Near-Term Space Fission Systems," Proceedings of Space Technology and Applications International Forum (STAIF–2004), M.S. El-Genk (ed.), *AIP Conf. Proceedings*, Vol. 699, pp. 713–719, Melville, NY, 2004.

6. Martin, J.J.; and Reid R.S.: "Sodium-Based Heat Pipe Modules for Space Reactor Concepts: Stainless Steel SAFE–100 Core," *International Congress on Advanced Nuclear Power Plants* (*ICAPP–2004a*), Conf. Proc. Published by ANS, Pittsburgh, PA, Paper No. 4275, pp. 2330–2338, 2004.

7. Lundberg, L.B.: "Alkali Heat Pipe Corrosion Phenomena," *Proc. VI Int. Heat Pipe Conf*., Grenoble, France, 1987.

8. Woloshun, K.A.; Merrigan, M.A.; and Best, E.B.: "HTPIPE: A Steady State Heat Pipe Analysis Program," *LA–11324–M*, Los Alamos National Laboratory, Los Alamos, NM, 1988.

9. Dickenson, T.J.; Woloshun, K.A.; and Stoyanof, M.: "Microgravity Experiment of Three Liquid Metal Heat Pipes," *Proc. 10th Int. Heat Pipe Conf*., Stuttgart, Germany, 1997.

10. Reid, R.S.: "Heat Pipe Transient Response Approximation," *Proc. Space Technology and Applications International Forum* (STAIF 2002), AIP Conf. Proc., Albuquerque, NM, February 2002.

11. Lundberg, L.B.: "A Critical Evaluation of Molybdenum and Its Alloys for Use in Space Reactor Core Heat Pipes," *Report No. LA–8685–MS*, Los Alamos Scientific Laboratory, Los Alamos, NM, January 1981.

12. Fuji, T.; and Watanabe, R.: "Secondary Recrystallization Kinetics in Molybdenum Sheet," *Journal of the Less-Common Metals*, Vol. 99, Issue 1, pp. 77–86, May 1984.

13. Incropera, F.P.; and Dewitt, D.P.: *Fundamentals of Heat Transfer*, John Wiley & Sons, New York, 1981.

14. Hewitt, G.F. (ed.): *Heat Exchanger Design Handbook 2002, Part 2 Fluid Mechanics and Heat Transfer*, Begell House, Inc., New York, ISBN 1–56700–181–5, 2002.

15. Dezani, V.B.; and Ginoux, J.L.: "Investigation of Breakdown Voltage Curves for Pure Helium and Silane-Helium Mixtures," *Phys. Plasmas*, Vol. 1, No. 4, AIP, pp. 1060–1063, 1994.

16. Furukawa, M.: "Empirical Expressions Selected as a Common Basis of Heat-Transfer and Pressure-Drop Calculations," *Trans. Japan Soc. Aero. Space Sci*., Vol. 36, No. 113, ISSN 0549–3811, pp. 188–208, November 1993.

17. Majumdar, A.K.; Bailey, J.W.; Schallhorn, P.A.; and Steadman, T.E.: "Generalized Fluid System Simulation Program," U.S. Patent No. 6748349, 2004.

18. Hendricks, R.C.; Baron, A.K.; and Peller, I.C.: "GASP—A Computer Code for Calculating the Thermodynamic and Transport Properties for Ten Fluids: Para Hydrogen, Helium, Neon, Methane, Nitrogen, Carbon Monoxide, Oxygen, Fluorine, Argon, and Carbon Dioxide," *NASA TN D–7808*, 1975.

19. Hendricks, R.C.; Peller, I.C.; and Baron, A.K.: "WASP—A Flexible Fortran IV Computer Code for Calculating Water and Steam Properties," *NASA TN D–7391*, 1973.

20. Cryodata Inc.: "User's Guide to GASPAK," Version 3.20, November 1994.

21. Holman, J.P.: *Heat Transfer*, 8th Edition, McGraw-Hill, New York, NY, 1997.

22. Reid, R.S.; and Martin, J.J: "Alkali Metal Heat Pipe Life Issues," *International Congress on Advanced Nuclear Power Plants* (ICAPP–2004a), Paper No. 4291, Conf. Proceedings Published by ANS, Pittsburgh, PA, pp. 2319–2329, 2004.

23. Reid, R.S.; Martin, J.J.; and Schmidt, G.L.: "Method for Determination of Less Than 5 pp Oxygen in Sodium Samples," *NASA/TM—2005–213902*, Marshall Space Flight Center, AL, July 2005.

24. Smith, D.L.; and Lee, R.H.: "Characterization of the Vanadium-Wire Equilibration Method for Measurement of Oxygen Activity in Liquid Sodium," *ANL–7891*, January 1, 1972.

25. Touloukian, Y.S.; and Ho, C.Y.: *Properties of Nonmetallic Fluid Elements*, McGraw-Hill, New York, ISBN 0070650330, 1981.

26. McCarty, R.D.: "Thermophysical Properties of Helium-4 from 2 to 1,500 K With Pressures to 1,000 Atmospheres," NBS Technical Note 631, 1972.

27. APT Materials Handbook, TID-26666, Oak Ridge National Laboratory, Oak Ridge, TN.

28. Lemmon, E.W.; McLinden, M.O.; and Friend, D.G.: "Thermophysical Properties of Fluid Systems," NIST Chemistry WebBook, NIST Standard Reference Database Number 69, P.J. Linstrom and W.G. Mallard (eds.), NIST, Gaithersburg, MD, 29899 (http://webbook.nist.gov), March 2003.

29. Majumdar, A.K.: "A Second Law-Based Unstructured Finite Volume Procedure for Generalized Flow Simulation," 37th AIAA Aerospace Sciences Meeting Conference and Exhibit, AIAA 99–0934, Reno, NV, January 11–14, 1999.

30. Majumdar, A.K.; and VanHooser, K.P.: "A General Fluid System Simulation Program to Model Secondary Flows in Turbomachinery," 31st AIAA/ASME/SAE/ASEE Joint Propulsion Conference, AIAA 95–2969, San Diego, CA, July 10–12, 1995.

31. VanHooser, K.P.; Bailey, J.W.; and Majumdar, A.K.: "Numerical Prediction of Transient Axial Thrust and Internal Flows in a Rocket Engine Turbopump," 35th AIAA/ASME/SAE/ASEE Joint Propulsion Conference, AIAA 99–2189, Los Angeles, CA, June 20–24, 1999.

32. Holt, K.; Majumdar, A.; Steadman, T.; and Hedayat, A.: "Numerical Modeling and Test Data Comparison of Propulsion Test Article Helium Pressurization System," 36th AIAA/ASME/ SAE/ ASEE Joint Propulsion Conference and Exhibit, AIAA 2000–3719, Huntsville, AL, July 16–19, 2000.

33. Schallhorn, P.; Elrod, D.; Goggin, D.; et al.: "A Fluid Circuit Model for Long Bearing Squeeze Film Damper Rotordynamics," *AIAA Journal of Propulsion and Power*, Vol. 16, No. 5, pp. 777–780, 2000.

34. Majumdar, A.K.; and Steadman, T.E.: "Numerical Modeling of Pressurization of a Propellant Tank," *Journal of Propulsion and Power*, Vol. 17, No. 2, pp. 385–390, 2001.

REPORT DOCUMENTATION PAGE

Form Approved
OMB No. 0704-0188

PLEASE DO NOT RETURN YOUR FORM TO THE ABOVE ADDRESS.

1. REPORT DATE *(DD-MM-YYYY)*	2. REPORT TYPE	3. DATES COVERED *(From - To)*
01–08–2010	Technical Publication	

4. TITLE AND SUBTITLE

Design of Refractory Metal Life Test Heat Pipe and Calorimeter

5a. CONTRACT NUMBER

5b. GRANT NUMBER

5c. PROGRAM ELEMENT NUMBER

6. AUTHOR(S)

J.J. Martin, R.S. Reid, and S.M. Bragg-Sitton

5d. PROJECT NUMBER

5e. TASK NUMBER

5f. WORK UNIT NUMBER

7. PERFORMING ORGANIZATION NAME(S) AND ADDRESS(ES)

George C. Marshall Space Flight Center
Marshall Space Flight Center, AL 35812

8. PERFORMING ORGANIZATION REPORT NUMBER

M–1284

9. SPONSORING/MONITORING AGENCY NAME(S) AND ADDRESS(ES)

National Aeronautics and Space Administration
Washington, DC 20546–0001

10. SPONSORING/MONITOR'S ACRONYM(S)

NASA

11. SPONSORING/MONITORING REPORT NUMBER

NASA/TP—2010–216435

12. DISTRIBUTION/AVAILABILITY STATEMENT

Unclassified-Unlimited
Subject Category 20
Availability: NASA CASI (443–757–5802)

13. SUPPLEMENTARY NOTES

Prepared by the Nuclear and Advanced Propulsion Development Branch, Engineering Directorate

14. ABSTRACT

Heat pipe life tests have seldom been conducted on a systematic basis. Typically, one or more heat pipes are built and tested for an extended period at a single temperature with simple condenser loading. Results are often reported describing the wall material, working fluid, test temperature, test duration, and occasionally the nature of any failure. Important information such as design details, processing procedures, material assay, power throughput, and radial power density are usually not mentioned. We propose to develop methods to generate carefully controlled data that conclusively establish heat pipe operating life with material-fluid combinations capable of extended operation. The test approach detailed in this Technical Publication will use 16 Mo-44.5%Re alloy/sodium heat pipe units that have an approximate12-in length and 5/8-in diameter. Two specific test series have been identified: (1) Long-term corrosion rates based on ASTM–G–68–80 (G-series) and (2) corrosion trends in a cross-correlation sequence at various temperatures and mass fluences based on a Fisher multifactor design (F-series). Evaluation of the heat pipe hardware will be performed in test chambers purged with an inert purified gas (helium or helium/argon mixture) at low pressure (10–100 torr) to provide thermal coupling between the heat pipe condenser and calorimeter. The final pressure will be selected to minimize the potential for voltage breakdown between the heat pipe and radio frequency (RF) induction coil (RF heating is currently the planned method of powering the heat pipes). The proposed calorimeter is constructed from a copper alloy and relies on a laminar flow water-coolant channel design to absorb and transport energy.

15. SUBJECT TERMS

alkali metal, sodium, heat pipes, refractory, metal, molybdenum, rhenium, radio frequency heating, fission power, space nuclear, life testing

16. SECURITY CLASSIFICATION OF:			17. LIMITATION OF ABSTRACT	18. NUMBER OF PAGES	19a. NAME OF RESPONSIBLE PERSON
a. REPORT	b. ABSTRACT	c. THIS PAGE			STI Help Desk at email: help@sti.nasa.gov
U	U	U	UU	116	19b. TELEPHONE NUMBER *(Include area code)* STI Help Desk at: 443–757–5802

National Aeronautics and
Space Administration
IS20
George C. Marshall Space Flight Center
Marshall Space Flight Center, Alabama
35812